frontiers in Earth Science

ORIGINAL RESEARCH
published: 11 December 2020
doi: 10.3389/feart.2020.568715

Mesozoic Paleo-Pacific Subduction Beneath SW Borneo: U-Pb Geochronology of the Schwaner Granitoids and the Pinoh Metamorphic Group

H. Tim Breitfeld[1,2], Lorin Davies[1,3], Robert Hall[1], Richard Armstrong[4], Marnie Forster[4], Gordon Lister[4], Matthew Thirlwall[1], Nathalie Grassineau[1], Juliane Hennig-Breitfeld[1,2] and Marco W. A. van Hattum[1]*

[1]Department of Earth Sciences, SE Asia Research Group, Royal Holloway University of London, Egham, United Kingdom, [2]Chemostrat Ltd., Buttington Cross Enterprise Park, Welshpool, United Kingdom, [3]Petryx Ltd., Menai Science Park, Gaerwen, United Kingdom, [4]Research School of Earth Sciences, The Australian National University, Canberra, ACT, Australia

OPEN ACCESS

Edited by:
Julia Ribeiro,
Chinese Academy of Sciences, China

Reviewed by:
Abigail Barker,
Uppsala University, Sweden
Alex Burton-Johnson,
British Antarctic Survey (BAS),
United Kingdom

***Correspondence:**
H. Tim Breitfeld
tim.breitfeld@rhul.ac.uk

Specialty section:
This article was submitted to Petrology, a section of the Frontiers in Earth Science

Received: 01 June 2020
Accepted: 20 October 2020
Published: 11 December 2020

Citation:
Breitfeld HT, Davies L, Hall R, Armstrong R, Forster M, Lister G, Thirlwall M, Grassineau N, Hennig-Breitfeld J and van Hattum MWA (2020) Mesozoic Paleo-Pacific Subduction Beneath SW Borneo: U-Pb Geochronology of the Schwaner Granitoids and the Pinoh Metamorphic Group. Front. Earth Sci. 8:568715. doi: 10.3389/feart.2020.568715

The Schwaner Mountains in southwestern Borneo form a large igneous province with a complex magmatic history and poorly known tectonic history. Previously it was known that Cretaceous granitoids intruded metamorphic rocks of the Pinoh Metamorphic Group assumed to be of Paleozoic age. Jurassic granitoids had been reported from the southern Schwaner Mountains. Most ages were based on K-Ar dating. We present new geochemistry, zircon U-Pb and $^{40}Ar/^{39}Ar$ age data from igneous and metamorphic rocks from the Schwaner Mountains to investigate their tectono-magmatic histories. We subdivide the Schwaner Mountains into three different zones which record rifting, subduction-related and post-collisional magmatism. The Northwest Schwaner Zone (NWSZ) is part of the West Borneo Block which in the Triassic was within the Sundaland margin. It records Triassic to Jurassic magmatism during early Paleo-Pacific subduction. In contrast, the North Schwaner Zone (NSZ) and South Schwaner Zone (SSZ) are part of the SW Borneo (Banda) Block that separated from NW Australia in the Jurassic. Jurassic granitoids in the SSZ are within-plate (A-type) granites interpreted to have formed during rifting. The SW Borneo (Banda) Block collided with eastern Sundaland at c. 135 Ma. Following this, large I-type granitoid plutons and arc volcanics formed in the NWSZ and NSZ between c. 90 and 132 Ma, associated with Cretaceous Paleo-Pacific subduction. The largest intrusion is the c. 110 to 120 Ma Sepauk Tonalite. After collision of the East Java-West Sulawesi (Argo) Block, subduction ceased and post-collisional magmatism produced the c. 78 to 85 Ma Sukadana Granite and the A-type 72 Ma Sangiyang Granite in the SSZ. Rocks of the Pinoh Metamorphic Group mainly exposed in the NSZ, previously assumed to represent Paleozoic basement, contain abundant Early Cretaceous (110 to 135 Ma) zircons. They are interpreted as volcaniclastic sediments that formed contemporaneously with subduction-related volcanic rocks of the NSZ subsequently metamorphosed during intrusion of Cretaceous granitoids. There are no igneous rocks older than Cretaceous in the NSZ

and older than Jurassic in the SSZ and there is no evidence for a continuation of a Triassic volcanic arc crossing Borneo from Sundaland to the east.

Keywords: zircon U-Pb geochronology, SHRIMP, LA-ICP-MS, Pinoh Metamorphic Group, Schwaner Mountains, Borneo, $^{40}Ar/^{39}Ar$ geochronology

INTRODUCTION

SE Asia is known to have been formed from continental fragments of Australian Gondwana origin from the Late Palaeozoic onwards to form the Sundaland continent. From the Triassic until early in the Late Cretaceous the eastern edge of Asia and Sundaland, at the western edge of the Paleo-Pacific, was a broadly north-south-trending subduction margin marked by abundant igneous rocks recording magmatic activity along an Andean-type continental margin. The margin (**Figure 1A**) can be traced from South China through Indochina into Borneo (e.g., Taylor and Hayes, 1983; Williams et al., 1988; Metcalfe, 2006; Metcalfe, 2017; Hall, 2012; Shellnutt et al., 2013; Hennig et al., 2017). Igneous and metamorphic rocks are exposed in the Schwaner Mountains of Indonesian Borneo (Kalimantan) and were for many years considered to be an ancient continental core of the island (e.g., van Bemmelen, 1949; Haile, 1974; Metcalfe, 1994) intruded by Cretaceous subduction-related granitoids. However, new mapping, sampling and dating (e.g., Setiawan et al., 2013; Davies et al., 2014; Breitfeld et al., 2017; Hennig et al., 2017) and new reconstructions (Hall et al., 2009; Metcalfe, 2009) have cast doubt on previously accepted ideas.

Despite their name, the Schwaner Mountains form a relatively low area (**Figure 2A**), with elevations mainly between 100 and 500 m, although there are a few high peaks of 1000 to 2000 m. The mountains cover an area almost 600 km wide, from close to the western coast of Borneo to the interior of the island further east, and more than 200 km from south to north (**Figures 2A,B**). Large parts of the Schwaner Mountains are mapped only at a reconnaissance level and access via rivers and logging

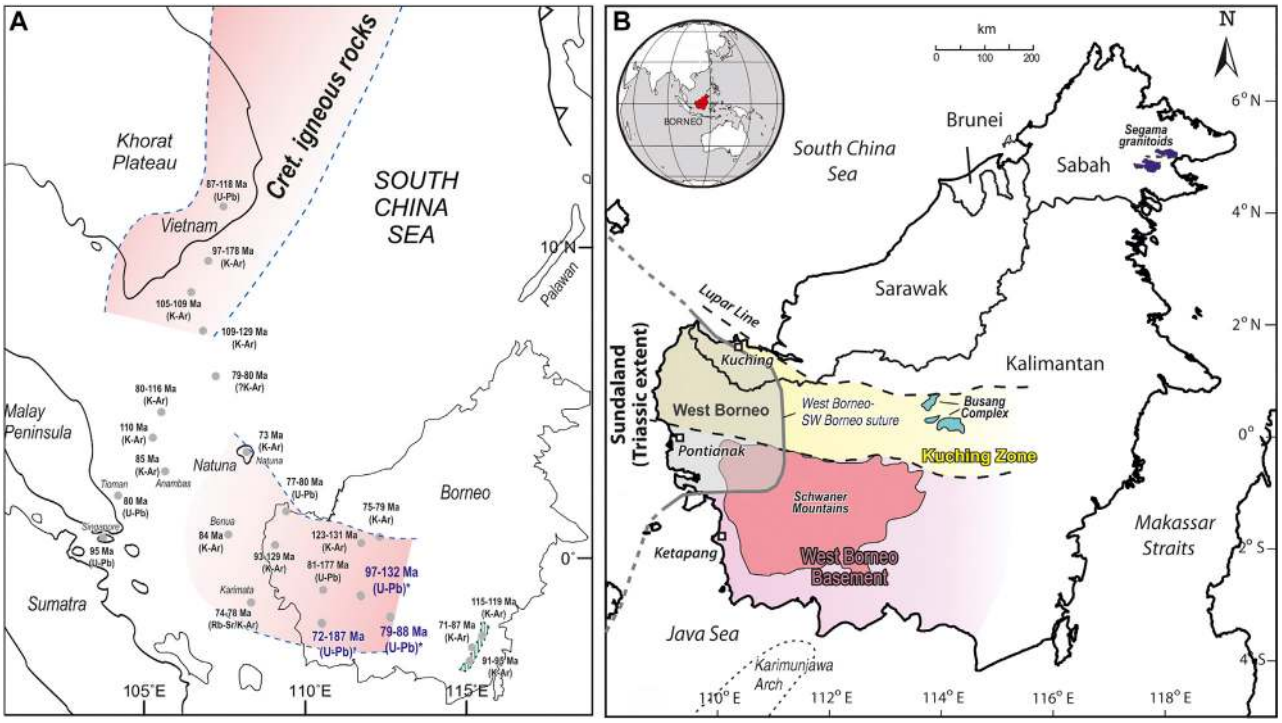

FIGURE 1 | (A) Cretaceous Paleo-Pacific subduction zone and spatial distribution of Cretaceous igneous rocks. Main belt with Lower to Upper Cretaceous granitoids extends from SE China and Taiwan in the north into SW Borneo in the south. A second smaller with predominantly Upper Cretaceous granites is located in central Borneo and extends to Natuna Island and the offshore South China Sea region. Locations marked in dark blue and with * are samples of this study. Literature data assembled from Haile (1970), Haile and Bignell (1971), Priem et al. (1975), Hamilton (1979), Hutchison (1989), Bladon et al. (1989), Areshev et al. (1992), Wu and Yang (1994), Rustandi et al. (1995), Nguyen et al. (2004), Searle et al. (2012), Hartono (2012), Shellnutt et al. (2013), Hennig et al. (2017), and Li et al. (2018). **(B)** Tectonic zones of western Borneo and location of the Schwaner Mountains (modified after Haile, 1974; Hennig et al., 2017). The West Borneo Basement correlates roughly to the SW Borneo Block of Hall (2017) and Hennig et al. (2017). The old West Borneo Basement term (Haile, 1974) should be replaced in the future by the term SW Borneo to avoid confusion.

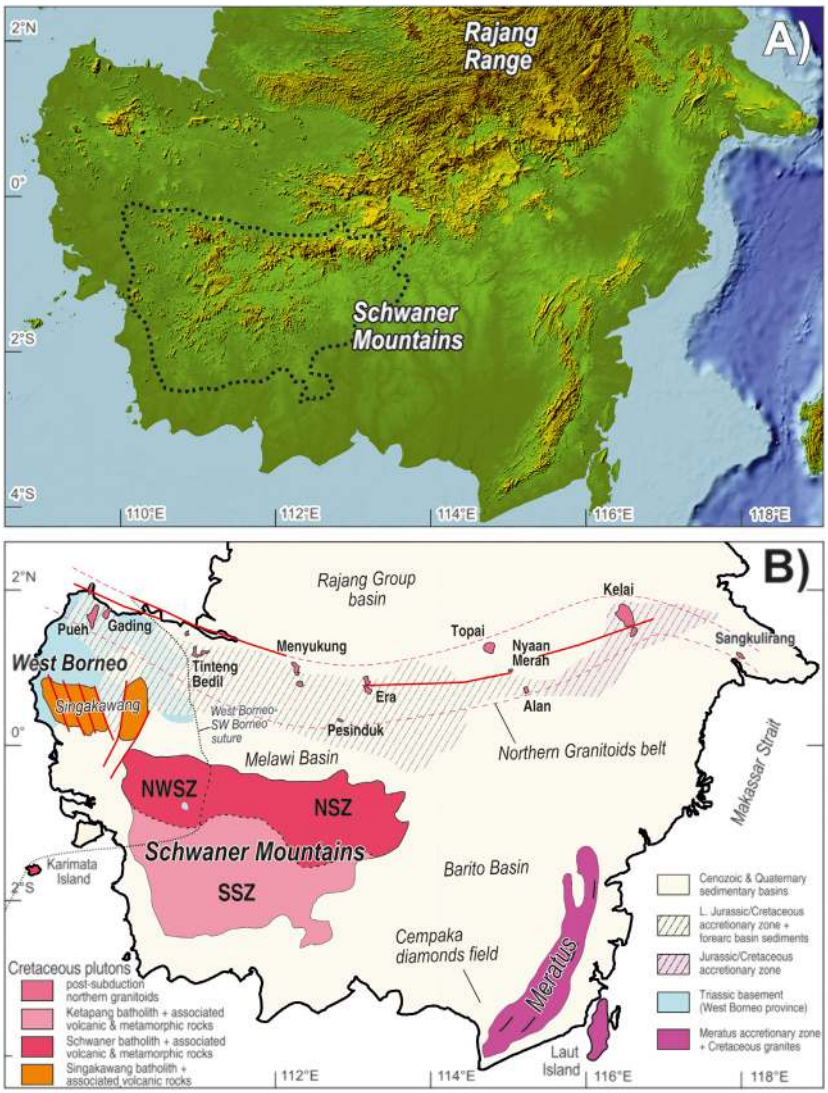

FIGURE 2 | (A) SRTM image showing location of the Schwaner Mountains. **(B)** Cretaceous granitoids and basement map of southern Borneo. NW Schwaner Zone (NWSZ) is part of the West Borneo province and has a Triassic and Jurassic basement intruded by Cretaceous granites. The North Schwaner Zone (NSZ) is dominated by the subduction-related Sepauk Tonalite. The South Schwaner Zone (SSZ) includes the Jurassic within-plate Belaban Granite and the post-subduction Cretaceous Sukadana Granite. The Upper Cretaceous Northern Granitoids belt follows the Lupar Line fault system. Southern boundary of West Borneo either is represented by the NWSZ or by an unidentified ENE-WSW striking line crossing the western part of the SSZ (modified from Hennig et al., 2017).

roads remains difficult, especially to the eastern parts of the region. We have carried out fieldwork and new sampling in the Schwaner Mountains, which, together with previous studies in NW Kalimantan and West Sarawak, provide the basis for new interpretations of the development of the southern part of the Paleo-Pacific margin. Here we present new U-Pb zircon geochronology, $^{40}Ar/^{39}Ar$ mica geochronology, whole-rock geochemistry, and garnet chemistry from these areas which elucidate the igneous history and tectonic evolution of this region. The evidence shows there was igneous activity within the Sundaland and Australian margins before the collision of SW Borneo with Sundaland, followed by subduction-related magmatism in the Schwaner Mountains, and further magmatism that occurred after subduction ceased.

REGIONAL BACKGROUND

Haile (1974) named the southern part of western Borneo, which included the Schwaner Mountains, the West Borneo Basement and this is bounded to the north by the Kuching Zone of NW Kalimantan and West Sarawak (**Figure 1B**). Granitoids in the Schwaner Mountains and associated volcanic rocks were known to range in age from Late Jurassic to Late Cretaceous based mainly on K-Ar geochronology (Haile et al., 1977; Williams et al., 1988;

Bladon et al., 1989). The Cretaceous igneous rocks in the northern Schwaner Mountains intruded metamorphic rocks of the Pinoh Metamorphic Group (PMG) which were generally interpreted as Palaeozoic basement (e.g., van Bemmelen, 1949; Haile, 1974). Metcalfe (1986) and Metcalfe (1990) introduced the term SW Borneo Block for this region and parts of the Kuching Zone, suggesting this was a pre-Mesozoic continental terrane or terranes, possibly of South China/Indochina origin (Metcalfe, 1996), added during the Mesozoic to a Sundaland continental core. Recent studies show that the Sundaland core can be identified in NW Kalimantan and West Sarawak where Triassic meta-granitoids in the NW Schwaner Mountains (Setiawan et al., 2013; Hennig et al., 2017) are interpreted to be part of the pre-Jurassic Sundaland margin and imply a West Borneo–SW Borneo suture in West Sarawak and NW Kalimantan. U-Pb dating has revealed abundant zircons with Early Cretaceous ages (Davies et al., 2014) in all the metamorphic rocks of the PMG casting doubt on the suggestion that the igneous and metamorphic rocks in the Schwaner Mountains were an ancient Borneo basement, whether a continental core or a pre-Mesozoic continental terrane.

Our interpretation (Breitfeld et al., 2017; Hall, 2017; Hennig et al., 2017) is that from the Late Triassic the Asian continent was broadly in its present position (**Figure 3A**) with Sundaland at its southern end. West Borneo (**Figure 2**) was the most southeastern part of Triassic Sundaland and includes the Northwest Schwaner Zone (NWSZ). Further east and south, the Schwaner Mountains are divided into two parts: the North Schwaner Zone (NSZ) and the South Schwaner Zone (SSZ) of the SW Borneo Block. The metamorphic rocks of the PMG are found mainly in the northeast part of the NSZ. Other metamorphic rocks are found near the southern margin of the SSZ.

From the Triassic onwards there was west-directed subduction beneath an Andean-type margin from South China to eastern Sundaland. Triassic arc-related sedimentary or volcanic rocks can be found in West Sarawak (e.g., Serian Volcanics, Sadong Formation, Jagoi Granodiorite), in NW Kalimantan (e.g., Balaisebut Group), and there are Triassic metamorphic and igneous rocks in the Embuoi Complex (Wilford and Kho, 1965; Williams et al., 1988; Rusmana et al., 1993; Supriatna et al., 1993). SW Borneo is interpreted as a block derived from the Gondwana margin of NW Australia (Hall et al., 2009; Metcalfe, 2009; Hall, 2012) which accreted to Sundaland in the Early Cretaceous. Hennig et al. (2017) suggested a suture between West Borneo and SW Borneo (**Figure 3B**) which can be traced through the NW Schwaner Mountains into West Sarawak based on the occurrence of Triassic basement rocks and Triassic sedimentary units in the West Borneo province. East of the suture, the Schwaner Mountains includes a substantial part of the SW Borneo Block and north of the SW Borneo Block is the Kuching Zone of Haile (1974) (**Figure 1B**). Within the Kuching Zone are remnants of the Cretaceous forearc basin of the Paleo-Pacific margin which include the turbiditic Pedawan and Selangkai Formations; and Jurassic to Cretaceous accretionary complexes (e.g., Sebangan and Sejingkat Formations, Lubok Antu

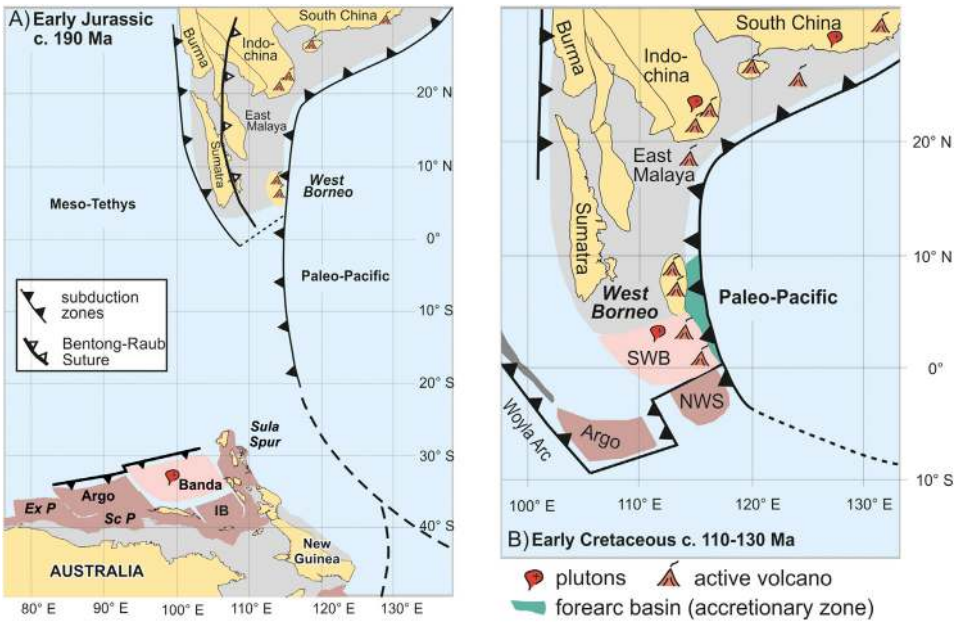

FIGURE 3 | Paleogeography maps (modified from Hall, 2012; Hennig et al., 2016; Hennig et al., 2017), showing **(A)** beginning of separation of the Banda (SW Borneo, SWB) and Argo blocks from NW Australia. Rifting began in the Triassic or Early Jurassic and the blocks finally separated in the Middle to Late Jurassic. The Paleo-Pacific subduction margin followed the eastern side of Sundaland and South China, and **(B)** accretion of SW Borneo to Sundaland before c. 135 Ma and continuation of subduction-related magmatism associated with the Paleo-Pacific in West Borneo and initiation of magmatism in SW Borneo that formed the Menunuk Volcanics, Sepauk Tonalite, and Pinoh Metamorphic Group between c. 130 to 110 Ma. Subduction ceased later with the collision of the Argo Block with SW Borneo around 90 Ma. NWS (Northwest Sulawesi-East Sabah) is the Inner Banda Block (IB). ExP—Exmouth Plateau, ScP—Scott Plateau. Forearc basin fill by the Pedawan and Selangkai Formations.

Melange, Boyan Melange) described by a number of authors (e.g., Tan, 1979; Williams et al., 1988; Pieters et al., 1993a; Hutchison, 2005; Breitfeld et al., 2017). These are overlain by terrestrial to marginal marine sediments of Late Cretaceous to Eocene age of the Kuching Supergroup (Heryanto and Jones, 1996; Hutchison, 2005; Breitfeld et al., 2018; Breitfeld and Hall, 2018) which postdate the docking of SW Borneo with Sundaland.

The Cretaceous igneous belt can be traced from SW Borneo along the western side of the South China Sea into Indochina and further north into SE China (e.g., Taylor and Hayes, 1983; Williams et al., 1988; Hutchison, 1996; Li, 2000; Zhou et al., 2008; Metcalfe, 2013; Shellnutt et al., 2013; Xu et al., 2016; **Figure 1A**), although this connection is uncertain since there is a gap between Vietnam and Borneo in the area of the submerged Sunda Shelf where thick Cenozoic sediments cover older basement rocks. Granitoids in SE Vietnam show U-Pb zircon crystallisation ages of 87 to 118 Ma (Nguyen et al., 2004; Shellnutt et al., 2013) and K-Ar age data from offshore SE Vietnam basement (Nam Con Son Basin, Cuu Long Basin) ranges from 97 to 178 Ma (Hutchison, 1989; Areshev et al., 1992; Wu and Yang, 1994). Cretaceous granitoids with K-Ar ages of c. 116 to 80 Ma have been dated from offshore wells east of the Thai-Malay Peninsula (Hutchison, 1989). Granitoids in the Anambas, Karimata, Tambelan (Benua) and Natuna Islands have K-Ar ages of 74 to 78 Ma (Priem et al., 1975), c. 84 Ma (Haile, 1970; Haile and Bignell, 1971) and c. 85 Ma (Hamilton, 1979). Offshore Natuna granitoids have K-Ar ages of 79–80 Ma (Wu and Yang, 1994; Li et al., 2018). Those all support the interpretation of a continuous igneous belt. There are also Cretaceous granitoids in Tioman Island, east of the Malay Peninsula, and Singapore with U-Pb zircon ages of c. 80 and 95 Ma (Searle et al., 2012). These could also be part of a granite belt between Vietnam and Borneo, but their position and restricted age range suggested they are more likely a western granite belt traceable between Singapore and Thailand related to east-directed Neo-Tethyan subduction below Sundaland (Searle et al., 2012).

In southern Borneo granitoids are the dominant lithology of the Schwaner Mountains, accompanied by other less abundant intrusive rocks, associated with metamorphic and volcanic rocks. We use the term Schwaner batholith for the whole area of granitoid rocks and refer to different bodies mapped separately as plutons. The stratigraphy and ages of igneous and metamorphic rocks of western Borneo are summarised in the following section. **Figure 4** shows the principal subdivisions of the region used in this study, based on Davies et al. (2014) and Hennig et al. (2017), although the precise boundaries between them are uncertain reflecting the size of the region, nature of terrain and quality of exposure.

IGNEOUS AND METAMORPHIC ROCKS OF SW BORNEO

Below we summarise the principal features, including dating, of the igneous rocks of SW Borneo based on work carried out before this study.

Granitoids of the North Schwaner Zone: Sepauk Tonalite

The Sepauk Tonalite is the largest pluton in the Schwaner batholith and occupies the major part of the NWSZ, NSZ and possibly some parts of the SSZ (**Figures 2B**, **4**). K-Ar ages range from 103 to 123 Ma (Haile et al., 1977; Williams et al., 1988; Bladon et al., 1989; Amiruddin and Trail, 1993; **Table 1**). Dominant rock types are tonalite and granodiorite with minor syenogranite, monzogranite, diorite, gabbro and monzonite with an I-type signature and a subduction-related origin (Williams et al., 1988; Pieters and Sanyoto, 1993). Williams et al. (1988) suggested, based on composition and age, that at least two different plutons are present in the northern Schwaner Mountains and a second body, the Laur Granite, was later mapped by Pieters and Sanyoto (1993) and Amiruddin and Trail (1993) in the NWSZ, but no new mapping in the NSZ has been conducted and the extent of the Laur Granite in the NSZ or occurrence of other granitoid bodies remain uncertain.

Granitoids of the Northwest Schwaner Zone: West Borneo

The NWSZ (**Figures 2B**, **4**) as part of the early Mesozoic Sundaland is characterised by the occurrence of Triassic and Jurassic metagranitoids (Setiawan et al., 2013; Hennig et al., 2017) and extensive areas of Cretaceous igneous rocks that intrude them, mapped as the Sepauk Tonalite, the Laur Granite, and possibly the Sukadana Granite (Pieters and Sanyoto, 1993). As in the NSZ, the Sepauk Tonalite is the largest body in the NWSZ. K-Ar ages for the Sepauk Tonalite in the NWSZ range from c. 107 to 128 Ma (Haile et al., 1977; Bladon et al., 1989; **Table 1**).

The Laur Granite was reported to be an equivalent of the Sepauk Tonalite (Supriatna et al., 1993). The main rock type is monzogranite accompanied by syenogranite, granodiorite, tonalite, quartz diorite and diorite (Pieters and Sanyoto, 1993; Supriatna et al., 1993). As parts of the Laur Granite suite are petrographically similar to rocks of the Sepauk Tonalite and Sukadana Granite of the SSZ (De Keyser and Rustandi, 1993) it remains difficult to clearly identify it in the field. No detailed geochemical study has been carried out on the Laur Granite and its spatial extent is unknown. There are also no age data available, but a granitoid dated by the K-Ar method with an age of 103 ± 1 Ma from the Ketapang area of the SSZ (De Keyser and Rustandi, 1993; **Table 1**) is suspected to represent the Laur Granite (Supriatna et al., 1993). Within the NWSZ, Haile et al. (1977) and Bladon et al. (1989) reported K-Ar ages from granitoids that range from c. 91 to 103 Ma (**Table 1**) which might also represent the Laur Granite. It was interpreted as a subduction-related intrusion and possibly a partly contemporaneous and co-genetic equivalent of the Sepauk Tonalite (Amiruddin and Trail, 1993; Pieters and Sanyoto, 1993).

In the southern part of the NWSZ Haile et al. (1977), Williams et al. (1988), Bladon et al. (1989) also reported granitoids with K-Ar ages of 77–87 Ma which might represent the Sukadana Granite of the SSZ (**Table 1**). U-Pb zircon ages presented by

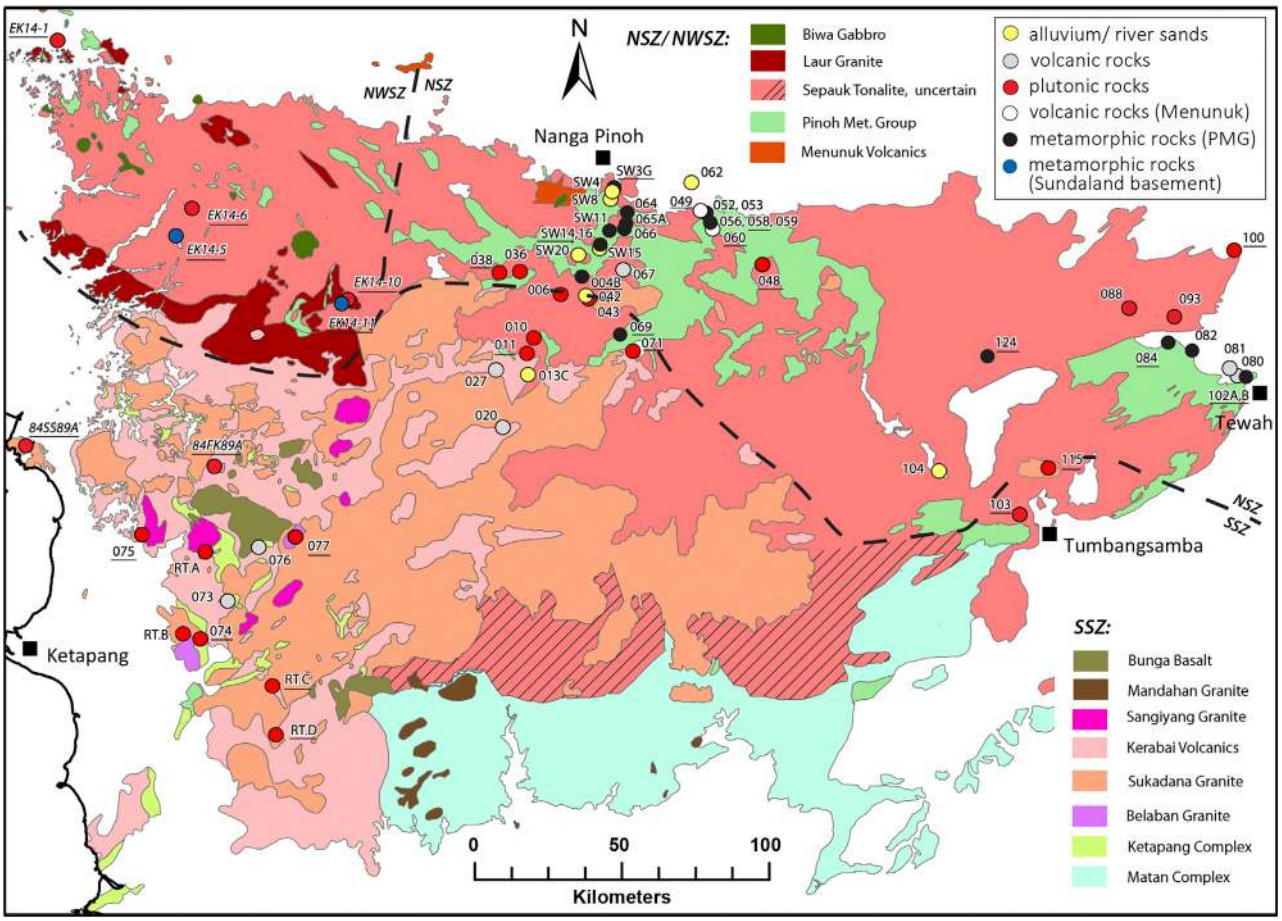

FIGURE 4 | Geological map of the Schwaner Mountains with sample locations, modified after Borneo maps of Pieters and Supriatna (1990) and Tate (2001). Underlined samples are dated with zircon U-Pb geochronology. Italic labelled samples are literature data (Ketapang area: De Keyser and Rustandi, 1993; NWSZ: Hennig et al., 2017). Dashed lines indicate approximate boundaries of the NWSZ, NSZ and SSZ. The extent of plutons is inferred from geological maps. The distribution of the Sepauk Tonalite is possibly overestimated in the SSZ.

Hennig et al. (2017) confirm separate magmatic phases at 118 ± 1.1 Ma, 101.5 ± 0.6 Ma, and 81.1 ± 1.1 Ma in the NWSZ.

The Biwa Gabbro (**Figure 4**) of Pieters and Sanyoto (1993) intrudes the Sepauk Tonalite in the NWSZ and is dated by the K-Ar method from hornblende as 88 ± 3.6 Ma (Bladon et al., 1989; **Table 1**).

Granitoids of the South Schwaner Zone: Belaban Granite, Sukadana Granite, Sangiyang Granite

Haile et al. (1977) and Bladon et al. (1989) reported an age of c. 157 Ma for an S-type monzodiorite-monzonite, since named the Belaban Granite (**Figure 4**; **Table 1**), found so far only in one outcrop at Bukit Belabantujuh (De Keyser and Rustandi, 1993).

The SSZ is dominated by the Sukadana Granite (**Figure 4**) which forms a large pluton dominated by potassic granites also named the Ketapang batholith (Williams et al., 1988; De Keyser and Rustandi, 1993; Hartono, 2012). There is a wide range of compositions from alkali to syenogranite with rare diorite and gabbro. U-Pb zircon ages reported by De Keyser and Rustandi (1993) and van Hattum et al. (2013) range from c. 80 to 85 Ma (**Table 1**). K-Ar and Rb-Sr geochronology yielded similar ages with a slightly wider range for K-Ar ages (Haile et al., 1977; Bladon et al., 1989; De Keyser and Rustandi, 1993; **Table 1**). The Sukadana Granite was interpreted as a post-collisional intrusion based on geochemistry (De Keyser and Rustandi, 1993).

The Sangiyang Granite (**Figure 4**) forms a fine-grained small alkali granite pluton that intrudes the Sukadana Granite at Bukit Sangiyang and has been mapped more widely in the SSZ based on remote sensing (De Keyser and Rustandi, 1993). No age or chemical data are available, but a Late Cretaceous age was assumed based on the intrusive contact with the Sukadana Granite (De Keyser and Rustandi, 1993).

A number of isolated small plutons in the southern SSZ were mapped as Mandahan Granite (Hermanto et al., 1994). No age or geochemical data are available, but it was interpreted to be Late

TABLE 1 | Literature age data of Jurassic to Cretaceous rocks of the Schwaner Mountains and western Borneo. Phases marked with * are here reinterpreted based on their ages compared to their original interpretation.

Sample	Location	Phase	Rock type	Method	Mineral	Age (Ma)	Error 1SD (Ma)	Reference
NSZ								
83BA62A	NSZ	Sepauk	qz diorite	K-Ar	Biotite	110	1	Bladon et al. (1989), Amiruddin and Trail (1993)
83BA70A	NSZ	Sepauk	Granodiorite	K-Ar	Biotite	110	1	Bladon et al. (1989), Amiruddin and Trail (1993)
83CP115A	NSZ	Sepauk	Monzodiorite	K-Ar	Biotite	111	1	Bladon et al. (1989), Amiruddin and Trail (1993)
83CP115A	NSZ	Sepauk	Monzodiorite	K-Ar	hbl	118	1	Williams et al. (1988), Bladon et al. (1989), Amiruddin and Trail (1993)
83CP115C	NSZ	Sepauk	qz diorite/tonalite	K-Ar	Biotite	109	1	Bladon et al. (1989), Amiruddin and Trail (1993)
83CP115C	NSZ	Sepauk	qz diorite/tonalite	K-Ar	hbl	116	1	Bladon et al. (1989), Amiruddin and Trail (1993)
83CP116B	NSZ	Sepauk	Tonalite	K-Ar	Biotite	110	1	Bladon et al. (1989), Amiruddin and Trail (1993)
83CP116B	NSZ	Sepauk	Tonalite	K-Ar	hbl	123	1	Williams et al. (1988), Bladon et al. (1989), Amiruddin and Trail (1993)
83CP122A	NSZ	Sepauk	Tonalite	K-Ar	Biotite	107	1	Williams et al. (1988), Bladon et al. (1989), Amiruddin and Trail (1993)
83CP125A	NSZ	Sepauk	Tonalite	K-Ar	hbl	112	2	Williams et al. (1988), Bladon et al. (1989), Amiruddin and Trail (1993)
83HZ34C	NSZ	Sepauk	Tonalite	K-Ar	Biotite	110	1	Bladon et al. (1989), Amiruddin and Trail (1993)
83HZ36A	NSZ	Sepauk	Granodiorite	K-Ar	Biotite	112	1	Bladon et al. (1989), Amiruddin and Trail (1993)
83HZ39A	NSZ	Sepauk	Granodiorite	K-Ar	Biotite	110	1	Bladon et al. (1989), Amiruddin and Trail (1993)
84DT08B	NSZ	Sepauk	Tonalite	K-Ar	Biotite	122	1	Bladon et al. (1989), Amiruddin and Trail (1993)
84DT08B	NSZ	Sepauk	Tonalite	K-Ar	hbl	114	1	Bladon et al. (1989), Amiruddin and Trail (1993)
RI116	NSZ	?Sepauk	Tonalite	K-Ar	Whole rock	130	5	JICA (1979) (in Bladon et al., 1989)
RI113	NSZ	Laur*	Granodiorite	K-Ar	Whole rock	100	5	JICA (1979) (in Bladon et al., 1989)
84DT03D	NSZ	Sepauk-Laur*	Granodiorite	K-Ar	hbl	105	1	Williams et al. (1988), Bladon et al. (1989), Amiruddin and Trail (1993)
84UM48A	NSZ	Sepauk-Laur*	Tonalite	K-Ar	hbl	104	1	Williams et al. (1988), Bladon et al. (1989), Amiruddin and Trail (1993)
FM8988	NSZ	Menunuk	Altered porphyritic basic lava	K-Ar	Whole rock	81.5	2.8	Mouret (in Bladon et al., 1989)
FM8989	NSZ	PMG	Biotite hornfels	K-Ar	Whole rock	189	2	Mouret (in Bladon et al., 1989)
NWSZ								
EK14-6	NWSZ	Sepauk-Laur	Tonalite	U-Pb	Zircon	101.5	0.6	Hennig et al. (2017)
EK14-10	NWSZ	Sukadana*	Diorite	U-Pb	Zircon	81.1	1.1	Hennig et al. (2017)
EK14-1	NWSZ	Sepauk	Granite	U-Pb	Zircon	118.6	1.1	Hennig et al. (2017)
EK14-11	NWSZ	Jurassic pluton	meta-Granodiorite	U-Pb	Zircon	149.8+	4.4	Hennig et al. (2017)
K30	NWSZ	Sepauk	Tonalite	K-Ar	Biotite	114.1	2.6	Haile et al. (1977), recalculated by Bladon et al. (1989)
K30	NWSZ	Sepauk	Tonalite	K-Ar	hbl	113.7	4.5	Haile et al. (1977), recalculated by Bladon et al. (1989)
K32	NWSZ	Sepauk	Monzogranite	K-Ar	Biotite	115.5	2.6	Haile et al. (1977), recalculated by Bladon et al. (1989)
K32	NWSZ	Sepauk	Monzogranite	K-Ar	hbl	118.3	2.6	Haile et al. (1977), recalculated by Bladon et al. (1989)
K34	NWSZ	Sepauk	Granite	K-Ar	Biotite	115.6	1.5	Haile et al. (1977), recalculated by Bladon et al. (1989)
K34	NWSZ	Sepauk	Granite	K-Ar	hbl	116.8	3	Haile et al. (1977), recalculated by Bladon et al. (1989)
K35	NWSZ	Sepauk	Tonalite	K-Ar	Biotite	107.3	2.4	Haile et al. (1977), recalculated by Bladon et al. (1989)
85PR022A	NWSZ	Sepauk	bt-hbl granodiorite	K-Ar	Biotite	119	1	Bladon et al. (1989), Pieters and Sanyoto (1993)
85PR022A	NWSZ	Sepauk	bt-hbl granodiorite	K-Ar	hbl	128	1	Bladon et al. (1989), Pieters and Sanyoto (1993)
K75	NWSZ	Sepauk-Laur*	Tonalite	K-Ar	Biotite	103.1	2.2	Haile et al. (1977), recalculated by Bladon et al. (1989)
84PP044A	NWSZ	Laur*	Granodiorite	K-Ar	hbl	99.5	0.6	Bladon et al. (1989), Pieters and Sanyoto (1993)
K52	NWSZ	Laur*	Tonalite	K-Ar	hbl	97.7	3	Haile et al. (1977), recalculated by Bladon et al. (1989)
K52	NWSZ	?Rantau Asem*	Tonalite	K-Ar	Biotite	91.2	1.3	Haile et al. (1977), recalculated by Bladon et al. (1989)
K76	NWSZ	Sukadana*	Granodiorite	K-Ar	Biotite	77.4	1.7	Haile et al. (1977), recalculated by Bladon et al. (1989)
K76	NWSZ	Sukadana*	Granodiorite	K-Ar	Hbl	78.3	3.2	Haile et al. (1977), recalculated by Bladon et al. (1989)
84PP043A	NWSZ	Sukadana*	Diorite	K-Ar	Hbl	87	0.8	Williams et al. (1988), Bladon et al. (1989), Pieters and Sanyoto (1993)
K74	NWSZ	Biwa Gabbro	Gabbro	K-Ar	Hbl	88	3.6	Haile et al. (1977), recalculated by Bladon et al. (1989)
SSZ								
RT.C	SSZ	Sukadana	qz monzonite	U-Pb	Zircon	84.7	1.3	van Hattum et al. (2013)
RT.D	SSZ	Sukadana	qz monzonite	U-Pb	Zircon	81.7	1	van Hattum et al. (2013)
84FK89A	SSZ	Sukadana	qz monzonite	U-Pb	Zircon	80.8	0.7	Bladon et al. (1989), de Keyser and Rustandi (1993)
84SS89A	SSZ	Sukadana	Monzogranite	U-Pb	Zircon	84	1	Bladon et al. (1989), de Keyser and Rustandi (1993)

(Continued on following page)

TABLE 1 | (*Continued*) Literature age data of Jurassic to Cretaceous rocks of the Schwaner Mountains and western Borneo. Phases marked with * are here reinterpreted based on their ages compared to their original interpretation.

Sample	Location	Phase	Rock type	Method	Mineral	Age (Ma)	Error 1SD (Ma)	Reference
K43	SSZ	Belaban	Granite	K-Ar	Biotite	157.2	3.5	Haile et al. (1977), recalculated by Bladon et al. (1989)
K22	SSZ	?Mentembah*	Granite	K-Ar	Hbl	130.2	2.8	Haile et al. (1977), recalculated by Bladon et al. (1989)
84ER180C	SSZ	Laur*	qz monzodiorite	K-Ar	Hbl	103	1	Bladon et al. (1989), de Keyser and Rustandi (1993)
84DT262A	SSZ	Laur*	Tonalite	K-Ar	Hbl	104	1	Bladon et al. (1989), Amiruddin and Trail (1993)
84DT263A	SSZ	Laur*	Tonalite	K-Ar	Hbl	105	1	Bladon et al. (1989), Amiruddin and Trail (1993)
84ER234C	SSZ	Sukadana	hyp-aug-bt-qz monzonite	K-Ar	Biotite	86.3	0.5	Williams et al. (1988), Bladon et al. (1989), de Keyser and Rustandi (1993)
84FK101B	SSZ	Sukadana	Leucocratic bt monzogranite	K-Ar	Biotite	88.6	0.8	Williams et al. (1988), Bladon et al. (1989), de Keyser and Rustandi (1993)
84FK142B	SSZ	?Sukadana	Syenogranite	K-Ar	Biotite	91.4	0.6	Williams et al. (1988), Bladon et al. (1989), de Keyser and Rustandi (1993)
84FK89A	SSZ	Sukadana	qz monzonite	Rb-Sr	Bt, whole rock	81.4	NA	Bladon et al. (1989), de Keyser and Rustandi (1993)
84FK89C	SSZ	Sukadana	qz monzonite	Rb-Sr	Bt, whole rock	83.1	NA	Bladon et al. (1989), de Keyser and Rustandi (1993)
K14B	SSZ	Sukadana	Granodiorite	K-Ar	Biotite	85.4	1.9	Haile et al. (1977), recalculated by Bladon et al. (1989)
K1	SSZ	Sukadana	Monzogranite	K-Ar	Biotite	88.4	2	Haile et al. (1977), recalculated by Bladon et al. (1989)
K15	SSZ	Sukadana	Granite	K-Ar	Biotite	82.1	2	Haile et al. (1977), recalculated by Bladon et al. (1989)
K15	SSZ	Sukadana	Granite	K-Ar	hbl	81.1	4.8	Haile et al. (1977), recalculated by Bladon et al. (1989)
K16	SSZ	Sukadana	Granite	K-Ar	Biotite	81.5	1.2	Haile et al. (1977), recalculated by Bladon et al. (1989)
K16	SSZ	Sukadana	Granite	K-Ar	hbl	80.7	3.3	Haile et al. (1977), recalculated by Bladon et al. (1989)
K17	SSZ	Sukadana	Monzogranite	K-Ar	Biotite	83.2	2	Haile et al. (1977), recalculated by Bladon et al. (1989)
K19	SSZ	Sukadana	Granite	K-Ar	Biotite	83.1	2	Haile et al. (1977), recalculated by Bladon et al. (1989)
84DT160B	SSZ	Dyke - Kerabai	Trachyandesite	K-Ar	Whole rock	68.5	0.5	Bladon et al. (1989), de Keyser and Rustandi (1993)
84FK159A	SSZ	Dyke - Kerabai	hbl-basalt/andesite	K-Ar	Hbl	74.8	0.7	Bladon et al. (1989), de Keyser and Rustandi (1993)
84PP162B	SSZ	Dyke - Kerabai	Dolerite	K-Ar	Pyroxene	65.6	1.1	Bladon et al. (1989), de Keyser and Rustandi (1993)
Upper Cretaceous Northern Granitoids								
TB76	Northern belt	Pueh	Granite	U-Pb	Zircon	78.6	3	Hennig et al. (2017)
TB71a	Northern belt	Gading	Two-mica granite	U-Pb	Zircon	79.7	1	Hennig et al. (2017)
S7984	Northern belt	Pueh	quartz monzonite	K-Ar	Biotite	75.6	4	Kirk (1968)
S9677	Northern belt	Gading	quartz monzonite	K-Ar	Biotite	77	4	Kirk (1968)
S7285	Northern belt	Gading	Granodiorite	K-Ar	Biotite	78	5	Kirk (1968)
S6299	Northern belt	Tinteng Bedil	quartz monzonite	K-Ar	Biotite	79	5	Kirk (1968)
S1900	Northern belt	Sebuyau	Granodiorite	K-Ar	Biotite	101	5	Kirk (1968)
85PR078B	Northern belt	Era	Granodiorite	K-Ar	hbl	74.9	2	Williams et al. (1988), Bladon et al. (1989), Pieters et al. (1993c)
85UM012A	Northern belt	Era	Biotite granite	K-Ar	Biotite	78.2	0.6	Williams et al. (1988), Bladon et al. (1989), Pieters et al. (1993c)
85SR064C	Northern belt	Era	Granodiorite	K-Ar	Biotite	78.6	0.8	Williams et al. (1988), Bladon et al. (1989), Pieters et al. (1993c)
85RS160A	Northern belt	Pueh	Monzogranite	K-Ar	Biotite	80.6	0.6	Williams et al. (1988), Bladon et al. (1989), Rusmana et al. (1993)
86DT6C	Northern belt	Topai	Granite	K-Ar	Biotite	75.9	0.9	Bladon et al. (1989)
86PP118B	Northern belt	Topai	Granodiorite	K-Ar	Biotite	76	0.04	Bladon et al. (1989)
86PP118A	Northern belt	Topai	Granodiorite	K-Ar	Biotite	77.5	0.3	Bladon et al. (1989)
86AM071A	?Northern belt	Alan	Diorite	K-Ar	hbl	131	1.6	Bladon et al. (1989), Pieters et al. (1993a)
86PP008D	?Northern belt	Alan	Granite	K-Ar	hbl	123	1	Bladon et al. (1989), Pieters et al. (1993a)
86PP009A	?Northern belt	Alan	Diorite	K-Ar	hbl	126	1	Bladon et al. (1989), Pieters et al. (1993a)
85DT066C	?Northern belt	Menyukung	Granite	K-Ar	Biotite	125	1	Bladon et al. (1989), Pieters et al. (1993b)
West Borneo—NW Kalimantan								
80RD45	NW Kalimantan	Mensibau	Granodiorite	K-Ar	Whole rock	111	6	JICA (1982) (in Bladon et al., 1989)
80RE52	NW Kalimantan	Mensibau	Granodiorite	K-Ar	Whole rock	107	5	JICA (1982) (in Bladon et al., 1989)
81RX53	NW Kalimantan	Mensibau	Granodiorite	K-Ar	Whole rock	124	8	JICA (1982) (in Bladon et al., 1989)
85SR214A	NW Kalimantan	Mensibau	Granodiorite	K-Ar	hbl	128	1	Bladon et al. (1989), Supriatna et al. (1993)
85SS067A	NW Kalimantan	Mensibau	Granodiorite	K-Ar	hbl	120	1	Bladon et al. (1989), Supriatna et al. (1993)
85SS167A	NW Kalimantan	Mensibau	qz diorite	K-Ar	hbl	116	2	Bladon et al. (1989), Supriatna et al. (1993)
85ER79A	West Borneo	Mensibau	Biotite granite	K-Ar	Biotite	125	1	Bladon et al. (1989), Suwarna et al. (1993)

(Continued on following page)

TABLE 1 | (*Continued*) Literature age data of Jurassic to Cretaceous rocks of the Schwaner Mountains and western Borneo. Phases marked with * are here reinterpreted based on their ages compared to their original interpretation.

Sample	Location	Phase	Rock type	Method	Mineral	Age (Ma)	Error 1SD (Ma)	Reference
85ER81A	West Borneo	Mensibau	Granodiorite	K-Ar	hbl	121	1	Bladon et al. (1989), Suwarna et al. (1993)
85ER103A	West Borneo	Mensibau	Adamellite	K-Ar	Hbl	92.8	0.9	Bladon et al. (1989), Suwarna et al. (1993)
85ER110A	West Borneo	Mensibau	Diorite	K-Ar	Hbl	129	1	Bladon et al. (1989), Suwarna et al. (1993)
85ER135A	West Borneo	Mensibau	Biotite granite	K-Ar	hbl	121	2	Bladon et al. (1989), Suwarna et al. (1993)
85ER160A	West Borneo	Mensibau	Granodiorite	K-Ar	Biotite	125	1	Bladon et al. (1989), Suwarna et al. (1993)
85NS182A	West Borneo	Mensibau	Granite	K-Ar	hbl	119	2	Bladon et al. (1989), Suwarna et al. (1993)
85PW161A	West Borneo	Mensibau	Granodiorite	K-Ar	hbl	60.1	0.7	Bladon et al. (1989), Suwarna et al. (1993)
85SS85A	West Borneo	Mensibau	Granodiorite	K-Ar	Biotite	118	1	Bladon et al. (1989), Suwarna et al. (1993)
85YN233A	West Borneo	Mensibau	Granite	K-Ar	Biotite	120	1	Bladon et al. (1989), Suwarna et al. (1993)
85YN234B	West Borneo	Mensibau	Granite	K-Ar	Biotite	121	1	Bladon et al. (1989), Suwarna et al. (1993)
79RE-50	West Borneo	Mensibau	Diorite	K-Ar	hbl	98.6	4.9	JICA (1982) (in Suwarna et al., 1993)
79RP-19	West Borneo	Mensibau	Granodiorite	K-Ar	hbl	103.7	5.2	JICA (1982) (in Suwarna et al., 1993)
80RC-64	West Borneo	Mensibau	Granodiorite	K-Ar	Whole rock	114	6	JICA (1982) (in Suwarna et al., 1993)
80RD-67	West Borneo	Mensibau	Diorite	K-Ar	Whole rock	95.1	4.8	JICA (1982) (in Suwarna et al., 1993)
85YN260B	West Borneo	Raya	hbl-bearing extrusive	K-Ar	hbl	106	1	Bladon et al. (1989), Suwarna et al. (1993)
Meratus								
82PW106	Meratus	Batang Alai	Microgabbro xenolith	K-Ar	hbl	119	1	Bladon et al. (1989)
82PW107	Meratus	Batang Alai	Granodiorite	K-Ar	hbl	115	1	Bladon et al. (1989)
82PW113	Meratus	?Batang Alai	Rhyodacite	K-Ar	hbl	105	1	Bladon et al. (1989)
NA	Meratus	Batang Alai	Tonalite	K-Ar	hbl	118.6	1.5	Hartono (2012)
NA	Meratus	Batang Alai	Tonalite	K-Ar	Biotite	101	2.6	Hartono (2012)
NA	Meratus	Hajawa	Gabbro, diorite, tonalite	K-Ar	?	71-87	NA	Hartono (2012)
NS352	Meratus	Kintap	Granite	K-Ar	Whole rock	95.3	NA	Sikumbang (1986) (in Bladon et al., 1989)
NA	Meratus	?Kintap	Diorite	K-Ar	?	91	NA	Rustandi et al. (1995)
NS834	Meratus	Bennarian	basaltic andesite	K-Ar	Whole rock	85.6	NA	Sikumbang (1986) (in Bladon et al., 1989)

Cretaceous (Hermanto et al., 1994) and could be an equivalent of the Sangiyang Granite.

Granitoids Northwest of the Schwaner Mountains: Singakawang Batholith

Northwest of the Schwaner Mountains (**Figure 2B**) is the Mensibau Granodiorite (Suwarna et al., 1993) also known as Singakawang batholith (Amiruddin, 1989; Hartono, 2012). Based on geochemistry it was interpreted as an I-type subduction-related granitoid that may be a continuation of the Sepauk Tonalite (Suwarna et al., 1993). Most K-Ar ages range from 116 to 129 Ma, but there are also some ages of 93–100 Ma (JICA, 1982; Supriatna et al., 1993; Suwarna et al., 1993; **Table 1**) suggesting at least two different magmatic episodes. The Setinjam Gabbro (Suwarna et al., 1993) intrudes the Mensibau Granodiorite and is interpreted as a possible equivalent of the Biwa Gabbro of the NWSZ.

Upper Cretaceous Northern Granitoids

Upper Cretaceous granites are present as small isolated plutons in a belt north of the Schwaner Mountains from West Sarawak, in the Kuching Zone and close to the Lupar Line, to central Kalimantan (**Figure 2B**). They include the Pueh, Gading and Tinteng Bedil granites of West Sarawak, and the Pesinduk Granodiorite, the Era and Topai granites of central Kalimantan (**Figure 2B**). This belt has been named the Northern Belt of granite plutons (Williams et al., 1988) and the Sambas-Mangkaliat Isolated Granite Belt (Hartono, 2012). The plutons include granites, granodiorites, tonalites and diorites usually with I- and S-type signatures and volcanic arc granite (VAG) to within plate granite (WPG) character (Hennig et al., 2017). Kirk (1968) interpreted a post-collision emplacement. Hartono (2012) included the Nyaan Merah, Kelai, and Sangkulirang granites in this belt, but there are no age or geochemical data from them. Hennig et al. (2017) reported U-Pb zircon ages of 78.6 ± 3 to 79.7 ± 1 Ma for the Pueh and Gading plutons. K-Ar ages of Kirk (1968), Bladon et al. (1989) and Pieters et al. (1993c) for the other granitoids are similar and indicate intrusion after c. 90–85 Ma. **Table 1** summarises the age data for the Upper Cretaceous post-collision plutons.

Two relatively small granitoid plutons in this belt include the Menyukung and Alan Granite (**Figure 2B**) which are slightly older than the Sepauk Tonalite and significantly older than other plutons in the northern belt; K-Ar ages range from 123 ± 1 to 131 ± 1.6 Ma (Pieters et al., 1993a, Pieters et al., 1993b; **Table 1**). Hartono (2012) grouped them with post-subduction granitoids of this belt.

Volcanic Rocks

Volcanic rocks occur throughout the Schwaner Mountains and were assigned mainly to the Menunuk and Kerabai Volcanics (**Figure 4**). Northwest of the Schwaner Mountains the Raya Volcanics form the extrusive equivalent of the Mensibau Granodiorite. Age data from the rocks is very limited and the volcanics are only tentatively assigned to these units.

Menunuk Volcanics (?Early Cretaceous)—North Schwaner Zone

The Menunuk Volcanics comprise felsic lithic tuff, volcaniclastic siltstone and mudstone, quartzite and turbiditic volcaniclastics and are exposed in the northern part of the Schwaner Mountains (Amiruddin and Trail, 1993) (**Figure 4**). They were interpreted as the downfaulted volcanic cover of the Sepauk Tonalite with a possible Early Cretaceous age (Amiruddin and Trail, 1993). Bladon et al. (1989) reported a whole-rock K-Ar age of 81.5 ± 2.8 Ma from an altered sample (**Table 1**), interpreted as age of metamorphism.

Kerabai Volcanics (Latest Cretaceous)—South Schwaner Zone

The Kerabai Volcanics (**Figure 4**) consist predominantly of mafic volcanics and pyroclastics with some rhyolites and are exposed in the western and central part of the Schwaner Mountains (Amiruddin and Trail, 1993; De Keyser and Rustandi, 1993; Pieters and Sanyoto, 1993). They were interpreted as co-magmatic volcanic equivalents of the Sukadana Granite based on geochemistry and stratigraphy (De Keyser and Rustandi, 1993). K-Ar dating (whole rock, hornblende, pyroxene) of dykes yielded latest Cretaceous ages (c. 66 to 75 Ma, **Table 1**), and they were interpreted as part of the Kerabai Volcanics (De Keyser and Rustandi, 1993; Pieters and Sanyoto, 1993).

Bunga Basalt (Latest Cretaceous)—South Schwaner Zone

The Bunga Basalt is a mafic volcanic unit at Bunga Hill in the SSZ that lies above the Kerabai Volcanics, Sukadana Granite and the Sangiyang Granite (De Keyser and Rustandi, 1993) (**Figure 4**). No age data are available but De Keyser and Rustandi (1993) suggested it is partly contemporaneous with the Sangiyang Granite based on stratigraphic relations.

Raya Volcanics (Early Cretaceous)—Northwest of the Schwaner Mountains

The Raya Volcanics outcrop NW of the Schwaner Mountains in the area of the Mensibau Granodiorite (**Figure 2B**) where they are interpreted to form its volcanic cover (Suwarna et al., 1993) and the contemporaneous volcanic equivalent of the Sepauk Tonalite and Laur Granite (Supriatna et al., 1993). They include predominantly basic volcanics with some intercalated sandstones, conglomerates and mudstones (Suwarna et al., 1993). There is a single K-Ar hornblende age of 106 ± 1 Ma from a dacite (Suwarna et al., 1993, **Table 1**).

Metamorphic Rocks

Pinoh Metamorphic Group

The PMG (**Figure 4**) consists of thermally and regionally metamorphosed muscovite-quartz schists, quartzites, phyllites, slates, calc-silicates, gneisses and meta-tuffs that are found predominantly in the NSZ, but also within the NWSZ and SSZ (Amiruddin and Trail, 1993; De Keyser and Rustandi, 1993; Pieters and Sanyoto, 1993). The metamorphic rocks were originally interpreted as Permo-Carboniferous basement of

SW Borneo (e.g., van Bemmelen, 1949) and Paleozoic to Triassic (e.g., Amiruddin and Trail, 1993), although they were undated. A single whole rock K-Ar age of 189 ± 2 Ma from a biotite hornfels by Mouret was reported in Bladon et al. (1989). The sample was poorly located and although identified as PMG, it appears to be from an area mapped as Cretaceous Sepauk Tonalite. More recent U-Pb ages from zircons (Davies et al., 2014) from the PMG indicate an Early Cretaceous age similar to the granitoids and associated volcanic rocks as discussed below.

Ketapang Complex

The Ketapang Complex (**Figure 4**) comprises thermally metamorphosed and hydrothermally altered pelitic and psammitic rocks including siltstones, sandstones, shales, calc-silicate rocks, slates, and tuffaceous lithic arenites in the western part of the SSZ (De Keyser and Rustandi, 1993). Van Bemmelen (1939) and van Emmichoven (1939) considered that the Ketapang Complex included rocks of possible Permo-Carboniferous, Late Triassic and Cenozoic age, without providing evidence. Limited palynology analyses (Haile, 1973; De Keyser and Rustandi, 1993) yielded Albian to Cenomanian ages and one sample was rich in possible Jurassic sponges.

Matan Complex

Like the Ketapang Complex, the Matan Complex (**Figure 4**) in the southeastern part of the SSZ was also assumed to include Permo-Carboniferous, and Late Triassic to Cenozoic rocks (van Bemmelen, 1939; van Emmichoven, 1939). These are predominantly volcanic and meta-volcanic, and De Keyser and Rustandi (1993) suggested the term Matan Complex should be abandoned and assigned the rocks to the mainly Cretaceous Kerabai Volcanics. The Matan Complex is also referred to as Kuayan Formation (Hermanto et al., 1994).

METHODOLOGY

Sampling

Rocks were collected from the northern part of the Schwaner Mountains south of Nanga Pinoh, from the southwest near Ketapang, and from the eastern part near Tumbangsamba and Tewah (**Figure 4**). Samples include Schwaner granitoids, PMG rocks, volcanics and meta-volcanics, and modern river sands. Sample locations are shown in **Figure 4**. Additional granitoid samples from the area near Ketapang were provided by Rio Tinto (samples labelled RT). Samples RT.C and RT.D were dated in van Hattum et al. (2013).

Zircon Geochronology (SHRIMP and LA-ICP-MS)

Zircons were separated from crushed rock samples and friable river sands using standard heavy liquids (sodium polytungstate, lithium heteropolytungstate, di-iodomethane) and a FRANTZ magnetic barrier separator. The analysed zircon fraction was 63–250 μm. Zircons from igneous and metamorphic rocks were dated with sensitive high-resolution ion microprobe (SHRIMP II) at the Research School of Earth Sciences, The Australian National University, Canberra, Australia. The zircons were mounted in resin with the TEMORA 2 zircon standard (416.8 ± 1.0 Ma: Black et al., 2004) and polished to expose mid-sections of each grain. Photomicrographs were taken in reflected and transmitted light to detect cracks and inclusions and cathodoluminescence (CL) imaging was carried out on a JEOL JSM 6610 A scanning electron microscope to detect internal features of the zircons (i.e., growth zonations, core-rim sites). The beam size varied from 10 to 20 μm for rim and core analyses respectively. The TEMORA 2 U-Pb standard and SL13 uranium concentration (U = 238 ppm) standard were used for calibration. Analyses followed the procedure of Williams (1997). Analytical data for SHRIMP geochronology is listed in **Supplementary Table S1**.

Zircons from other igneous rocks and modern river sands were dated by laser ablation inductively coupled plasma mass spectrometry (LA-ICP-MS) at the Birkbeck College, University of London (UCL) using a New Wave NWR 213 nm and 193 nm laser ablation system coupled to an Agilent 7500 and Agilent 7700 quadrupole-based plasma mass spectrometer (ICP–MS). Zircons were mounted in epoxy resin and polished to expose mid-grain sections. Analysis spots for each grain were selected using transmitted light and cathodoluminescence scanning electron microscope (CL-SEM) imagery to avoid cracks and inclusions. The Plešovice zircon standard (337.13 ± 0.37 Ma; Sláma et al., 2008) and a NIST 612 silicate glass bead (Pearce et al., 1997) were used to correct for instrumental mass bias and depth-dependent inter-element fractionation of Pb, Th and U. Real-time data were processed using the GLITTER data reduction software (Griffin et al., 2008). A laser spot size of 35 μm for the NWR 213 nm and 25 μm for the NWR 193 nm was used. The data were corrected using the common lead correction method by Andersen (2002), which is used as a ^{204}Pb common lead-independent procedure. Ages were calculated using the ^{238}U/^{206}Pb ratios for samples dated as younger than 1000 Ma and the ^{207}Pb/^{206}Pb ratios were used for grains older than 1000 Ma (Nemchin and Cawood, 2005). Ages greater than 1000 Ma were considered to be concordant if the difference between the ^{207}Pb/^{206}Pb and ^{206}Pb/^{238}U age is 15% or less and ages smaller 1000 Ma were considered to be concordant if the ^{207}Pb/^{235}U—^{206}Pb/^{238}U age is 15% or less. The 15% concordance range was chosen to better compare results from the older Agilent 7500 system with the newer 7700, and with the SHRIMP data. Analytical data for LA-ICP-MS geochronology is listed in **Supplementary Table S2** for igneous and metamorphic rocks, and **Supplementary Table S3** for modern river sands.

Isoplot 4.15 (Ludwig, 2008) was used for graphical illustration of Tera-Wasserburg concordia diagrams (Tera and Wasserburg, 1972), conventional concordia plots (Wetherill, 1956), and probability density plots. Tera-Wasserburg plots were used to identify individual peaks or visually assess outliers (e.g., lead loss, inheritance or common lead) within the population which were excluded from the weighted mean age calculation. In some metamorphic samples several subpeaks were identified and the unmix function of Sambridge and Compston (1994) was used to calculate a mean age for these populations. Additional zircon age

histograms and probability density plots were calculated using an R script written by I. Sevastjanova based on the approach of Sircombe (2004).

$^{40}Ar/^{39}Ar$ Geochronology

PMG sample LD10-084 (garnet-sillimanite schist) was crushed to gravel sized chips using the jaw crusher at Royal Holloway University of London. It was washed and sieved into 420–600 μm and 250–420 μm grain fractions. Biotite and white mica flakes were concentrated using flotation techniques and separated using a FRANTZ magnetic separator. Samples were finally hand-picked in order to ensure purity of >99%. Two biotite fractions (L2—250–420 μm & L3—420–600 μm) and one white mica fraction (L1—420–600 μm) were selected for analysis. The mica separates were analysed using the furnace step-heating technique in the Argon Laboratory at the Research School of Earth Science, The Australian National University, Canberra, Australia. Separates were irradiated in canister ANU#13 at the USGS Nuclear Reactor in Denver (USA) with the GA1550 biotite standard (98.5 ± 0.8 Ma; Spell and McDougall, 2003). Flux monitor standard GA1550 was analysed with the fusion technique with the LED continuous wave laser, and samples and standards were analysed in the VG1200 mass spectrometer with 100% gas release of ^{39}Ar. Separates were analysed with 18–21 steps and with temperatures rising from 450°C to 1450°C (Lovera et al., 1989).

The reported data have been corrected for system backgrounds, mass discrimination, fluence gradients and atmospheric contamination. Errors associated with the age determinations are one sigma uncertainties and exclude errors in the age of the standard GA1550. Decay constants are those of Steiger and Jager (1977). The $^{40}Ar/^{39}Ar$ dating technique is described in detail by McDougall and Harrison (1999) and Forster and Lister (2009). Data reduction was done with a new adapted version of *Noble* Software. The data reduction was based on optimising MSWD on isotope intensities with an exponential best fit methodology. Data interpretation was carried out using the eArgon software using the approach by Forster and Lister (2004) and Beltrando et al. (2009). Data tables are presented in **Supplementary Table S4**, and a detailed methodology description is given in the **Supplementary Material**.

Geochemistry

Whole rock geochemical analyses were obtained for 16 igneous and 17 metamorphic samples at Royal Holloway University of London. Major element analyses were acquired by inductively coupled plasma atomic emission spectroscopy (ICP-AES) on a Perkin Elmer Optima 3300RL instrument with an Echelle spectrometer and a segmented-array charge-coupled-device detector. Sample powders were prepared with Li-metaborate flux for the fusion procedure. Data were averaged from 5 analyses and calibrated using international reference materials and a Gallium internal standard (**Supplementary Table S5**). Precision on triplicates was better than ±0.07%, and RSD was better than 5%. X-ray fluorescence (XRF) was used for trace element analyses. Sample powders were set in a PVP-MC binding solution and pressed into pellets. Analyses were performed using a PANalytical Axios sequential X-ray fluorescence spectrometer with 4 kW Rh-anode X-ray tube. Analyses were run four times to check for reproducibility. 30 to 40 international rock standards were used for calibration. Calibration graphs and comparisons between XRF and isotope dilution data for several elements are publicly available at https://www.royalholloway.ac.uk/research-and-teaching/departments-and-schools/earth-sciences/research/research-laboratories/x-ray-fluorescence-laboratory/. The quality of the straight line fit of these graphs is the best indicator of accuracy over a wide range of concentrations. Where there is more scatter, this can reflect poor precision of the XRF analyses relative to the calibrated concentration range (e.g., Sn, where precision is about ±2 ppm, and the calibrated range only 15 ppm); inaccuracies in the published standard data (e.g., S, Cl), or inaccuracies in the XRF data (e.g., at ≪100 ppm F). A wider range of trace elements were analysed for RT samples using ICP-AES for major and trace elements. Geochemical data were plotted using GCDkit by Janoušek et al. (2006). Data tables for major and trace elements are supplied in **Supplementary Table S5** along with quality control data.

Chemical data for garnets of PMG samples LD10-084 and SW16 were acquired at Birkbeck College, University of London using a JEOL-733 Superprobe equipped with an Oxford Instruments ISIS energy dispersive system. Data tables for garnets are supplied in **Supplementary Table S6**.

RESULTS

Zircon Geochronology

Intrusive Rocks

Zircons from intrusive rocks of the Schwaner Mountains were analysed in samples LD10-038, LD10-048, LD10-100 and LD10-071 from the NSZ, LD10-103 and LD10-115 from close to the easternmost part of the NSZ-SSZ boundary, and LD10-011, LD10-074, LD10-75 and LD10-77 from the SSZ. Zircons typically show oscillatory zoning.

Three NSZ tonalite samples from the Sepauk Tonalite yielded Early Cretaceous (Aptian) ages of c. 112 to 114 Ma. 20 U-Pb zircon ages by SHRIMP from tonalite sample LD10-048 (**Figure 5A**) have a weighted mean age of 111.8 ± 1.1 Ma (MSWD = 1.2). For tonalite sample LD10-100 (**Figure 5B**) 25 ages by SHRIMP gave a weighted mean age of 114.2 ± 0.7 Ma (MSWD = 1.1). 15 concordant U-Pb zircon ages were obtained by LA-ICP-MS for tonalite LD10-038 (**Figure 5C**) and a coherent cluster of 12 were used to calculate a weighted mean age of 114.4 ± 1.1 Ma (MSWD = 1.3). An NSZ alkali granite (LD10-071) interpreted as Laur Granite yielded a Late Cretaceous (Cenomanian) age. 29 U-Pb zircon ages by SHRIMP (**Figure 5D**) yielded a weighted mean age of 96.8 ± 0.6 Ma (MSWD = 0.9).

Tonalite LD10-103 (**Figure 5E**) from the easternmost NSZ-SSZ boundary yielded 50 concordant U-Pb zircon ages determined by LA-ICP-MS and 45 were used to calculate a weighted mean age of 88.1 ± 0.6 Ma (MSWD = 2.8). Granite sample LD10-115 (**Figure 5F**) from the same area (**Figure 4**)

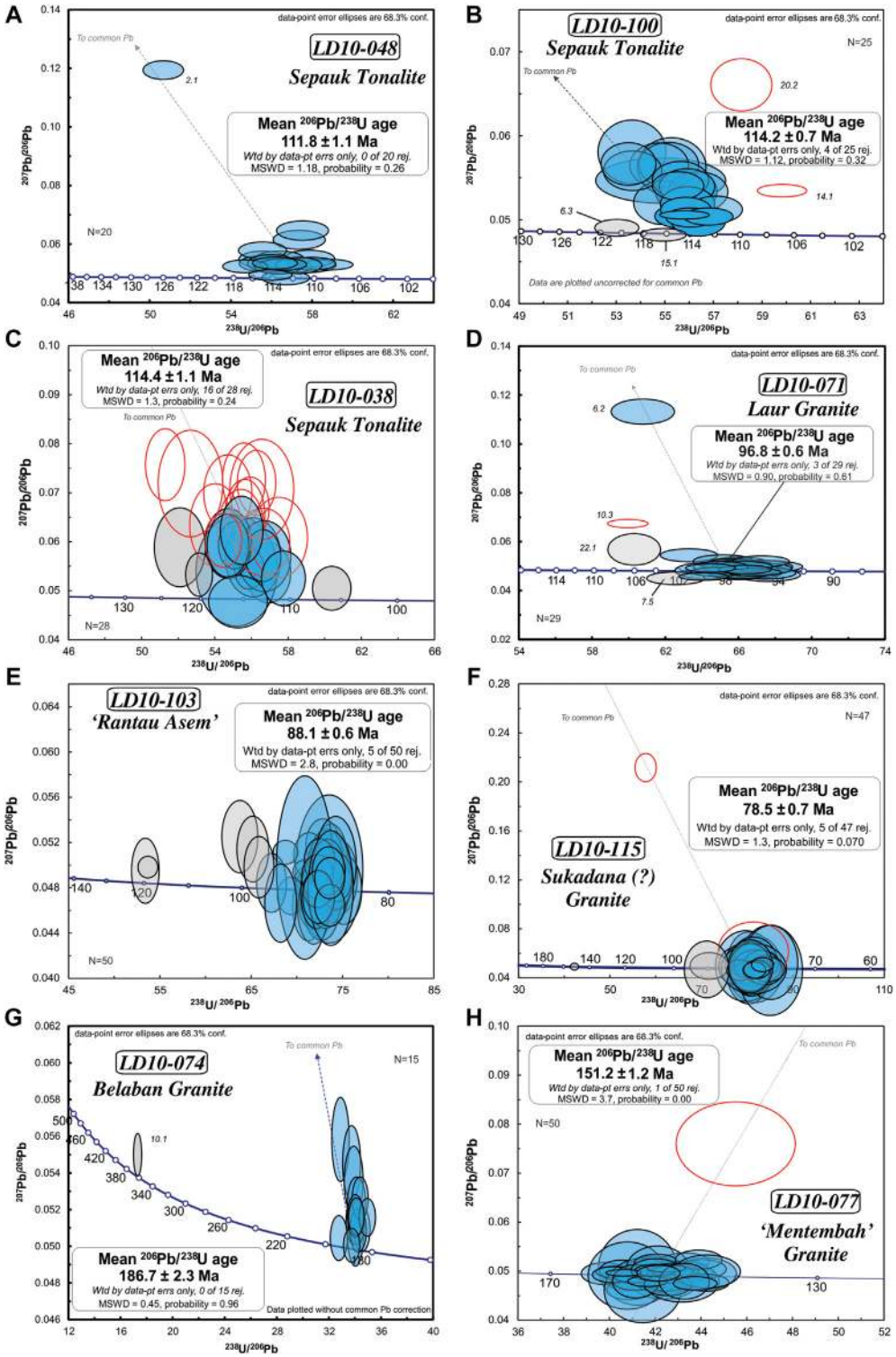

FIGURE 5 | Zircon U-Pb weighted mean age calculation and Tera-Wasserburg diagrams for plutons in the NSZ, the eastern part of the Schwaner Mountains (potentially SSZ), and the Jurassic basement of the SSZ. **(A)** LD10-048 Sepauk Tonalite NSZ, **(B)** LD10-071 Laur Granite NSZ, **(C)** LD10-100 Sepauk Tonalite NSZ, **(D)** LD10-038 Sepauk Tonalite NSZ, **(E)** LD10-103 Rantau Asem Tonalite NSZ-SSZ?, **(F)** LD10-115 Sukadana Granite SSZ?, **(G)** LD10-074 Belaban Granite SSZ, **(H)** LD10-077 Mentembah Granite SSZ. SHRIMP diagrams display ages uncorrected for common Pb and for LA-ICP-MS results common Pb corrected ages are displayed. Common Pb correction after Andersen (2002).

yielded 45 concordant LA-ICP-MS U-Pb zircon ages of which 42 gave a weighted mean age of 78.5 ± 0.7 Ma (MSWD = 1.3). The sample location is within the area mapped as the Sepauk Tonalite (Sumartadipura and Margono, 1996; Tate, 2001), but as the age is significantly younger than all other NSZ granitoids and comparable to the Sukadana Granite (van Hattum et al., 2013), we suggest that the Sukadana Granite and the SSZ extend into the easternmost Schwaner Mountains.

Samples from the SSZ include Jurassic and Cretaceous plutons. The oldest igneous rock dated is granite LD10-074 (Belaban Granite) (**Figure 5G**). 16 U-Pb zircon ages were determined by SHRIMP, and a cluster of 15 ages gave a weighted mean age of 186.7 ± 2.3 Ma (MSWD = 0.45). The sample contained one inherited age of 357.8 ± 4.2 Ma LD10-077 (**Figure 5H**) is another Jurassic granite sample with 49 concordant LA-ICP-MS U-Pb zircon ages, which gave a weighted mean age of 152.2 ± 1.2 Ma (MSWD = 3.7). No Early Cretaceous ages in the SSZ have been reported and none were found in this study. Granite LD10-011 (**Figure 6A**) from the northernmost SSZ yielded 44 concordant LA-ICP-MS U-Pb zircon ages and 43 gave a weighted mean age of 78.4 ± 0.5 Ma (MSWD = 1.1), comparable to the Sukadana Granite (van Hattum et al., 2013). The youngest igneous rock from the Schwaner batholith dated in this study is an alkali granite LD10-075 (**Figure 6B**) from the Sangiyang Granite. 19 U-Pb zircon ages acquired by SHRIMP yielded a weighted mean age of 72.1 ± 0.6 Ma (MSWD = 1.4).

Volcanic and Sheared Volcanic Rocks—Menunuk Volcanics

Samples LD10-49 and LD10-60 are volcanic and sheared volcanic rocks from the NSZ at the northern margin of the Schwaner Mountains, and are Early Cretaceous. They were sampled from an area mapped as PMG 20 km east of Sungai Menunuk. No contacts with PMG rocks were observed. 20 U-Pb ages acquired by SHRIMP for sample LD10-049 (**Figure 6C**) range between 125 and 135 Ma (weighted mean age of 130.8 ± 1.1 Ma; MSWD = 1.3). 19 U-Pb SHRIMP ages for sample LD10-060 (**Figure 6D**) range between 127 and 135 Ma with one discordant slightly younger outlier. The weighted mean age of the sample is 132.1 ± 1.4 Ma (MSWD = 1.4).

Pinoh Metamorphic Group

The dated samples from the PMG include metapelites, metavolcanic rocks, schists, and quartzites. Most zircons show oscillatory zoning, while a few zircons exhibit convolute zoned rims. Samples LD10-102A and LD10-124 are schistose metavolcanic rocks with Cretaceous ages. 55 U-Pb ages were acquired by SHRIMP from sample LD10-102A (**Figure 6E**) with 48 being concordant. Except for one Triassic core age, the majority of ages are Early Cretaceous and form a group between c. 127 Ma and 110 Ma. They are from unaltered inner cores or grains that show some recrystallisation textures. This group has an Isoplot unmix age of c. 118.5 ± 0.4 Ma (**Figure 6E**). A younger age group (c. 88 Ma, **Figure 6E**) is from rims of zircons that show recrystallisation textures. Seven discordant Paleogene and Neogene ages have large common Pb (>10%) or high U, and were excluded from age calculations. 16 U-Pb SHRIMP ages from LD10-124 (**Figure 6F**) range from c. 120 to 130 Ma and gave a weighted mean age of 124.0 ± 3.7 Ma (MSWD = 6.7). A small number of ages cluster around c. 111–118 Ma. The older ages are interpreted as the age of volcanic activity and the younger ages to record later recrystallisation.

Samples LD10-004B, LD10-084, SW3G, LD10-058, LD10-069 and SW14 are schists and quartzites. 62 concordant U-Pb zircon ages were acquired with SHRIMP from quartzite LD10-004B (**Figure 6G**). 58 are Cretaceous, and 4 are inherited Permian, Carboniferous and Neoproterozoic ages. The Cretaceous population ranges from 76–141 Ma with a bimodal distribution. There is a major age peak at c. 110 Ma probably related to magmatism and a smaller one at c. 82 Ma likely related to recrystallisation. A small number of grains have ages close to c. 127 Ma.

There were no inherited pre-Cretaceous ages in samples LD10-084, SW3G and LD10-058. 17 U-Pb zircon ages acquired by SHRIMP from LD10-084 (**Figure 6H**) range from 90–133 Ma with the main population at c. 115 Ma. 44 U-Pb zircon SHRIMP ages were acquired from SW03G (**Figure 7A**). The distribution is unimodal with a major cluster in the Early Cretaceous that has a weighted mean age of 128.2 ± 1.5 Ma (MSWD = 2.5). One grain (2 spots) has an age of c. 105 Ma and may indicate recrystallisation at this time (**Figure 7A**). 43 U-Pb zircon SHRIMP ages from LD10-058 (**Figure 7B**) range from 110 to 140 Ma. The largest age cluster has a weighted mean age of 131.3 ± 1.0 Ma (MSWD = 1.2). The youngest age in the sample is c. 111 Ma (**Figure 7B**) and comes from a possibly recrystallised grain.

25 concordant U-Pb zircon ages were acquired with LA-ICP-MS for LD10-069 (**Figure 7C**). The majority of ages range from 105 to 125 Ma and there are seven Permo-Carboniferous and three Proterozoic (1.56 to 1.83 Ga) inherited ages. Two major peaks were calculated at c. 110 and 120 Ma with the Isoplot unmix function and could both be related to magmatism. Three Neogene ages of 5.8 to 6.7 Ma were acquired from zircons with very bright CL images; they have high U contents (similar to LD10-102) and were ignored in the age calculations.

There are 62 concordant SHRIMP U-Pb ages (**Figure 7D**) from quartzite SW14. Cretaceous grains have a population with a peak at c. 80 Ma and a minor population at c. 117 Ma. The weighted mean age calculation for the three youngest grains yielded an age of 78.7 ± 1.3 Ma, which is similar to the Sukadana Granite and interpreted as metamorphic overprint. Other Cretaceous ages are c. 90, 105, 126, 135 and 142 Ma. The Early Cretaceous ages are likely related to magmatism contemporaneously with the deposition of the protolith of SW14. There are some Jurassic grains with ages between 161 and 175 Ma. In contrast to other PMG samples, the quartzite has a large number of inherited grains, and also a number of rounded zircons not seen the other samples. There is a Permo-Triassic age population with peaks at c. 200, 230 and 250–260 Ma (**Figure 7D**). Palaeozoic zircons include a small Silurian-Devonian population and scattered Cambrian, Ordovician and Carboniferous ages (**Figure 7D**). 14 Proterozoic ages have a peak at c. 1.8–1.9 Ga and are

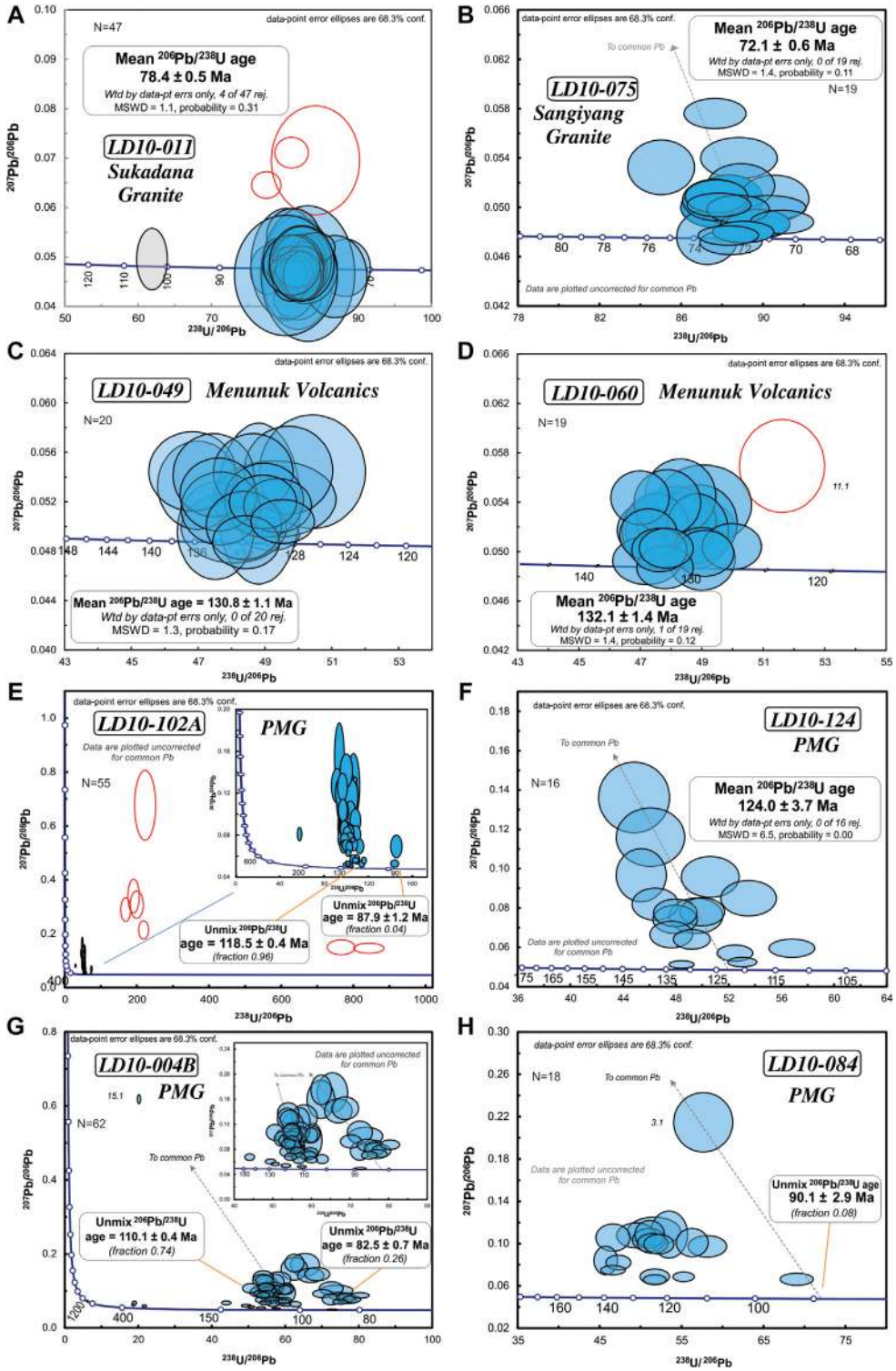

FIGURE 6 | Zircon U-Pb weighted mean age calculation and Tera-Wasserburg diagrams for post-subduction plutons in the SSZ: **(A)** Sukadana Granite LD10-011, **(B)** Sangiyang Granite LD10-075, **(C, D)** Menunuk Volcanics from the NSZ, and **(E–H)** metamorphic rocks from the Pinoh Metamorphic Group with **(E)** LD10-102 A, **(F)** LD10-124, **(G)** LD10-004B, **(H)** LD10-084. SHRIMP diagrams display ages uncorrected for common Pb and for LA-ICP-MS results common Pb corrected ages are displayed. Common Pb correction after Anderson (2002). Age cluster calculation for PMG rocks with the unmix function of Isoplot.

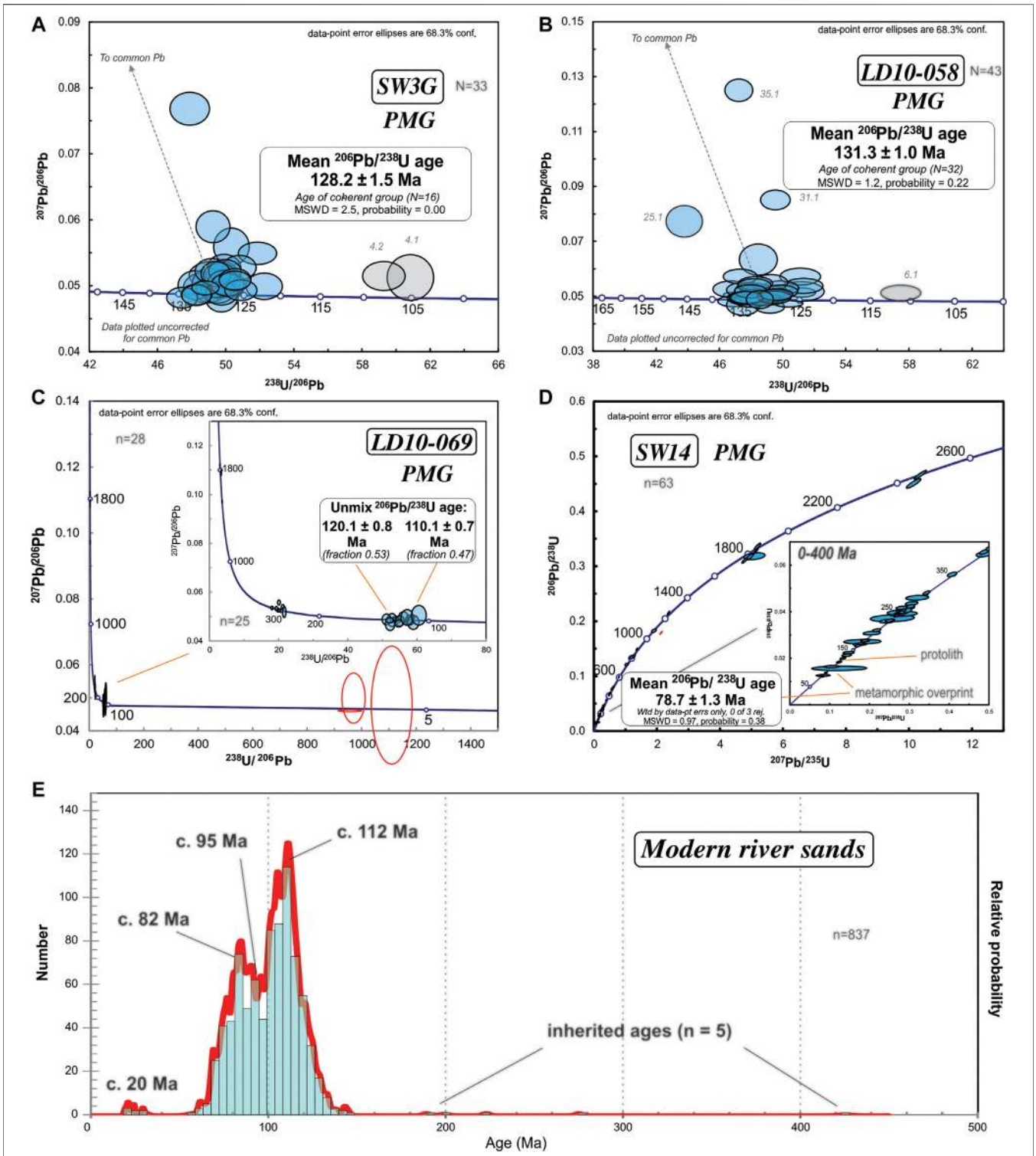

FIGURE 7 | Zircon U-Pb weighted mean age calculation, Tera-Wasserburg diagrams for metamorphic rocks from the Pinoh Metamorphic Group (continued), and concordia plots and age histogram for metamorphic rocks from the PMG with inherited ages. SHRIMP diagrams display ages uncorrected for common Pb. **(A)** Terra-Wasserburg plot for SW3G with weighted mean age calculation. **(B)** Terra-Wasserburg plot for LD10-058 with weighted mean age calculation. **(C)** Tera-Wasserburg diagram for sample LD10-069 from the Pinoh Metamorphic Group. Two main age cluster calculated with the unmix function of Isoplot. Ages are plotted corrected for common Pb. **(D)** Conventional concordia diagram for sample SW14 from the Pinoh Metamorphic Group to display the abundant inherited ages. **(E)** Detrital zircon U-Pb histogram and probability density from modern river sand samples. Main population peaks at c. 112 Ma, 95 Ma, 82 Ma, and at c. 20 Ma.

accompanied by scattered ages at c. 800 Ma, 1060–1250 Ma and 2.5 Ga (**Figure 7D**).

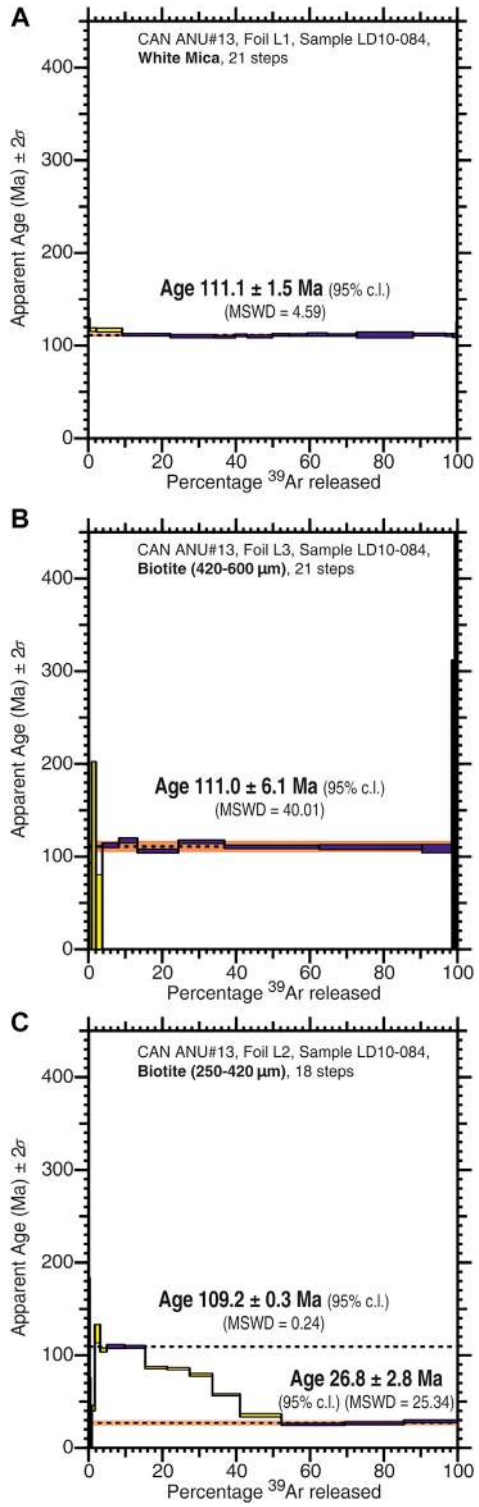

FIGURE 8 | $^{40}Ar/^{39}Ar$ plateaus and apparent age calculation for sample LD10-084. **(A)** L1: white mica, **(B)** L3: coarse biotite, **(C)** L2: fine-grained biotite.

Modern River Sands

The metamorphic rocks of the Schwaner Mountains, and to some extent the intrusive and volcanic rocks, are difficult to access. Sampling requires long journeys up rivers, and logging and mining activity in some areas made access restricted or impossible. In order to check if any important age populations were missed, zircons from a number of modern river sands were dated with LA-ICP-MS. Although the precise source of zircons in river sands cannot be known it can be expected that if there are igneous and metamorphic rocks in the region with other age populations, these would be represented in river sands. 1025 zircon grains were dated from 8 samples collected from rivers that drain an area of c. 10,000 km^2 of the central northern Schwaner Mountains, mainly the NSZ, including the Pinoh River and Melawi River near Nanga Pinoh, and the Mendawai River in the east. The areas drained by rivers from which these samples were collected are shown on **Supplementary Figure S1** based on rivers and drainage basins in the global Hydro1K (2020) dataset. There were 837 concordant ages. The overwhelming majority (818 ages) are Cretaceous, with peaks between 115 to 110 Ma, at c. 95 Ma and at c. 82 Ma (**Figure 7E**). Early Cretaceous ages between 125 to 105 Ma are the most common. Inherited ages are very rare with only 5 grains older than Cretaceous. Two grains are Early Jurassic (199–189 Ma), one is Late Triassic (223 Ma), one is Permian (275 Ma), and the oldest grain is Silurian (425 Ma). Besides the dominant Cretaceous ages, there is a small age cluster of seven Paleocene ages and another seven Oligocene to Miocene ages (31 to 19 Ma).

$^{40}Ar/^{39}Ar$ Geochronology

$^{40}Ar/^{39}Ar$ geochronology of PMG garnet-sillimanite schist LD10-084 was conducted using one white mica fraction (L1) and two biotite fractions (L2 and L3) as explained in the **Methodology** section *$^{40}Ar/^{39}Ar$ Geochronology*.

White mica (L1) analysis yielded a single plateau age of 111.1 Ma ± 1.5 (MSWD = 4.6) indicated by the age spectrum (**Figure 8A**) and represents ~80% of the ^{39}Ar released. Thin section study indicates that white mica growth occurred during prograde replacement of staurolite porphyroblasts and the plateau age records this event.

Coarse-grained biotite (L3) is present throughout the sample. A similar single plateau of 111.0 ± 6.1 Ma (MSWD = 40.0) was obtained (**Figure 8B**), which accounts for ~80% of ^{39}Ar released. The large error and MSWD is a result of the age range of c. 116 to 110 Ma in the sample that may indicate two separate events during an earlier period of metamorphism (116.5 Ma) that has been overprinted by high temperature metamorphism at 110.1 Ma, or a long period of biotite growth.

Fine-grained biotite (L2) occurs along shear planes intergrown with fibrolitic sillimanite. Analysis yielded a complex age spectrum with two distinct age domains (**Figure 8C**): an age of 109.2 ± 0.3 Ma (~10% of total ^{39}Ar released), and an age of 26.8 ± 2.8 Ma (~50% of total ^{39}Ar released). Using methods described by Forster and Lister (2004) we interpret the older age at c. 109 Ma to come from

TABLE 2 | Zircon U-Pb ages of this study and literature data from the igneous and metamorphic rocks of the Schwaner Mountains. PMG samples marked with * are ages calculated with the unmix function of Isoplot and represent the igneous protolith ages and metamorphic overprint. Samples from Bladon et al. (1989) are marked with ** because there is no information given on how many zircons were analysed. + marks informal names for new plutons found in this study.

Sample	Longitude	Latitude	Name/phase	Sample type	Method	Lithology	Location	Number of analyses	Number of zircon ages used for mean age calculation	Weighted mean age (Ma)	Error (Ma)	MSWD	Reference
NSZ													
LD10-060	112.0657	−0.5474	Menunuk Volc	Outcrop	SHRIMP	Ignimbrite	Nanga Pinoh	19	18	132.1	1.4	1.4	This study
LD10-049	112.0289	−0.4907	Menunuk Volc	Outcrop	SHRIMP	Sheared ignimbrite	Nanga Pinoh	20	20	130.8	1.1	1.3	This study
LD10-038	111.4128	−0.6792	Sepauk	Outcrop	LA-ICP-MS	Tonalite	Nanga Pinoh	28	12	114.4	1.1	1.3	This study
LD10-100	113.6605	−0.6106	Sepauk	Outcrop	SHRIMP	Granodiorite	Tewah	25	21	114.2	0.7	1.1	This study
LD10-048	112.2170	−0.6544	Sepauk	Outcrop	SHRIMP	Amphibole tonalite	Nanga Pinoh	20	20	111.8	1.1	1.2	This study
LD10-071	111.8214	−0.9194	Laur	Outcrop	SHRIMP	Alkali granite	Nanga Pinoh	29	26	96.8	0.6	0.9	This study
NWSZ													
EK14-1	110.0633	0.03001	Sepauk	Outcrop	LA-ICP-MS	Granite	Pontianak	57	30	118.6	1.1	4.9	Hennig et al. (2017)
EK14-6	110.475	−0.48421	Sepauk-Laur	Float	LA-ICP-MS	Tonalite	Pontianak	58	53	101.5	0.6	1.7	Hennig et al. (2017)
EK14-10	110.9521	−0.76219	Sukadana	Outcrop	LA-ICP-MS	Diorite	Pontianak	25	22	81.1	1.1	2.3	Hennig et al. (2017)
EK14-11	110.9317	−0.77402	Jurassic plutons	Outcrop	LA-ICP-MS	meta-Granodiorite	Pontianak	25	5	149.8	4.4	3.2	Hennig et al. (2017)
EK14-5	110.4265	−0.56635	Triassic plutons	Outcrop	LA-ICP-MS	meta-Granodiorite	Pontianak	57	5	213.0	3.0	0.7	Hennig et al. (2017)
84MS89A	110.44501	−0.48853	Triassic plutons	Outcrop	LA-ICP-MS	meta-Tonalite	Pontianak	23	23	233.0	3.0	2.3	Setiawan et al. (2013)
TB114	109.99646	1.33366	Jagoi	Float	LA-ICP-MS	Granodiorite	West Sarawak	108	91	208.3	0.9	4.6	Breitfeld et al. (2017)
SSZ													
LD10-074	110.4978	−1.7988	Belaban	Outcrop	SHRIMP	Alkali granite	Ketapang	16	15	186.7	2.3	0.5	This study
LD10-077	110.7906	−1.4872	*Mentembah+*	Outcrop	LA-ICP-MS	Granite	Ketapang	50	49	151.2	1.2	3.7	This study
LD10-103	113.0038	−1.4186	*Rantau Asem+*	Outcrop	LA-ICP-MS	Tonalite	Tumbangsamba	50	45	88.1	0.6	2.8	This study
LD10-115	113.0928	−1.2777	Sukadana	Outcrop	LA-ICP-MS	Granite	Tumbangsamba	45	42	78.5	0.7	1.3	This study
LD10-011	111.4978	−0.9263	Sukadana	Outcrop	LA-ICP-MS	Granite	Northern SSZ	47	43	78.4	0.5	1.1	This stidy
LD10-075	110.3198	−1.4798	Sangiyang	Outcrop	SHRIMP	Alkali granite	Ketapang	19	19	72.1	0.6	1.4	This study
RT.C	110.71977	−1.941991	Sukadana	Outcrop	SHRIMP	Monzogranite	Ketapang	36	27	84.7	1.3	NA	van Hattum et al. (2013)
RT.D	110.73125	−2.092264	Sukadana	Outcrop	SHRIMP	Monzogranite	Ketapang	13	12	81.7	1.0	NA	van Hattum et al. (2013)
84FK89A	110.543	−1.2713	Sukadana	Outcrop	NA	quartz monzogranite	Ketapang	NA	NA	80.8	0.7	NA	Bladon et al. (1989)**
84SS89A	109.9656	−1.2075	Sukadana	Outcrop	NA	Monzogranite	Ketapang	NA	NA	84.0	1.0	NA	Bladon et al. (1989)**
Upper Cretaceous Northern Granitoids													

(Continued on following page)

TABLE 2 | (*Continued*) Zircon U-Pb ages of this study and literature data from the igneous and metamorphic rocks of the Schwaner Mountains. PMG samples marked with * are ages calculated with the unmix function of Isoplot and represent the igneous protolith ages and metamorphic overprint. Samples from Bladon et al. (1989) are marked with ** because there is no information given on how many zircons were analysed. + marks informal names for new plutons found in this study.

Sample	Longitude	Latitude	Name/phase	Sample type	Method	Lithology	Location	Number of analyses	Number of zircon ages used for mean age calculation	Weighted mean age (Ma)	Error (Ma)	MSWD	Reference
TB76	109.69632	1.63922	Pueh	Float	LA-ICP-MS	Granite	West Sarawak	101	78	78.6	0.3	1.9	Hennig et al. (2017)
TB71a	109.86466	1.73467	Gading	Float	LA-ICP-MS	Two-mica granite	West Sarawak	47	26	79.7	1.0	3.3	Hennig et al. (2017)
West Borneo basement													
TB114	109.99646	1.33366	Jagoi	Float	LA-ICP-MS	Granodiorite	West Sarawak	108	91	208.3	0.9	4.6	Breitfeld et al. (2017)
Metamorphic rocks of the NSZ of the Schwaner Mountains (Pinoh Metamorphic Group)													
LD10-004B	111.6671	−0.6912	PMG	Outcrop	SHRIMP	Biotite schist	Nanga Pinoh	62	40/14	110.1/82.5*	0.4/0.7	NA	This study
LD10-084	113.4575	−0.8934	PMG	Outcrop	SHRIMP	Garnet sillimanite schist	Tewah	18	2	90.1*	2.9	NA	This study
LD10-102A	113.6961	−0.9981	PMG	Outcrop	SHRIMP	Schist	Tewah	55	47/2	118.5/87.9*	0.4/1.2	NA	This study
LD10-124	112.9057	−0.9344	PMG	Outcrop	SHRIMP	Schist	Tewah	16	16	124.0	3.7	6.5	This study
LD10-058	112.0581	−0.5277	PMG	Outcrop	SHRIMP	quartzite	Nanga Pinoh	43	32	131.3	1.0	1.2	This study
SW3G	111.7640	−0.4228	PMG	Float	SHRIMP	quartzite	Nanga Pinoh	33	16	128.2	1.5	2.5	This study
SW14	111.7201	−0.6059	PMG	Outcrop	SHRIMP	quartzite	Nanga Pinoh	63	3	78.7	1.3	1.0	This study
LD10-069	111.7831	−0.8687	PMG	Outcrop	LA-ICP-MS	Schist	Nanga Pinoh	28	8/7	120.1/110.1*	0.8/0.7	NA	This study

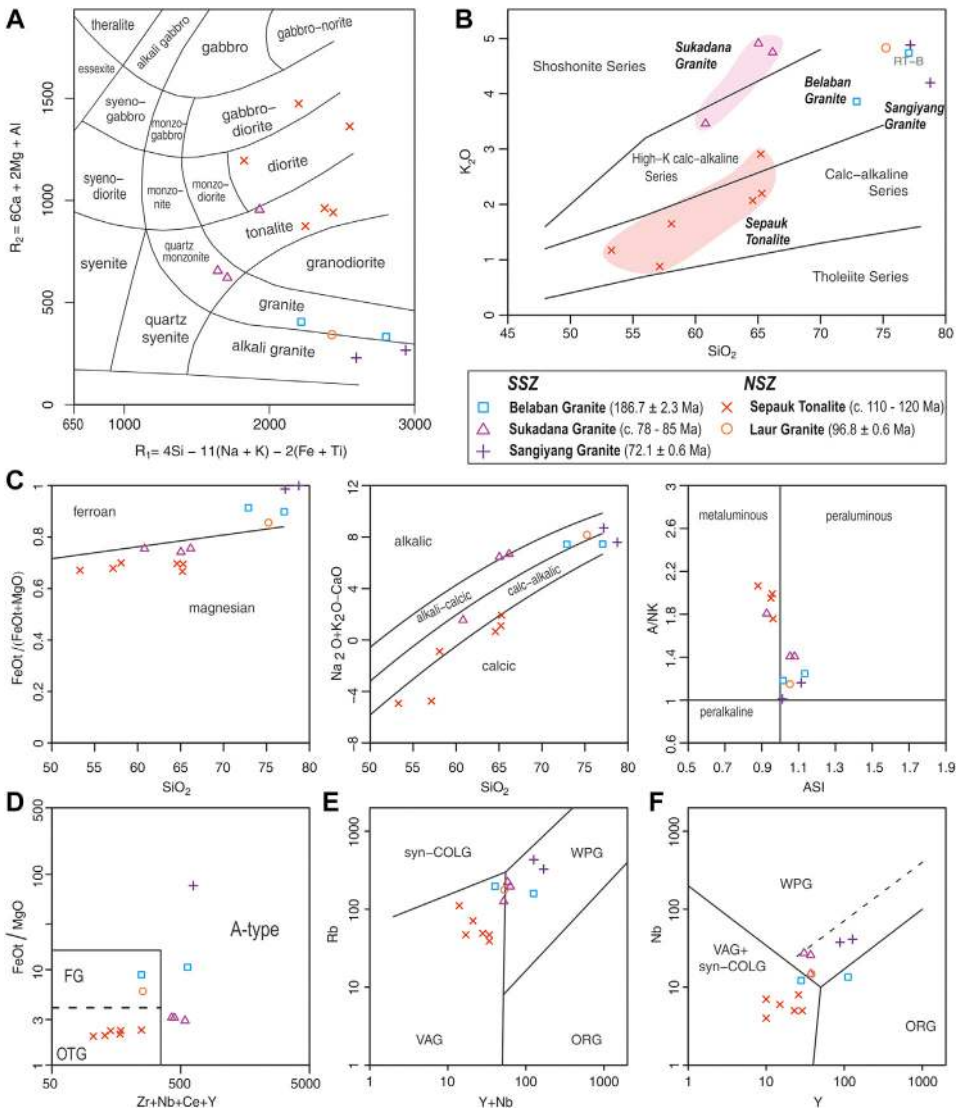

FIGURE 9 | Geochemistry classification diagrams of intrusive rocks of the Schwaner Mountains. **(A)** R1-R2 classification diagram (after De La Roche et al., 1980). **(B)** K_2O-SiO_2 classification (after Peccerillo and Taylor, 1976). **(C)** Granite classification diagrams (Frost et al., 2001). **(D)** A-type granite classification (after Whalen et al., 1987). **(E, F)** Tectonic setting of granitoids of the Schwaner Mountains (after Pearce et al., 1984).

larger grains (L3) broken in the crushing process and incorporated into the fine-grained fraction. The younger age is from fine-grained biotite formed probably during shearing of the rock at around 26.8 ± 2.8 Ma.

Petrography and Geochemistry

Major and trace element results from analysis of 14 intrusive, 9 volcanic and meta-volcanic, and 14 metamorphic rocks of the NSZ and the SSZ are displayed in **Supplementary Table S5**. Below we group our samples from different bodies by the ages determined. **Table 2** summarises the U-Pb zircon ages of this and previous studies.

Igneous Rocks

Intrusive Rocks of the South Schwaner Zone

Samples of intrusive rocks from the SSZ include RT.A from the type locality of the Sangiyang Granite and LD10-075 west of Sangiyang Hill, RT.B from the type locality of the Belaban Granite and LD10-074 near the Belaban Granite type locality, and RT.C, RT.D and LD10-010 from the Sukadana Granite.

The Belaban Granite (186.7 ± 2.3 Ma, **Table 2**) samples (RT.B, LD10-074) consist predominantly of quartz, alkali feldspar and biotite which form large crystals. Quartz grains have straight boundaries and occasionally exhibit undulose extinction or a "chicken-wire" fracture pattern. Alkali feldspar microperthite

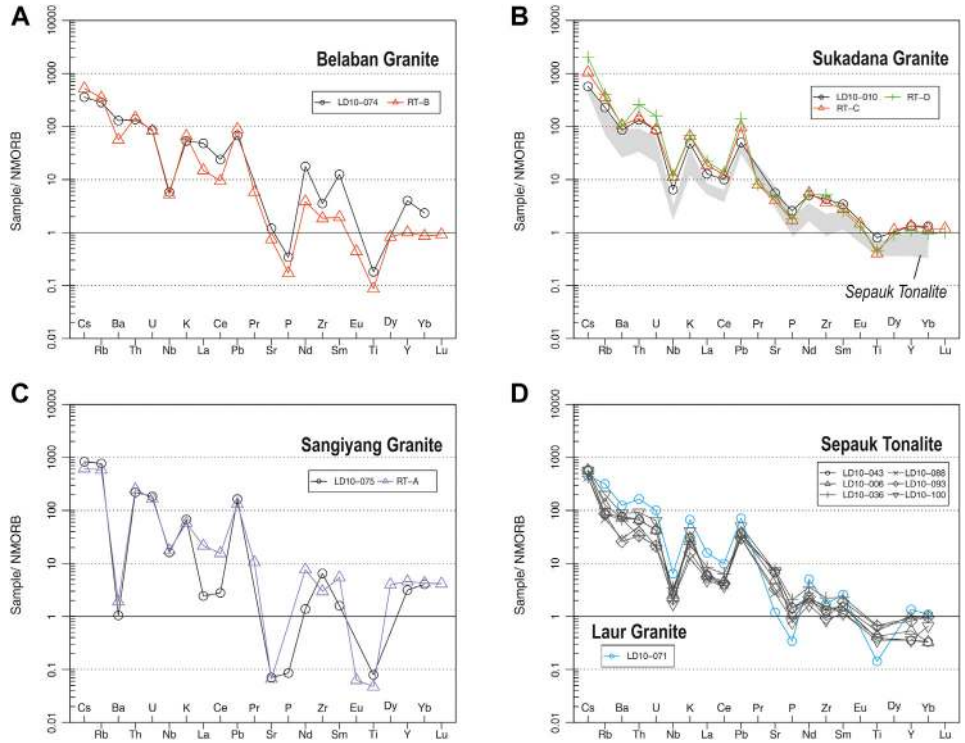

FIGURE 10 | Trace element spider diagrams for intrusive rocks of the Schwaner Mountains normalised to NMORB (Sun and McDonough, 1989). **(A)** Belaban Granite samples, **(B)** Sukadana Granite samples, **(C)** Sangiyang Granite samples, **(D)** Sepauk Tonalite samples and Laur Granite sample.

grains also have straight boundaries and are often concentrically zoned. Biotite shows some irregular grain boundaries. Plagioclase and green amphibole are minor phases, and zircon and apatite are accessories. Titanite is relatively abundant, forming large prismatic grains. A few opaque minerals are present but no rutile. The lack of deformation textures indicates little deformation since emplacement. The samples have 73 to 77 wt% SiO_2 and 3.9 to 4.7 K_2O wt%, and are classed as high-K calc-alkaline granites (**Figures 9A,B**). They are peraluminous, calc-alkalic and alkali-calcic, ferroan (Frost et al., 2001; **Figure 9C**) and on trace element discrimination diagrams they plot as A-type and felsic granites (Whalen et al., 1987; **Figure 9D**) or as WPG, post-collision and VAG (Pearce et al., 1984; **Figures 9E,F**). According to Frost et al. (2001) ferroan granites can be A-type granites. Trace element spider plots show an enrichment of LILE over HFSE (**Figure 10A**). Most HFSE are enriched relative to N-MORB with pronounced depletions in P and Ti (**Figure 10A**). The trace element spider plots suggest A-type or WPG with enrichment in high field strength elements (e.g., Zr, Y) and depletion in large-ion lithophile elements (e.g., Ba, Sr).

Sukadana (c. 78.5 to 85 Ma, **Table 2**) samples (RT.C, RT.D, LD10-010) are quartz monzonite and tonalite (**Figure 9A**). Dominant mineral phases include quartz, alkali feldspar (including microcline), plagioclase, biotite, amphibole, titanite, apatite and some epidote. Alkali feldspar can be up to 2 mm in length and is more abundant than plagioclase. Both form zoned crystals with some sericitisation. The Sukadana samples have high K_2O (>3.5% wt%) with SiO_2 of 60–68 wt% (**Figure 9B**). Samples with the greatest SiO_2 content have K_2O values close to 5 wt%. RT.C and RT.D are shoshonitic and LD10-010 is close to the shoshonite and high-K calc-alkaline boundary (**Figure 9B**). All samples are magnesian, with two being alkalic and peraluminous, and one calc-alkaline and metaluminous in the Frost classification (**Figure 9C**). The samples plot into the A-type granite field (Whalen et al., 1987; **Figure 9D**), and plot in the WPG field or at the boundary with VAG (Pearce et al., 1984; **Figures 9E,F**). The three samples show similar patterns on trace element spider diagrams normalised to N-MORB (**Figure 10B**). LILE are enriched compared to HFSE, with a negative Nb anomaly and a pronounced peak in Pb. HFSE have a very smooth pattern with only minor enrichment, and a small depletion of Ti (**Figure 10B**). The relative enrichment of Ba and Sr, as seen for the Sukadana Granite, in an A-type granite was, for Ba, interpreted by Creaser et al. (1991) as partial melting of a tonalite or granodiorite source. The enrichment in high field strength elements (Zr, Y, Yb) is consistent with an A-type granitoid.

The Sangiyang (72.1 ± 0.6 Ma, **Table 2**) samples (RT.A, LD10-075) have a coarse grained phaneritic texture with abundant alkali feldspar and quartz, which has straight boundaries and no

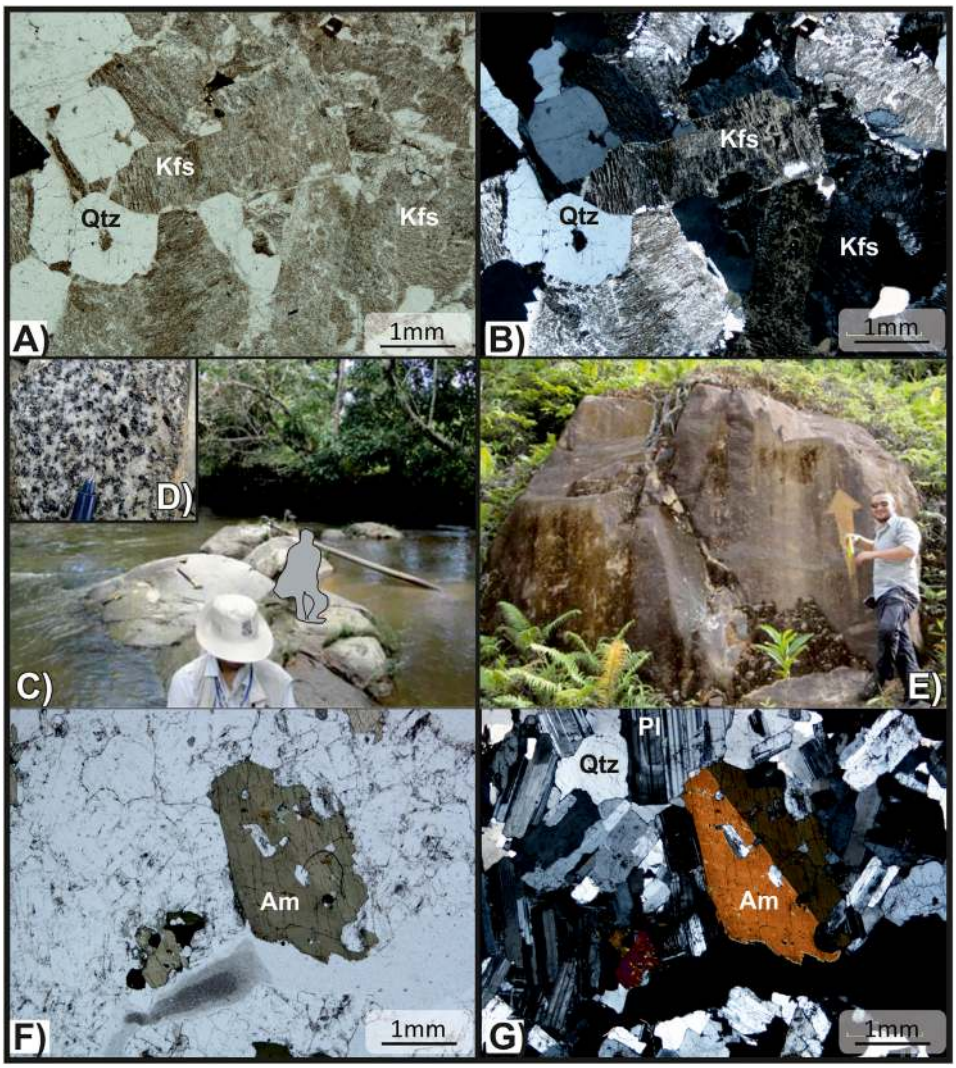

FIGURE 11 | Representative field photographs and photomicrographs of intrusive rocks of the Schwaner Mountains. **(A)** and **(B)** Photomicrograph (PPL and XPL) of the Sangiyang Granite (DL10-075). Large alkali feldspar grains commonly are exsolved to microperthite and show advanced sericitisation. **(C)** Sepauk Tonalite outcrop in river section (LD10-036). **(D)** Insert photograph shows a typical Sepauk Tonalite in hand specimen (LD10-100). **(E)** Outcrop of the Laur Granite (LD10-071). **(F, G)** Photomicrograph (PPL and XPL) of the Sepauk Tonalite (LD10-036), consisting predominantly of plagioclase, quartz and amphibole. Amphibole in the photomicrograph shows twinning and euhedral shape. (PPL—plane polarised light; XPL—cross-polarised light).

obvious fracturing or undulose extinction. Alkali feldspar grains are commonly exsolved to microperthite or show simple twinning with no zoning and advanced sericitic alteration (**Figures 11A,B**). Magnetite inclusions are abundant. Locally, intergrown feldspar and quartz grains produce a granophyric texture, likely the product of late cooling of liquid approaching the cotectic. Some amphibole is present, which is mostly green with irregular grain boundaries, but a few are blueish in transmitted light. This alkali amphibole is only observed in this granite of the SSZ. Biotite is conspicuous by its absence. Apatite and zircon are common, along with some opaque minerals but titanite and rutile are absent. The Sangiyang Granite is geochemically comparable to the Belaban samples. The samples are alkali granites with SiO_2 of 77 to 79 wt% and K_2O above 4 wt%, which classes them as high-K calc-alkaline (**Figures 9A,B**). The samples are peraluminous, calc-alkalic and alkali-calcic, and ferroan (Frost et al., 2001; **Figure 9C**). In the trace element discrimination plots (**Figures 9D–F**) they fall clearly in the A-type field of Whalen et al. (1987) and in the WPG field of Pearce et al. (1984). LILE and HFSE are generally enriched relative to N-MORB, with LILE enriched over HFSE (**Figure 10C**). There are pronounced depletions in Ba, Sr, P, Eu and Ti, and a small trough in La and Ce (**Figure 10C**). Trace element spider plots indicate an A-type or WPG character with enrichment in high field strength elements (e.g., Zr, Y) and depletion in large-ion lithophile elements (e.g., Ba, Sr).

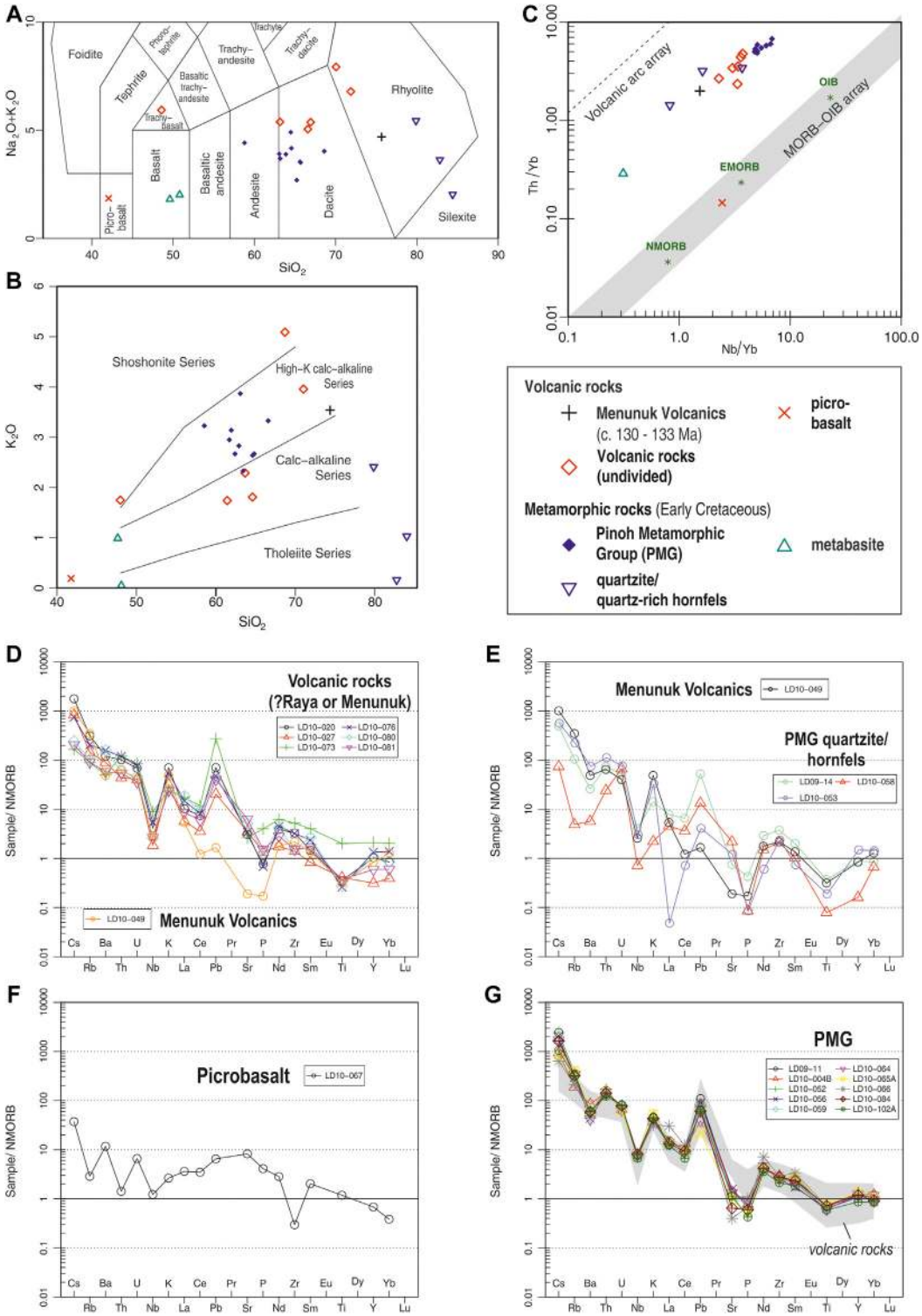

FIGURE 12 | Geochemistry classification diagrams and trace element spider diagrams of volcanic and metamorphic rocks of the Schwaner Mountains. **(A)** TAS diagram for classification of extrusive rocks (after Le Bas et al., 1986). **(B)** K_2O-SiO_2 classification (after Peccerillo and Taylor, 1976). **(C)** Th/Yb-Nb/Yb classification diagram for extrusive rocks (after Pearce, 2008). **(D–G)** Trace element spider diagrams of volcanic and metamorphic rocks of the Schwaner Mountains normalised to NMORB (Sun and McDonough, 1989) for: **(D)** Volcanic rock samples, **(E)** Menunuk Volcanic sample and PMG quartzites and hornfels, **(F)** Picrobasalt sample, and **(G)** PMG samples.

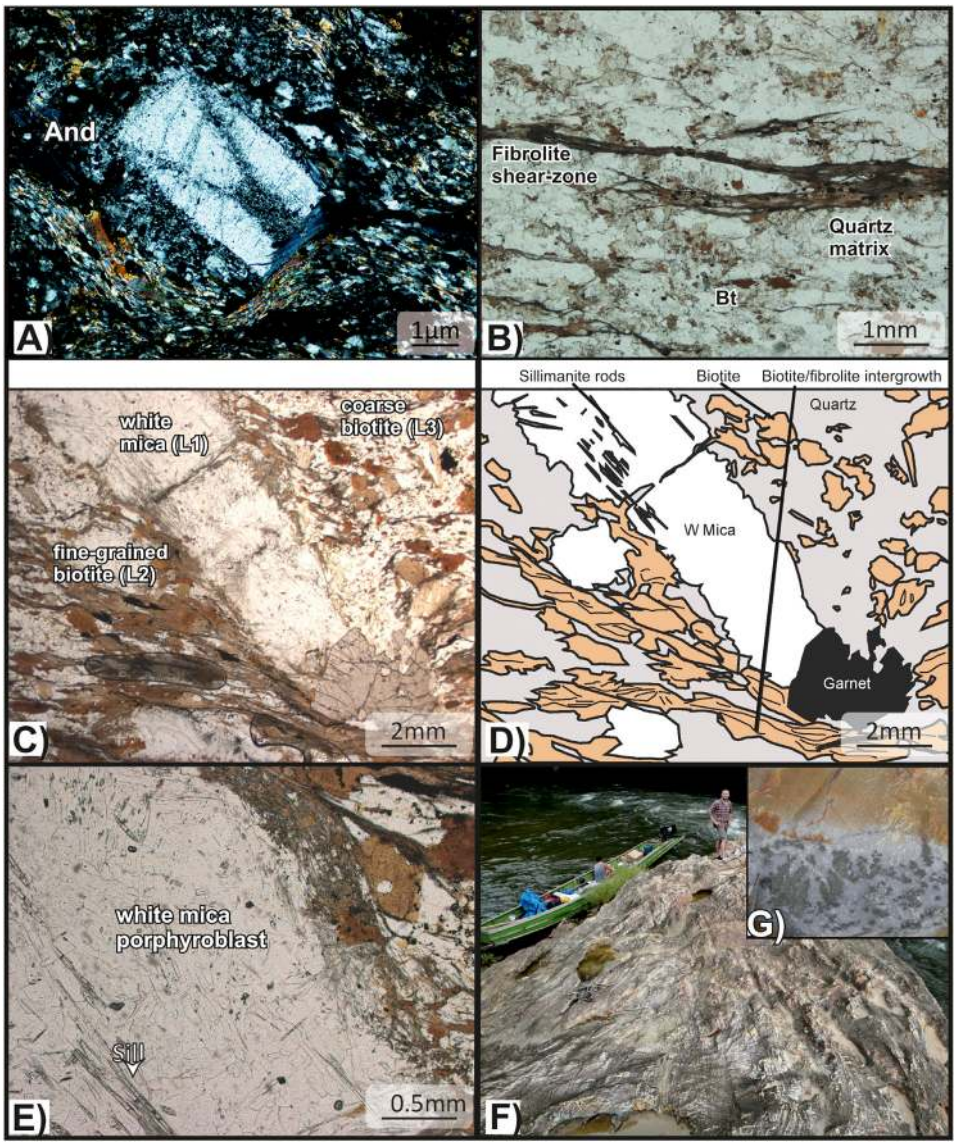

FIGURE 13 | Representative field photographs and photomicrographs of metamorphic rocks of the Schwaner Mountains. **(A)** Photomicrograph (XPL) of andalusite porphyroblast with chiastolite-type inclusion trail morphology (LD10-064, andalusite-cordierite schist). **(B)** Photomicrograph (PPL) of fibrolitic sillimanite growth along shear fabric in biotite schist (LD10-004B). **(C, D)** Photomicrograph (PPL and sketch) of garnet-sillimanite schist LD10-084. Shear fabric of sillimanite-biotite intergrowth deforms around white mica, biotite and garnet porphyroblasts. **(E)** Photomicrograph (PPL) of replacement white mica pseudomorph showing abundant sillimanite rods. **(F)** Quartzite outcrop in river section showing remnants of compositional layering (LD10-058). Close-up of quartzite hand specimen with alteration on surface.

Intrusive Rocks of the North Schwaner Zone

Intrusive rocks from the NSZ include the Sepauk Tonalite (c. 111.8 to 118.6 Ma) samples LD10-006, LD10-036 (**Figure 11C**), LD10-043 from the northern and central part, LD10-088, LD10-093 and LD10-100 (**Figure 11D**) from the easternmost part, and Laur Granite (**Figure 11E**) sample LD10-071 (96.8 ± 0.6 Ma). Sepauk samples contain plagioclase, quartz, amphibole, and biotite (**Figures 11F,G**). Accessory minerals include chlorite, epidote, titanite, rutile, zircon, apatite, and magnetite. Some samples exhibit myrmekitic textures, indicative of late stage metasomatism (Collins and Collins, 2013). Most samples are phaneritic, but a few have granoblastic textures, indicating that later recrystallisation has taken place. Some samples show evidence of shearing, with quartz recrystallisation along shear planes. Samples from the northern part have SiO_2 of 58 to 65 wt%. Two of the eastern samples have the lowest SiO_2 contents of 53 to 57 wt%. Samples with higher SiO_2 are tonalites, which is the dominant rock type of the NSZ intrusive rocks, and those with lower SiO_2 are diorites to gabbro-diorite (**Figure 9A**). Most samples have low K_2O, many below 2.2 wt%, which classes them as calc-alkaline

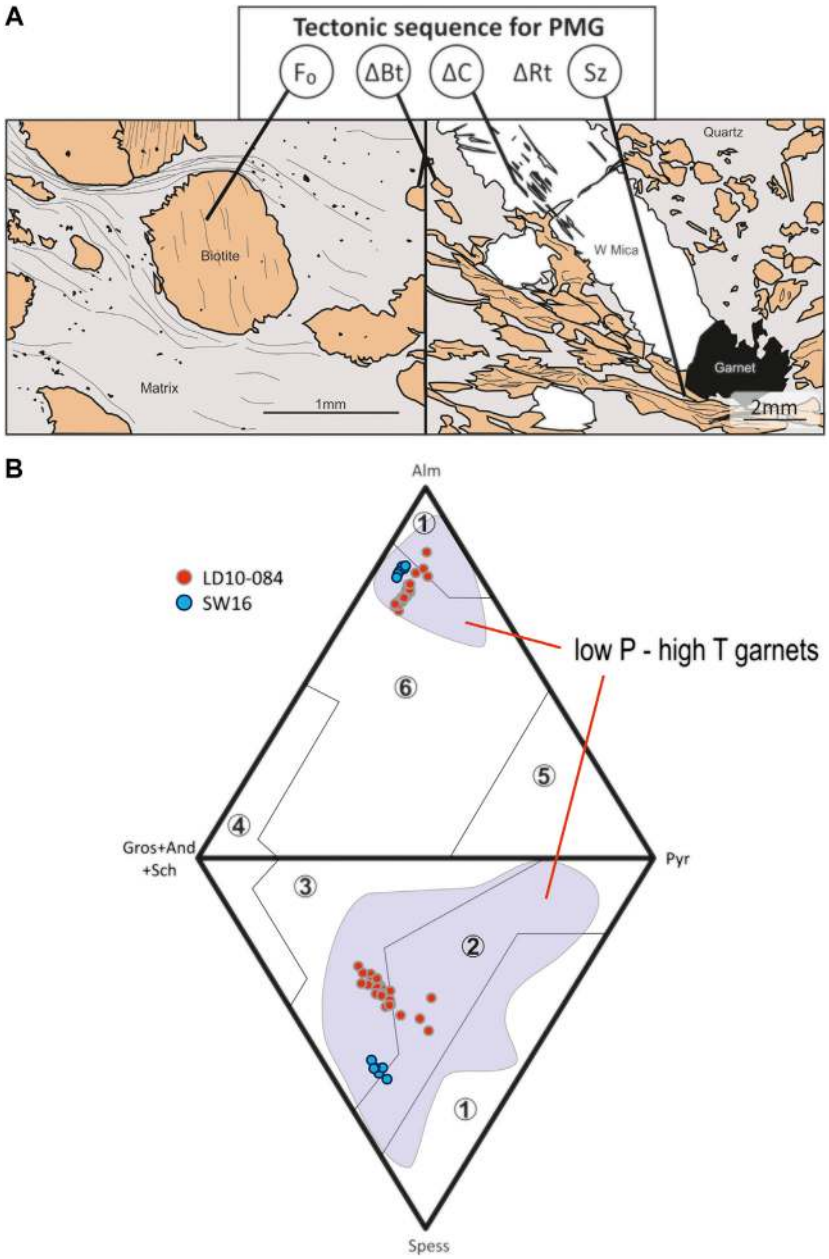

FIGURE 14 | (A) Tectonic Sequence Diagram for the Pinoh Metamorphic Group (PMG), illustrated by sketches of thin sections. F_O is earliest fabric, ΔBt is biotite growth, ΔC is low pressure-high temperature metamorphism characterised by andalusite- and cordierite-bearing mineral assemblages, and Sz is shearing. **(B)** Double ternary garnet end-member diagram for garnet-sillimanite schist samples LD10-084 and SW16 of the Pinoh Metamorphic Group (after Suggate and Hall, 2014). Garnets in both samples are spessartine-rich almandines. Shaded area shows garnets from low pressure-high temperature terranes for comparison (data from Suggate and Hall, 2014). Fields: 1) granites, 2) granulite and high-Mg pelites, 3) blueschists, 4) calc-silicates, skarns and rodingites, 5) ultrabasics, 6) basic rocks sub-ophiolites.

(**Figure 9B**). Sample LD10-100 has K_2O of 2.9 wt% which brings it into the high-K calc-alkaline field. The samples are magnesian, calcic or calc-alkalic, and metaluminous (Frost et al., 2001; **Figure 9C**). In the tectonic discrimination diagrams (**Figures 9D–F**) they plot in the unfractionated OTG (I & S-type) field of Whalen et al. (1987) and clearly in the VAG field (Pearce et al., 1984). With ASI (aluminium saturation index) values below 1.0 (**Figure 9F**) and relatively high Na_2O (>3.1 wt%) the rocks are I-type granitoids. The trace element patterns show a strong enrichment of LILE relative to N-MORB and HFSE with a pronounced negative Nb anomaly and a trough in La and Ce (**Figure 10D**). HFSE are close to N-MORB with slight depletion of heavy incompatible elements. The trace element pattern suggests a volcanic arc origin.

The only exception to the relative uniform geochemical character of the NSZ samples is LD10-071 (Laur Granite), which is significantly younger (c. 97 Ma) than the dominantly Early Cretaceous ages in the NSZ. It has a

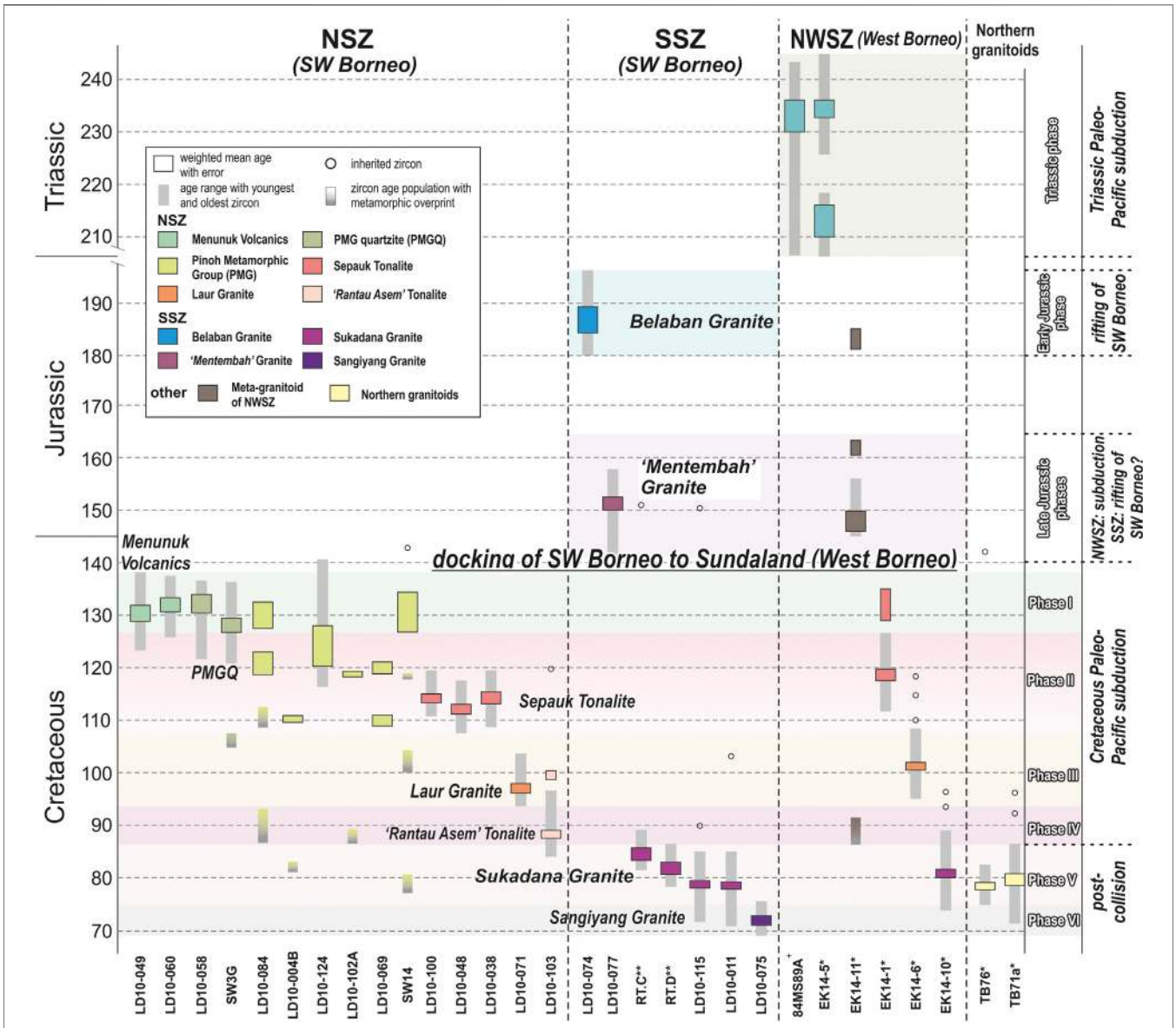

FIGURE 15 | Summary plot of Triassic to Cretaceous zircon U-Pb ages and subdivision of igneous phases in western Borneo. NSZ and SSZ from SW Borneo Block. NWSZ from West Borneo (part of Triassic Sundaland). Northern Granitoids from West Sarawak and central Kalimantan (Kuching Zone). (* age data from Hennig et al. (2017); ** age data from van Hattum et al. (2013); + age data from Setiawan et al. (2013)).

coarse-grained phaneritic texture with abundant quartz, alkali feldspar and plagioclase. Biotite and amphibole form large crystals with irregular grain boundaries. Chlorite is often present at biotite grain margins. Quartz occurs as large grains with undulose extinction, and smaller irregular grains around large feldspars. Alkali feldspar occurs as large grains, commonly with concentric zoning and simple twinning. Small epidote veins are present in some larger grains. Plagioclase occurs as smaller grains, commonly enclosed within alkali feldspar. This sample has 75 wt% SiO_2 and 4.8 wt% K_2O giving a high-K calc-alkaline character (**Figure 9B**). The Laur Granite sample is classed as alkali granite (**Figure 9A**). According to the Frost et al. (2001) classification, the sample is ferroan, alkali-calcic and peraluminous (**Figure 9C**). It plots in the felsic granite field of Whalen et al. (1987), but depending which elements are used it can also be classed as an I & S type or an A-type granitoid (**Figure 9D–F**). In the tectonic discrimination diagrams (**Figures 9E–F**) of Pearce et al. (1984) it falls at the boundary of VAG and WPG, which is also the field for post-collision granites (Pearce, 1996). Trace element spider diagrams show an enrichment of LILE relative to N-MORB and HFSE typical for a volcanic arc (**Figure 10D**). The sample has a negative Nb anomaly, depletion of P, and enrichment of Pb. HFSE show a slight enrichment relative to N-MORB with depletion of Ti.

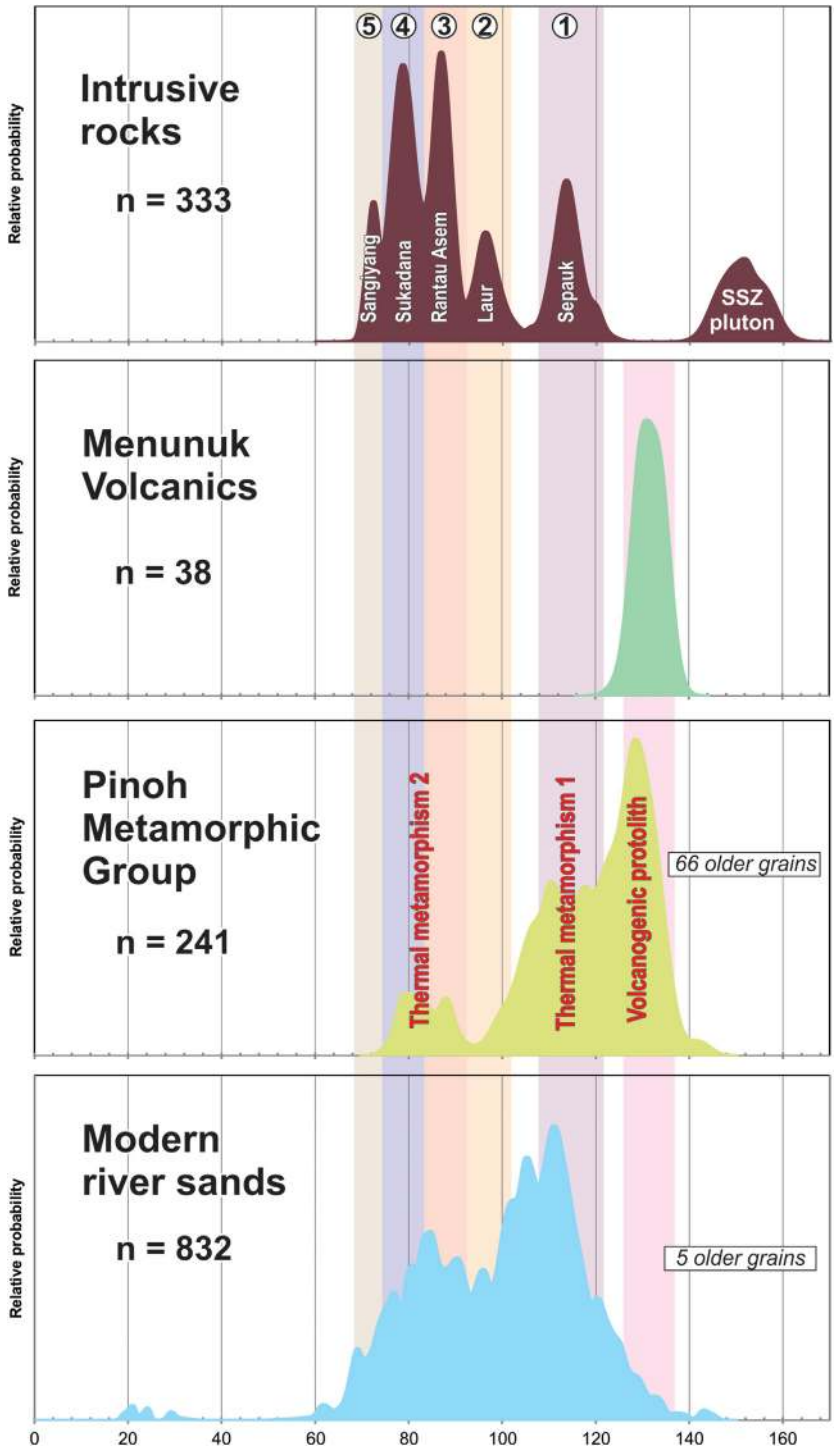

FIGURE 16 | Probability density summary of Cretaceous (to Jurassic) zircon populations for comparison. Intrusive rocks: 1) Sepauk Tonalite, 2) Laur Granite, 3) Rantau Asem Tonalite, 4) Sukadana Granite, and 5) Sangiyang Granite. Menunuk Volcanics correspond to the volcanogenic protolith of the PMG. Sepauk Tonalite corresponds to thermal metamorphism phase 1) Rantau Asem Tonalite and Sukadana Granite correspond to thermal metamorphism phase 2) Modern river sands show multiple age populations that correspond to the intrusive rocks with additional ages being derived from so far not discovered igneous rocks.

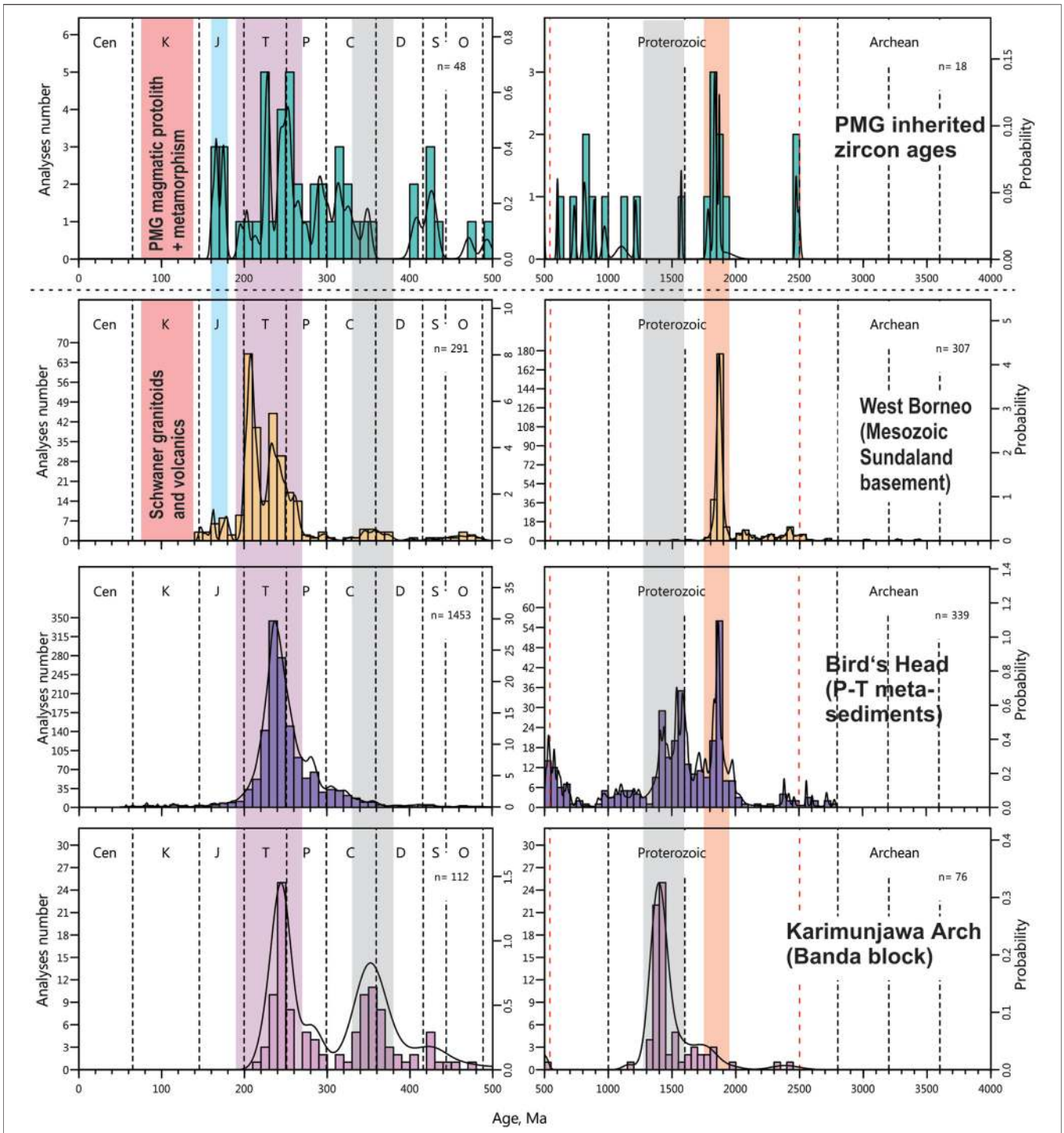

FIGURE 17 | Display of inherited zircon ages of the Pinoh Metamorphic Group and comparison to the Karimunjawa Arch (Banda Block) (data from Witts et al., 2012), Bird's Head of West Papua (data from Gunawan et al., 2012), and Mesozoic basement rocks in the West Borneo province (data from Breitfeld et al., 2017; Hennig et al., 2017). The Karimunjawa Arch and the Bird's Head data are from Triassic rocks, therefore no Jurassic zircons are present.

Volcanic and Sheared Volcanic Rocks

Volcanic rocks from the NSZ that extend into the northern part of the SSZ include tuffs, ignimbrites and lava flows of intermediate to acidic composition. Quartz, biotite and plagioclase are the dominant minerals that form porphyroblasts in a fine-grained matrix. The matrix consists of quartz, muscovite-sericite and biotite. In some cases the volcanic rocks appear to have a thermal metamorphic

overprint, identifiable as mineral recrystallisation and alteration. Some samples have been overprinted by a shear fabric similar to that observed in the intrusive rocks of the NSZ and the PMG, and could therefore be assigned to the PMG. Porphyroblasts can be rotated by this shear fabric.

Geochemical analyses indicate that the volcanic rocks are dacites and rhyolites with one mafic trachybasalt from the SSZ and one picrobasalt from the NSZ (**Figure 12A**). K_2O contents range from 1.7 to 5 wt% and the samples are calc-alkaline, high-K or shoshonitic (**Figure 12B**). The very wide range of K_2O and SiO_2 contents suggest that the samples may represent different magmatic phases or were affected by alteration. Trace element compositions suggest a subduction-related volcanic arc character (**Figure 12C**). The trace element spider diagram shows an enrichment of LILE over HFSE with depletion in Nb and enrichment in Pb (**Figure 12D**). HFSE are slightly enriched or depleted relative to N-MORB. The dated sample LD10-049 (Menunuk Volcanics) has a slightly different trace and major element composition compared to the rest of the volcanic samples with significant lower Ce, Pb, Sr and P values (**Figures 12D,E**), which may indicate that this sample is part of a different magmatic phase. Trace element discrimination diagrams for the picrobasalt sample suggest an N- to E-MORB character. The trace element spider diagram shows a pattern that is slightly enriched relative to N-MORB (**Figure 12F**).

Pinoh Metamorphic Group

The PMG rocks crop out almost exclusively in the NSZ of the Schwaner Mountains. The rocks are predominantly metapelites, although metabasites and quartzites are also found. Metapelites are predominantly andalusite-cordierite schists (**Figure 13A**), andalusite schists, biotite schists (**Figure 13B**), garnet-andalusite schists and garnet-sillimanite schists (**Figures 13C–E**). Rocks of higher metamorphic grade are garnet-biotite gneisses and andalusite gneisses. There are also a number of contact metamorphic andalusite-cordierite hornfels. Mineral assemblages include biotite, quartz, feldspar, andalusite, fibrolitic sillimanite, cordierite and garnet. Andalusite, cordierite, biotite and garnet usually form porphyorblasts in fine-grained matrix (**Figures 13A,C,D**) within a shear fabric. Muscovite pseudomorphs (replacement of possible andalusite) were also observed (**Figure 13E**). Quartzites (**Figures 13F,G**) contain >80 wt% quartz with other mineral phases, including biotite, muscovite and chlorite. Remnant compositional layering is formed by biotite-rich horizons. Textures suggest static recrystallisation of quartz grains followed by deformation-induced high temperature recrystallisation. Metabasites are foliated amphibolites consisting of abundant amphibole with plagioclase, epidote and apatite. The scarcity of sand-sized detrital grains such as zircon in all PMG samples, and the small grain size of those which are present, indicate that the protoliths were fine grained sedimentary rocks, such as muds or volcanic ashes.

Petrographic observations of the metamorphic rocks were recorded and summarised on Tectonic Sequence Diagrams (Forster and Lister, 2008; **Figure 14A**). At least three major periods of deformation are recorded: 1) low grade metamorphism (F0) interpreted as recording burial of sedimentary protoliths, 2) low pressure-high temperature metamorphism (ΔC), characterised by andalusite- and cordierite-bearing mineral assemblages and 3) shearing (Sz), often in association with fibrolitic sillimanite growth.

The mineral assemblages of the PMG are broadly similar to Buchan rocks from the Grampian Terrane in NE Scotland (Hudson, 1985; Viete et al., 2010; Viete et al., 2011). Garnets from two garnet-mica sillimanite schists of the PMG were analysed by electron microprobe. Garnet formulae were calculated for 24 oxygens (**Supplementary Table S6**), and garnet end-members calculated using the method of Suggate and Hall (2014). The garnets are almandine-rich (Fe^2) with 59.8 to 65.8% in sample LD10-084 and 57.4 to 60.8% in sample SW16, but have relatively high amounts of the spessartine (Mn) end-member. Garnets of sample SW14 have up to 24.1% and garnets in LD10-084 up to 14.5% of the spessartine end-member. The presence of garnet is often suggested to indicate medium to high pressure metamorphism, but high-Mn almandine garnets similar to the observed PMG garnets are found in rocks of the Buchan succession of NE Scotland and formed at pressures below 3.5 kbar (Viete et al., 2010). **Figure 14B** displays the garnet end-member composition of the analysed samples in double ternary diagrams in comparison to garnets of low pressure-high temperature terranes (after Suggate and Hall, 2014).

Geochemical analyses indicate compositional trends for PMG rocks that resemble igneous rocks. Metapelites have a dacitic composition, quartzites and quarzitic hornfels have rhyolitic character and metabasites have a basaltic composition (**Figure 12A**). Metapelites have relatively restricted SiO_2 contents of 58.5 to 66.6 wt% with K_2O contents of 2.3 to 3.9 wt%, which are higher than those of the volcanic rocks of similar SiO_2 contents (**Figure 12B**). Trace element compositions closely resemble those observed in intrusive and volcanic samples and the PMG rocks have a volcanic arc affinity (**Figure 12C**). What is particularly striking is the similarity of plots of the metamorphic rocks and the volcanic rocks of the Schwaner Mountains on trace element spider diagrams (**Figure 12G**). Some metapelites of the PMG also resemble slightly sheared volcanic rocks and can also be named meta-volcanic rocks (e.g., LD10-102 A, LD10-124). Some PMG quartzites/hornfels also resemble the Menunuk Volcanics sample (**Figure 12D**).

DISCUSSION

Magmatism in the Schwaner Mountains

The new and literature U-Pb geochronology results from the Schwaner Mountains are displayed on **Figure 15** and are listed in **Table 2**. Based on the results of this study and previous work (e.g., Williams et al., 1988; Bladon et al., 1989; van Hattum et al., 2013; Hennig et al., 2017), there were several pulses of magmatism.

Triassic Magmatism in Sundaland

The oldest magmatic rocks in the Schwaner Mountains are Triassic. They are from the NWSZ which was part of West Borneo at the SE edge of Sundaland in the Triassic and are separated from SW Borneo by a suture (**Figures 1B**, **2B**) as

explained by Hennig et al. (2017). The I-type granitoids were interpreted as the product of Triassic Paleo-Pacific subduction beneath Sundaland (Hennig et al., 2017). No other Triassic igneous rocks have been found in the large area of the Schwaner Mountains (NSZ and SSZ) investigated in this study or in previous studies (e.g., Williams et al., 1988).

Jurassic Within-Plate Magmatism

Early Jurassic Phase at c. 190 Ma: Belaban Granite

The Belaban Granite is the oldest granitoid found in the SSZ with a zircon U-Pb age of 186.7 ± 2.3 Ma (**Figure 15**), significantly older than the biotite K-Ar age of 153.5 ± 3.5 Ma of Haile et al. (1977) and Bladon et al. (1989). It also contains the only pre-Jurassic inherited zircon (357.8 ± 4.2 Ma) identified in the igneous rocks of the NSZ and SSZ of the Schwaner Mountains. Geochemically it is a WPG or A-type granite (**Figures 9**, **10**), and we suggest this reflects a rift-related character. Rifting of the Australian margin was underway from the Triassic (e.g., Longley et al., 2002) and the Belaban Granite is suggested to be associated with extension in the Gondwana margin in NW Australia.

Late Jurassic Phase at c. 150 Ma: Mentembah Granite

In the area of the Belaban Granite we found another Jurassic granitoid provisionally named the Mentembah Granite after the highest mountain nearby. The U-Pb age of 151.2 ± 1.2 (**Figure 15**) is similar to the 153.5 ± 3.5 Ma K-Ar age for the Belaban Granite (Haile et al., 1977) which may indicate that the K-Ar age was reset during Late Jurassic magmatism. The U-Pb age is also similar to an inherited zircon age in the Sukadana Granite (van Hattum et al., 2013). This suggests widespread Jurassic magmatism in the SSZ during extension within the NW Australian margin which led to separation of the Banda (SW Borneo) and the Argo (East Java-West Sulawesi) blocks in the Late Jurassic (Hall, 2012; Hennig et al., 2016, Hennig et al., 2017).

Cretaceous Subduction-Related Magmatism

The different phases of Cretaceous magmatism are shown on **Figures 15**, **16**.

Early Cretaceous Phase I at c. 130 Ma: Menunuk Volcanics

Volcanic and sheared volcanic rocks were sampled from the northern margin of the NSZ relatively close to the type locality of the Menunuk Volcanics to which we conclude they belong. The rocks have a rhyolitic composition and a volcanic arc signature (**Figure 12**). They yielded ages of c. 130 to 132 Ma (**Figure 15**) which are the first radiometric ages for this volcanic group. Two quartzites of the PMG have similar protolith ages (**Figure 15**) and geochemistry (**Figure 12**), and are interpreted here to represent metamorphosed Menunuk Volcanics. Several other PMG samples also have inherited zircons of this age (**Figure 15**). We interpret all these ages as marking a major Cretaceous magmatic phase I at c. 132 Ma following subduction initiation beneath SW Borneo. This implies docking of SW Borneo with southeastern Sundaland before this, since both (NSZ and NWSZ) record this magmatic phase (Hennig et al., 2017).

Early Cretaceous Phase II at c. 115 Ma: Sepauk Tonalite

The predominant tonalites and diorites of the NSZ have ages between 110 and 120 Ma (**Figure 15**), a volcanic arc trace element signature and relatively low K_2O (**Figures 9**, **10**). The Sepauk Tonalite is the main batholith in the NSZ (**Figure 4**) which we interpret formed during Cretaceous phase II of Paleo-Pacific subduction. As with the older magmatic rocks, no inherited zircons were found. This is probably a result of remelting immature volcanic arc material or may indicate they are mantle derived.

Several PMG samples show magmatic or recrystallised zircons of this age, suggesting they are either volcanic products of phase II or slightly older volcanic rocks subsequently recrystallised at c. 110 Ma (**Figure 15**). A granodiorite of 118.6 ± 1.1 Ma from the NWSZ (Hennig et al., 2017) is interpreted as part of phase II further supporting the suturing of West Borneo and SW Borneo before this time.

Late Cretaceous Phase III at c. 100 Ma: Laur Granite

The Laur Granite is an alkali granite which is significantly younger (96.8 ± 0.6 Ma) than the Early Cretaceous Sepauk Tonalite (**Figure 15**). It is a felsic granite which plots at the VAG and WPG boundary (**Figure 9**). On the trace element spider plot there are some similarities to the Sepauk Tonalite (**Figure 10D**). A subduction-related tonalite from the NWSZ (Hennig et al., 2017) yielded an age of 101.5 ± 0.6 Ma relative similar to the Laur Granite (**Figure 15**), and is geochemically more similar to the Sepauk Tonalite. This supports a subduction-related origin interpretation for the Laur Granite. Inherited zircons in the Rantau Asem Tonalite have also similar ages around 100 Ma (**Figure 15**). We interpret this to indicate that phase III extended from the NWSZ to the easternmost part of the Schwaner Mountains where the Rantau Asem Tonalite was found. We interpret the Laur Granite as subduction-related, and this phase produced a range of rock types from alkali granite to tonalite.

Late Cretaceous Phase IV at c. 90 Ma: Rantau Asem Tonalite

A tonalite at the eastern end of the Schwaner Mountains yielded an age of c. 90 Ma (**Figure 15**). It is petrographically similar to the Sepauk Tonalite samples, but as it is significantly younger, we name it the Rantau Asem Tonalite (derived from a nearby village). Two PMG samples yielded recrystallised zircons with this age and a Jurassic meta-granitoid from the NWSZ was interpreted by Hennig et al. (2017) to be metamorphosed at this time (**Figure 15**). This indicates a large area was affected and we interpret this widespread c. 90 Ma magmatism to be the final subduction-related phase in the NSZ.

Late Cretaceous Within-Plate Magmatism

Late Cretaceous Phase V Within-Plate Magmatism at c. 80 Ma: Sukadana Granite

The Sukadana Granite of the SSZ was dated in this study from samples collected close to the boundary with the NSZ and in the

far east of the Schwaner Mountains where granitoids were previously assumed to be part of the Sepauk Tonalite. The new U-Pb ages of c. 79 Ma (**Figure 15**) are slightly younger than K-Ar ages of c. 81 to 89 Ma (**Table 1**) reported by Haile et al. (1977), Bladon et al. (1989) and De Keyser and Rustandi (1993), and biotite/whole-rock Rb-Sr and zircon U-Pb ages of c. 80 to 85 Ma (**Tables 1**, **2**) of De Keyser and Rustandi (1993) and van Hattum et al. (2013), indicating that the phase of magmatism that produced the Sukadana Granite was probably from c. 78 to 85 Ma based on the more precise U-Pb zircon and Rb-Sr data.

The Sukadana Granite is characterised by high K_2O values that led Williams et al. (1988) to identify a suite of Schwaner Mountains Potassic Granites. Geochemically it comprises mainly granites with a WPG or A-type signature (**Figures 9**, **10**). Sample LD10-010 has a trace element signature similar to the Sepauk Tonalite with slight enrichment in HFSE suggesting partly remelting of a Sepauk Tonalite. Sample EK14-10 from the NWSZ has a similar age (Hennig et al., 2017) and we interpret it as Sukadana Granite or contemporaneous equivalent (**Figure 15**). The Pueh and Gading granites, which are part of the Upper Cretaceous Northern granites in Sarawak and Kalimantan (**Figure 2**), have similar ages to the Sukadana Granite (Hennig et al., 2017) and indicate that smaller plutons were intruded near the northern margin of the Kuching Zone close to the Lupar Line at the same time as the Sukadana Granite (**Figure 15**).

Late Cretaceous Phase VI Within-Plate Magmatism at c. 70 Ma: Sangiyang Granite

The youngest phase of Cretaceous magmatism in the Schwaner Mountains found in this study is recorded by the Sangiyang Granite, dated as 72.1 ± 0.6 Ma (**Figure 15**). The sample was collected from a NNW-SSE striking mountain complex previously mapped as Sukadana Granite west of the type locality Bukit Sangiyang. The Sangiyang Granite samples are alkali granites and are the most SiO_2-enriched granitoids of this study. In the tectonic discrimination diagrams they are clearly identified as WPG or A-type granites, supported by the trace element spider plot (**Figures 9**, **10**), which we interpret to have been emplaced after the larger Sukadana Granite.

Modern River Sands

The river sands were collected mainly from the central NSZ and SSZ from rivers that drain approximately 10,000 km^2 of the total 74,000 km^2 area mapped as granites (Pieters and Supriatna, 1990; Tate, 2001), based on rivers and drainage basins in the global Hydro1K (2020) dataset. **Figure 16** suggests the majority of zircons were derived from the intrusive rocks of the NSZ with minor contributions from the Menunuk Volcanics and PMG, and from the Sukadana Granite of the SSZ. The area drained by the sampled rivers suggests little or no contribution from the Jurassic plutons of the SSZ as there are only two Jurassic zircons in the sands. The main peak in the river sands correlates with the Sepauk Tonalite age of c. 112 Ma (**Figure 16**). A strong peak at c. 105 Ma indicates a granite that has so far not been found. The Laur Granite age correlates with a peak at c. 96 Ma, and the Rantau Asem Tonalite broadly correlates with a wider peak between 88 to 92 Ma in the river sands. A relatively broad peak between 76 and 85 Ma corresponds to the Sukadana Granite. The abundance of zircons of Sukadana Granite age supports the suggestion that the Sukadana Granite is more widespread in the Schwaner Mountains than previously assumed. The youngest peak in the river sands is at c. 70 Ma and slightly younger than the Sangiyang Granite indicating that magmatism did not stop until the end of the Cretaceous (**Figure 16**). A small population at c. 61 Ma suggests some Paleocene magmatism. The youngest ages around 20 to 25 Ma belong to zircons probably derived from the Neogene Sintang Suite that intruded the Schwaner granitoids (Breitfeld et al., 2019). There is one Triassic, one Permian and one Silurian zircon in the river sands, which we suggest is explained by recycling of the few older zircons from nearby PMG. There is no evidence that the Sundaland basement of the NWSZ extends into the NSZ, and the river sands support the conclusion that there are no Triassic granites anywhere in the NSZ and SSZ.

Age of the Pinoh Metamorphic Group

This study confirms the results of Davies et al. (2014) that the metamorphic rocks are not Paleozoic. Magmatic zircons within the PMG range from c. 110 to 135 Ma and indicate that most protoliths were initially formed in the Early Cretaceous (**Figures 15**, **16**) and incorporated some older detrital grains. The oldest Cretaceous ages of the PMG and the Menunuk Volcanics are indistinguishable and we conclude that some PMG rocks are the metamorphosed products of the Menunuk Volcanics or contemporaneous volcaniclastic equivalents. Early Cretaceous zircons (c. 110–120 Ma) correlate with the Sepauk Tonalite and suggest that other PMG rocks are metamorphic products of igneous activity contemporaneous with Cretaceous phase II (**Figure 15**). Recrystallised zircons of c. 110 Ma in PMG samples also indicate a thermal overprint that coincides with phase II (**Figure 15**). This thermal overprint is also recorded in the $^{40}Ar/^{39}Ar$ analysis of L3 coarse biotite (+broken biotite in L2) and L1 white mica (**Figure 8**). A later phase of thermal metamorphism is recorded only in recrystallised zircons (and not by Ar geochronology) and ranges from c. 80 to 90 Ma. This coincides with phase IV Rantau Asem Tonalite and phase V Sukadana Granite magmatism (**Figure 15**). The Mn-rich almandine garnets indicate Buchan-type HT-LP metamorphism which was associated either with phase II and/or phases IV/V magmatism implying contemporaneous extension.

After Cretaceous metamorphism, there was a PMG shearing event (Sz) in the Late Oligocene (**Figure 8**) recorded by $^{40}Ar/^{39}Ar$ ages of fine-grained biotite (L2) associated with biotite-fibrolite intergrowth. The age of c. 27 Ma is very similar to $^{40}Ar/^{39}Ar$ ages from the West Sarawak Metamorphics (Breitfeld et al., 2017) and to apatite fission-track ages in East Kalimantan interpreted as recording major denudation and uplift in central Borneo (Moss et al., 1998). This suggests that southern and central Borneo were likely affected by a major shearing event in the Late Oligocene which directly preceded the main Sintang Suite magmatism at c. 20 Ma in the same area (Breitfeld et al., 2019).

Origin of Triassic and Older Zircons

No inherited grains older than Jurassic have been found in igneous rocks of the NSZ. The Belaban Granite in the SSZ has a single Carboniferous inherited zircon. Four samples from the PMG yielded in total 66 inherited zircons older than 160 Ma (**Figure 17**). LD10-102B has one, LD10-069 and LD10-004 have a small number and there are abundant grains in SW14. The main Phanerozoic peak is Triassic-Late Permian (200–260 Ma) and there are 23 grains with ages from Permian to Cambrian. The 18 Precambrian ages are scattered between c. 0.6 to 2.5 Ga with a pronounced peak at c. 1.8 Ga. The paucity of older zircons is not a sampling problem; we spent considerable time processing samples trying to recover older zircons after the unexpected discovery of Cretaceous zircons in PMG samples. Although there was no previous dating of the PMG, we had expected, like others, the PMG to be much older. Furthermore, as noted above, there are only three pre-Jurassic zircons in the 837 concordant zircon ages from river sands.

A Sundaland West Borneo source for Triassic and older grains is possible but compared to the PMG (**Figure 17**) West Borneo has a bigger Late Triassic peak and lacks any Proterozoic ages between 0.6 and 1.8 Ga (Hennig et al., 2017). An alternative is that the inherited grains were detrital grains in sandstones that formed the sedimentary cover of the SW Borneo Block when it was within the Gondwana NW Australian margin. The Phanerozoic PMG ages resemble those from the Karimunjawa Arch (Witts et al., 2012), south of Borneo in the Java Sea (**Figure 1B**), which was at the southern edge of the Banda (SW Borneo) Block (**Figure 3**) before rifting. The Carboniferous zircons of the PMG are slightly younger than those in the Karimunjawa Arch, which could be explained by lead-loss. However, Precambrian ages differ markedly (**Figure 17**); the Karimunjawa Arch lacks the distinctive 1.8 Ga peak of the PMG and instead has its main peak at c. 1.4 Ga—a feature more similar to the Argo Block (**Figure 3**) (Zimmermann and Hall, 2019), but the Karimunjawa Arch lacks the common Archean zircons of that block (Smyth et al., 2008). Overall, the Triassic and older zircon ages from the PMG and the river sands are most similar to the Bird's Head (**Figure 17**; Gunawan et al., 2012; Zimmermann and Hall, 2016) and consistent with a Banda Block origin. There may have been also a West Borneo contribution in the Cretaceous to the PMG volcaniclastic sediments.

Early Mesozoic Position of SW Borneo

As plate tectonic models for SE Asia developed, the region was divided into terranes which were thought to have been derived from China or Australia. Metcalfe (e.g., 1990, 1996) suggested that there were two important continental terranes of possible South China/Indochina origin in western Borneo, Semitau and SW Borneo, separated from Sundaland (East Malaya) by a suture offshore in the Sunda Shelf. Later, SW Borneo was interpreted as continental terrane rifted from the NW Australian margin in the Jurassic (e.g., Hall et al., 2009; Metcalfe, 2009; Hall, 2012) which was added to Sundaland in the Early Cretaceous (**Figure 3**). Recent studies (Setiawan et al., 2013; Hennig et al., 2017) have shown there are Triassic meta-granitoids in the NWSZ meaning that the Sundaland-SW Borneo suture is within Borneo, rather than offshore as suggested by Metcalfe. West Borneo, of approximately similar extent to the Semitau terrane, was part of Sundaland by the Triassic (**Figure 3A**) and includes rocks with an Indochina affinity. In NW Kalimantan and West Sarawak there are Triassic arc-related sediments (e.g., Sadong Formation, Balaisebut Group), igneous rocks (e.g., Jagoi Granodiorite, Serian Volcanics) and metamorphic rocks (e.g., West Sarawak Metamorphics, Embuoi Complex). Sediments of the Sadong Formation have thereby a Cathaysian flora (Kon'no, 1972). Breitfeld et al. (2017) and Hennig et al. (2017) interpret these rocks to be the product of west-directed Triassic Paleo-Pacific subduction (**Figure 3A**). Thus, our interpretation (Hall, 2012; Hennig et al., 2017; Breitfeld et al., 2017) is that SW Borneo (Banda Block) separated from NW Australia in the Late Jurassic, was added to Sundaland in the Early Cretaceous to form the West Borneo-SW Borneo suture (**Figures 1**, **2**) and then the East Java-West Sulawesi (Argo Block) was added later in the Cretaceous at c. 90–80 Ma (Smyth et al., 2007) at the Meratus Suture which terminated subduction in the region until the Cenozoic.

Burton-Johnson et al. (2020) have recently challenged the view that SW Borneo was added in the Cretaceous and suggested that it was already part of Sundaland in the Triassic. Triassic and Jurassic granitoids in NE Sabah (Segama Valley) have long been known based on K-Ar dating (Kirk, 1968; Leong, 1974) but these and other pre-Cretaceous radiometric ages from Sabah were dismissed as spurious (e.g., Hutchison, 1992; Hutchison, 2005; Omang and Barber, 1996) because they were significantly older than the Cretaceous radiolarian ages from the Chert-Spilite Formation which were assumed to be the cover to a Sabah ophiolitic basement. U-Pb zircon geochronology by Burton-Johnson et al. (2020) confirmed the Triassic and Jurassic ages of the granitoids which they suggested were arc rocks that intrude ophiolitic rocks. They suggested these could be correlated with West Borneo granitoids (Hennig et al., 2017) and volcanics (Breitfeld et al., 2017) and proposed that a Triassic and Jurassic arc of Sabah was an autochthonous continuation of the Sundaland Paleo-Pacific arc, and that SW Borneo was part of Sundaland in the Triassic. We summarise in the next section the principal objections to this proposal.

Segama Granitoid Correlations: Sundaland or Australian Origin?

Burton-Johnson et al. (2020) interpreted the Segama granitoids to intrude older ophiolitic rocks although conceded that "it is hard to prove" that the [intruded] basalt is truly ophiolitic rather than the product of non-ophiolitic arc magmatism. They suggest that a 217 Ma K-Ar age from a metagabbro from Darvel Bay may support the ophiolitic option although they fail to observe that this is more than 30 Ma younger than their U-Pb ages from the Segama granitoids. The descriptions of the mainly basic metamorphic rocks intruded by the granitoids (Leong, 1974) do suggest an ophiolitic or arc origin. However, this provides no information on the position of the Segama granitoids in the Triassic which could have been almost anywhere in the West Pacific.

For example, Triassic sandstones, together with Jurassic-Cretaceous metamorphic rocks, have been dredged from the

South China Sea north of Sabah, and Triassic and older K-Ar ages were obtained from detrital biotites in the sandstones (Kudrass et al., 1986). Although Triassic granites have not yet been found, Jurassic and Cretaceous granitoids from the South China Sea contain Triassic and older inherited zircons and these are interpreted as part of a Mesozoic accretionary complex at an Andean-type Paleo-Pacific subduction margin (e.g., Yan et al., 2014; Xu et al., 2016). Thus, an East Asian margin origin is plausible. Triassic sandstones from the Bird's Head of New Guinea contain abundant Triassic and older zircons indicating a continental Andean-type subduction setting at the north Australian margin during the Paleozoic until the early Jurassic (e.g., Audley-Charles, 1991; Metcalfe, 1996; Gunawan et al., 2012; Zimmermann and Hall, 2016). Thus, northern Australia is another possible location.

The nearest possible correlative Triassic (Bladon et al., 1989) metamorphic rocks, gabbros and granitoids in Borneo are part of the Busang Complex in central Kalimantan 700 km from Sabah (**Figure 1B**). They are thought to be part of a melange (Tate, 1991; Pieters et al., 1993a) beneath Cretaceous sedimentary rocks (Heryanto and Jones, 1996). West Borneo is even further away (1000 km). But even if the hypothesis of a continuous arc over such a great distance is accepted all the arc rocks are north of the NSZ and separated from West Borneo and the Kuching Zone by sutures (the West Borneo-SW Borneo suture of this paper and the Boyan Suture of Metcalfe (1990).

As we have pointed out above there is no evidence of Triassic granites anywhere in the NSZ or SSZ of the SW Borneo Block, an area of c. 74,000 km^2. However, on the basis of similar Jurassic ages Burton-Johnson et al. (2020) suggest the Segama granitoids can be correlated with a NWSZ meta-granodiorite. However, this meta-granodiorite records multiple Jurassic igneous phases (Hennig et al., 2017; **Figure 15**), which are not present in the Segama granitoids. The Jurassic SSZ rock of this study is of WPG character, while the Segama granitoids are arc-related. We suggest a correlation of granitoids, across at least one suture zone, and in case of the SSZ rock of different character, is implausible.

Burton-Johnson et al. (2020) appear to consider all the ophiolites of Borneo to be a single unit. Given the number of suture zones identified in Borneo (e.g., Hutchison, 1989; Metcalfe, 1990; Metcalfe, 2013) which include ophiolites we question this assumption. They imply that a Pt-Os age of 197.8 ± 8.1 Ma (Coggon et al., 2011) obtained from alluvial grains of platinum-group minerals (PGM) collected at an uncertain location from a river in the Meratus Mountains not only dates the Meratus ophiolite but also indicates that the ophiolite formed at the southern margin of the SW Borneo Block in its present-day position. Ophiolitic, radiolarian-bearing (Wakita et al., 1998), volcanic (Sikumbang, 1986) and HP-LT metamorphic rocks (Parkinson et al., 1998) are found within the well-known Cretaceous Meratus suture (Metcalfe, 1990) east of SW Borneo. None of these rocks can be assumed to have formed in their present position and all are generally interpreted to have been accreted to SW Borneo during Cretaceous subduction (e.g., Metcalfe, 1990; Wakita et al., 1998). Thus, the Meratus ophiolite gives no information about the position of SW Borneo in the Triassic. Furthermore, it is worth noting that the source of alluvial grains found in rivers is commonly difficult to identify, and a Meratus ophiolite source for the PGM suggested by Coggon et al. (2011) is simply an assumption. Alluvial diamonds from rivers in the Meratus area and western Borneo illustrate this problem well and the source of these diamonds remains uncertain; nonetheless recent studies (e.g., Kueter et al., 2016; White et al., 2016) have been used to support the tectonic model we have proposed.

The confirmation of Triassic and Jurassic ages by Burton-Johnson et al. (2020) for arc-related igneous rocks in Sabah does not answer the question where they were located in the Early Mesozoic. As observed above, both northern Australia and East Asia/eastern Sundaland were subduction margins. Metcalfe (1990) identified a Mangkalihat terrane in NE Kalimantan that separated from NW Australia in the Late Jurassic, and included this (Metcalfe, 2013) as part of the East Java-West Sulawesi terrane of Hall et al. (2009). Hennig et al. (2016) identified an Australian-derived terrane spanning NW Sulawesi, NE Kalimantan and East Sabah as an Inner Banda Block rifted in the Late Jurassic. Igneous and metamorphic rocks from this block in Sulawesi have Triassic inherited zircons (Hennig et al., 2016; van Leeuwen et al., 2016). Other possibilities are that the Sabah arc rocks were situated somewhere further north in the East Asian margin, or were even in an intra-oceanic position in the Pacific. There is no possibility of obtaining faunal or palaeomagnetic evidence that could help to solve this problem since none of the granitoid areas retain any sedimentary cover and there are no suitable rocks or paleohorizontal markers to use in palaeomagnetic investigations. The only way to resolve this question is using zircon data, but currently there are too few analyses from the Segama granitoids, or other rocks in Sabah, that might help. Our study, and that of Burton-Johnson et al. (2020), both indicate the need for new high-quality dating studies in Borneo.

CONCLUSION

- Jurassic within-plate or A-type granites in the SSZ formed during rifting of the SW Borneo Block in the Jurassic from NW Australia and are not related to subduction.
- The rocks of the Schwaner Mountains in the NWSZ, NSZ and SSZ are mainly a product of Cretaceous magmatism indicated by Cretaceous zircons in all metamorphic and igneous rocks. Cretaceous igneous rocks in the NSZ and NWSZ are interpreted to record magmatism in a volcanic arc due to subduction from c. 135 to 90–85 Ma.
- After subduction ceased at c. 90–85 Ma, there were at least two phases of post-collision magmatism that are predominantly exposed in the SSZ. The large Sukadana Granite occupies most of the SSZ and is dated as c. 85 to 79 Ma. It was intruded by smaller stocks of the Sangiyang Granite at c. 72 Ma. Contemporaneous with the Sukadana Granite was the emplacement of smaller granitoid bodies near to the Lupar Line in West Sarawak and central Kalimantan.
- There is no evidence for a continuation of the Triassic and Jurassic Paleo-Pacific subduction margin from West Borneo (the Triassic eastern Sundaland margin) into SW and central Borneo. It is unlikely that the West Borneo basement extends south of the Ketapang area where within-plate granites indicate SWB rifting and are not related to subduction.

- The Pinoh Metamorphic Group, which has previously been interpreted as part of an ancient Paleozoic core to SW Borneo, is predominantly composed of Cretaceous metapelites. We suggest that the metapelites were derived from volcaniclastic sediments erupted between c. 135 to 110 Ma, and subsequently metamorphosed during granitoid emplacement from 120–80 Ma. Garnets of the PMG are spessartine-rich almandines that indicate HT-LP Buchan-type metamorphism and formed during Cretaceous granitoid emplacement.
- A few detrital pre-Jurassic zircons in the PMG rocks and river sediments recording ages from the Triassic to the Precambrian indicate reworking of some older material during deposition of the PMG protoliths. They are interpreted to be sourced by cover of the SW Borneo basement which originated close to the Bird's Head, with possible contributions from the Karimunjawa Arch and West Borneo basement.

DATA AVAILABILITY STATEMENT

All datasets presented in this study are included in the article/ **Supplementary Material**.

ETHICS STATEMENT

Written informed consent was obtained from the relevant individual(s) for the publication of any potentially identifiable images or data included in this article.

AUTHOR CONTRIBUTIONS

HTB: manuscript draft, visualisation, methodology, data validation, sample processing, LA-ICP-MS geochronology, data reduction, data interpretation. LD: field work, sample collection, sample processing, LA-ICP-MS geochronology, and paragraph drafting. RH: drafting the manuscript, editing and review. RA: SHRIMP analysis, data reduction, and age calculation. MF: sample preparation of Ar/Ar samples for irradiation and mass spec analysis. Analysis of Ar/Ar analysis, and interpretation of Ar/Ar results. GL: discussion and interpretation of Ar/Ar results. MT: XRF whole rock geochemistry and data reduction. NG: ICP-AES whole rock geochemistry and data reduction. JHB: visualisation, data interpretation, editing and review. MvH: sample processing for geochemistry.

FUNDING

This project was funded by the SE Asia Research Group of Royal Holloway University of London, which is supported by a consortium of oil companies.

ACKNOWLEDGMENTS

We thank Alfend Rudyawan, A. M. Surya Nugraha and Duncan Witts for assistance in the field. Martin Rittner, Pieter Vermeesch and Andy Carter (Birkbeck University of London) are thanked for help and support with the LA-ICP-MS analysis, and Anton Kearsley at the NHM for help with CL images for some LA-ICP-MS samples. Theo van Leeuwen, D. Hendrawan and Rio Tinto Exploration Indonesia helped in obtaining RT granite samples from west Kalimantan. Christina Manning (Royal Holloway University of London) assisted with the data reduction of the geochemical analyses. Andy Beard (Birkbeck University of London) helped with the microprobe analysis of garnets. We thank Julia Ribeiro for editorial support, and Alex Burton-Johnson and Abigail Barker for comments that helped to improve the manuscript.

SUPPLEMENTARY MATERIAL

The Supplementary Material for this article can be found online at: https://www.frontiersin.org/articles/10.3389/feart.2020.568715/full#supplementary-material.

REFERENCES

Amiruddin (1989). *The preliminary study of the granitic rocks of West Kalimantan, Indonesia (Project B-Geol.951)*. Wollongong, Australia: University of Wollongong.

Amiruddin and Trail, D. S. (1993). *Geology of the nangapinoh sheet area, Kalimantan. Map at 1: 250000 scale*. Bandung, Indonesia: Geological Research and Development Centre.

Andersen, T. (2002). Correction of common lead in U-Pb analyses that do not report 204Pb. *Chem. Geol.* 192, 59–79. doi:10.1016/s0009-2541(02)00195-x

Areshev, E. G., Dong, T. L., San, N. T., and Shnip, O. A. (1992). Reservoirs in fractured basement on the continental shelf of southern Vietnam. *J. Petrol. Geol.* 15, 451–464. doi:10.1111/j.1747-5457.1992.tb00719.x

Audley-Charles, M. G. (1991). Tectonics of the new Guinea area. *Annu. Rev. Earth Planet Sci.* 19, 17–41. doi:10.1146/annurev.ea.19.050191.000313

Beltrando, M., Lister, G. S., Forster, M., Dunlap, W. J., Fraser, G., and Hermann, J. (2009). Dating microstructures by the 40Ar/39Ar step-heating technique: deformation-pressure-temperature-time history of the penninic units of the western alps. *Lithos* 113, 801–819. doi:10.1016/j.lithos.2009.07.006

Black, L. P., Kamo, S. L., Allen, C. M., Davis, D. W., Aleinikoff, J. N., Valley, J. W., et al. (2004). Improved 206Pb/238U microprobe geochronology by the monitoring of a trace-element-related matrix effect; SHRIMP, ID-TIMS, ELA-ICP-MS and oxygen isotope documentation for a series of zircon standards. *Chem. Geol.* 205, 115–140. doi:10.1016/j.chemgeo.2004.01.003

Bladon, G. M., Pieters, P. E., and Supriatna, S. (1989). Preliminary Report. Catalogue of isotopic ages commissioned by the Indonesia-Australia Geological Mapping Project for igneous and metamorphic rocks in Kalimantan. Bandung, Indonesia: Geological Research and Development Centre.

Breitfeld, H. T., Hall, R., Galin, T., and BouDagher-Fadel, M. K. (2018). Unravelling the stratigraphy and sedimentation history of the uppermost cretaceous to Eocene sediments of the kuching zone in west Sarawak (Malaysia), Borneo. *J. Asian Earth Sci.* 160, 200–223. doi:10.1016/j.jseaes.2018.04.029

Breitfeld, H. T., Hall, R., Galin, T., Forster, M. A., and BouDagher-Fadel, M. K. (2017). A triassic to cretaceous sundaland-pacific subduction margin in west Sarawak, Borneo. *Tectonophysics* 694, 35–56. doi:10.1016/j.tecto.2016.11.034

Breitfeld, H. T. and Hall, R. (2018). The eastern Sundaland margin in the latest cretaceous to late Eocene: sediment provenance and depositional setting of the Kuching and Sibu zones of Borneo. *Gondwana Res.* 63, 34–64. doi:10.1016/j.gr.2018.06.001

Breitfeld, H. T., Macpherson, C., Hall, R., Thirlwall, M., Ottley, C. J., and Hennig-Breitfeld, J. (2019). Adakites without a slab: remelting of hydrous basalt in the crust and shallow mantle of Borneo to produce the Miocene Sintang suite and bau suite magmatism of west Sarawak. *Lithos* 344–345, 100–121. doi:10.1016/j.lithos.2019.06.016

Burton-Johnson, A., Macpherson, C. G., Millar, I. L., Whitehouse, M. J., Ottley, C. J., and Nowell, G. M. (2020). A triassic to Jurassic arc in north Borneo: geochronology, geochemistry, and genesis of the Segama Valley felsic intrusions and the Sabah ophiolite. *Gondwana Res.* 84, 229–244. doi:10.1016/j.gr.2020.03.006

Coggon, J. A., Nowell, G. M., Pearson, D. G., and Parman, S. W. (2011). Application of the 190Pt-186Os isotope system to dating platinum mineralization and ophiolite formation: an example from the Meratus Mountains, Borneo. *Econ. Geol.* 106, 93–117. doi:10.2113/econgeo.106.1.93

Collins, L. G. and Collins, B. J. (2013). Origin of myrmekite as it relates to K-, Na-, and Ca-metasomatism and the metasomatic origin of some granite masses where myrmekite occurs. *Contrib. Mineral. Petrol.* 213, 123–156.

Creaser, R. A., Price, R. C., and Wormald, R. J. (1991). A-type granites revisited: assessment of a residual-source model. *Geol.* 19, 163–166. doi:10.1130/0091-7613(1991)019<0163:atgrao>2.3.co;2

Davies, L., Hall, R., and Armstrong, R. (2014). "Cretaceous crust in SW Borneo: petrological, geochemical and geochronological constraints from the Schwaner Mountains," in Proceedings Indonesian Petroleum Association, 38th annual convention and exhibition. IPA14-G-025, Jakarta, Indonesia, 21–23 May 2014.

De Keyser, F. and Rustandi, E. (1993). *Geology of the Ketapang sheet area, Kalimantan. Map at 1: 250000 scale*. Bandung, Indonesia: Geological Research and Development Centre.

De La Roche, H., Leterrier, J., Grandclaude, P., and Marchal, M. (1980). A classification of volcanic and plutonic rocks using R 1 R 2 -diagram and major-element analyses—its relationships with current nomenclature. *Chem. Geol.* 29, 183–210. doi:10.1016/0009-2541(80)90020-0

Forster, M. A. and Lister, G. S. (2008). Tectonic sequence diagrams and the structural evolution of schists and gneisses in multiply deformed terranes. *J. Geol. Soc.* 165, 923–939. doi:10.1144/0016-76492007-016

Forster, M. A. and Lister, G. S. (2004). The interpretation of 40Ar/39Ar apparent age spectra produced by mixing: application of the method of asymptotes and limits. *J. Struct. Geol.* 26, 287–305. doi:10.1016/j.jsg.2003.10.004

Forster, M. and Lister, G. (2009). Core-complex-related extension of the Aegean lithosphere initiated at the Eocene-Oligocene transition. *J. Geophys. Res.: Solid Earth* 114 (B2). doi:10.1029/2007jb005382

Frost, B. R., Barnes, C. G., Collins, W. J., Arculus, R. J., Ellis, D. J., and Frost, C. D. (2001). A geochemical classification for granitic rocks. *J. Petrol.* 42, 2033–2048. doi:10.1093/petrology/42.11.2033

Griffin, W. L., Powell, W. J., Pearson, N. J., and O'Reilly, S. Y. (2008). "GLITTER: data reduction software for laser ablation ICP-MS," in *Laser ablation-ICP-MS in the earth sciences: current practices and outstanding issues mineralogical association of Canada, short course series 40*. Editor P. J. Sylvester (Quebec City, QC, Canada: Mineralogical Association of Canada), 308–311.

Gunawan, I., Hall, R., and Sevastjanova, I. (2012). "Age, character and provenance of the Tipuma Formation, West Papua: new insights from detrital zircon dating," in Proceedings indonesian petroleum association, 36th annual convention. IPA12-G-027, 1–14. Jakarta, Indonesia. May 2012. doi:10.29118/IPA.0.12.G.027

Haile, N. S. and Bignell, J. D. (1971). Late Cretaceous age based on K/Ar dates of granitic rock from the Tambelan and Bunguran islands, Sunda Shelf, Indonesia. *Geol. Mijnbouw* 50, 687–690.

Haile, N. S. (1974). "Borneo," in *Mesozoic-cenozoic orogenic belts*. Editor A.M. Spencer. (London, United Kingdom: Geological Society of London Special Publication) 4, 333–347.

Haile, N. S., McElhinny, M. W., and McDougall, I. (1977). Palaeomagnetic data and radiometric ages from the cretaceous of west Kalimantan (Borneo), and their significance in interpreting regional structure. *J. Geol. Soc. London* 133, 133–144. doi:10.1144/gsjgs.133.2.0133

Haile, N. S. (1970). Notes on the geology of the Tambelan, Annambas and Bunguran (Natuna) islands, Sunda shelf, Indonesia: including radiometric age determinations, U.N. ECAFE. Comm. Co-ordination of offshore proceedings (CCOP) 3. Geological Survey of Japan, Technical Bulletin, 55–89. doi:10.7186/bgsm03197011

Haile, N. S. (1973). West Borneo microplate younger than supposed?. *Nat. Phys. Sci.* 242, 28–29. doi:10.1038/physci242028a0

Hall, R., Clements, B., and Smyth, H. R. (2009). "Sundaland: basement character, structure and plate tectonic development," in Proceedings Indonesian petroleum association, 33rd annual convention, IPA09-G-134, Jakarta, Indonesia, 5–7 May 2009.

Hall, R. (2012). Late Jurassic-Cenozoic reconstructions of the Indonesian region and the Indian ocean. *Tectonophysics* 570–571, 1–41. doi:10.1016/j.tecto.2012.04.021

Hall, R. (2017). Southeast Asia: new views of the geology of the Malay archipelago. *Annu. Rev. Earth Planet Sci.* 45, 331–358. doi:10.1146/annurev-earth-063016-020633

Hamilton, W. (1979). *Tectonics of the Indonesian region*. Washington, DC: U.S.G.S. Prof. Paper, 1078, 345.

Hartono, U. (2012). *Magmatism in Kalimantan*. Bandung, Indonesia: Centre for Geological Survey, Geological Agency, Ministry of Energy and Mineral Resources, 199.

Hennig, J., Breitfeld, H. T., Hall, R., and Nugraha, A. M. S. (2017). The Mesozoic tectono-magmatic evolution at the Paleo-Pacific subduction zone in West Borneo. *Gondwana Res.* 48, 292–310. doi:10.1016/j.gr.2017.05.001

Hennig, J., Hall, R., and Armstrong, R. A. (2016). U-Pb zircon geochronology of rocks from west Central Sulawesi, Indonesia: extension-related metamorphism and magmatism during the early stages of mountain building. *Gondwana Res.* 32, 41–63. doi:10.1016/j.gr.2014.12.012

Hermanto, B., Bachri, S., and Atmawinata, S. (1994). *Geological map of the pankalanbuun quadrangle, Kalimantan, 1: 250,000*. Bandung, Indonesia: Geological Research and Development Centre (GRDC).

Heryanto, R. and Jones, B. G. (1996). Tectonic development of Melawi and Ketungau basins, Western Kalimantan, Indonesia 19. Bandung, Indonesia: Bulletin Geological Research and Development Centre, 151–179.

Hudson, N. F. C. (1985). Conditions of Dalradian metamorphism in the Buchan area, NE Scotland. *J. Geol. Soc.* 142, 63–76. doi:10.1144/gsjgs.142.1.0063

Hutchison, C. S. (1992). Evidence of multiphase deformation in the Rajang-Crocker Range (northern Borneo) from Landsat imagery interpretation: geodynamic implications-Comment (1). *Tectonophysics* 204, 175–177. doi:10.1016/0040-1951(92)90278-e

Hutchison, C. S. (1989). *Geological evolution of south-East Asia: Oxford monographs on geology and geophysics*, 13. Oxward, United Kingdom: Clarendon Press, 376.

Hutchison, C. S. (2005). *Geology of North-West Borneo. Sarawak, Brunei and Sabah*. Amsterdam, Netherlands: Elsevier, 421.

Hutchison, C. S. (1996). "The 'Rajang accretionary prism' and 'Lupar Line' problem of Borneo," in *Tectonic evolution of SE Asia*. Editors R. Hall and D. J. Blundell (London, United Kingdom: Geological Society of London Special Publication), 106, 247–261.

Hydro1K (2020). A global hydrologic database derived from 1996 GTOPO30 data. USGS EROS Archive—Digital Elevation—HYDRO1K. https://www.usgs.gov/centers/eros/science/usgs-eros-archive-digital-elevation-hydro1k/.

Janoušek, V., Farrow, C. M., and Erban, V. (2006). Interpretation of whole-rock geochemical data in igneous geochemistry: introducing Geochemical Data Toolkit (GCDkit). *J. Petrol.* 47, 1255–1259.

JICA (1979). *Report on the geological survey of central Kalimantan, republic of Indonesia*. Tokyo, Japan: Metal Mining Agency of Japan.

JICA (1982). *Report on the geological survey of west Kalimantan, republic of Indonesia (consolidated report)*. Tokyo, Japan: Metal Mining Agency of Japan.

Kirk, H. J. C. (1968). The igneous rocks of Sarawak and Sabah. Geological Survey of Malaysia, Borneo Region Bulletin 5, 210.

Kon'no, E. (1972). "Some late triassic plants from the southwestern border of Sarawak, east Malaysia," in *Geology and palaeontology of S.E. Asia*. Tokyo, Japan: University of Tokyo Press 10, 125–178.

Kudrass, H. R., Wiedicke, M., Cepek, P., Kreuzer, H., and Müller, P. (1986). Mesozoic and Cainozoic rocks dredged from the South China Sea (Reed Bank area) and Sulu Sea and their significance for plate-tectonic reconstructions. *Mar. Petrol. Geol.* 3, 19–30. doi:10.1016/0264-8172(86)90053-x

Kueter, N., Soesilo, J., Fedortchouk, Y., Nestola, F., Belluco, L., Troch, J., et al. (2016). Tracing the depositional history of Kalimantan diamonds by zircon

provenance and diamond morphology studies. *Lithos* 265, 159–176. doi:10.1016/j.lithos.2016.05.003

Le Bas, M. J., Le Maitre, R. W., Streckeisen, A., Zanettin, B., and IUGS Subcommission on the Systematics of Igneous Rocks. (1986). A chemical classification of volcanic rocks based on the total alkali-silica diagram. *J. Petrol.* 27, 745–750.

Leong, K. M. (1974). The geology and mineral resources of the Darvel Bay and upper Segama area Sabah. Geological Survey of Malaysia. Memoir 4 (revised).

Li, F., Sun, Z., and Yang, H. (2018). Possible spatial distribution of the Mesozoic volcanic arc in the present-day South China Sea continental margin and its tectonic implications. *J. Geophys. Res.: Solid Earth* 123, 6215–6235.

Li, X.-h. (2000). Cretaceous magmatism and lithospheric extension in Southeast China. *J. Asian Earth Sci.* 18, 293–305. doi:10.1016/s1367-9120(99)00060-7

Longley, I. M., Buessenschuett, C., Clydsdale, L., Cubitt, C. J., Davis, R. C., Johnson, M. K., et al. (2002). "The north west shelf of Australia—a Woodside perspective, the Sedimentary Basins of Western Australia 3," in Proceedings of the Petroleum Exploration Society of Australia Symposium. Perth. Pet. Explor. Soc. of Aust, Perth, WA, December 2002, 27–88.

Lovera, O. M., Richter, F. M., and Harrison, T. M. (1989). The40Ar/39Ar thermochronometry for slowly cooled samples having a distribution of diffusion domain sizes. *J. Geophys. Res.* 94, 17917–17935. doi:10.1029/jb094ib12p17917

Ludwig, K. R. (2008). *User's manual for Isoplot 4.15. A geochronological toolkit for microsoft excel, berkeley geochronology center*. Berkeley, CA: Special Publications.

McDougall, I. and Harrison, T. M. (1999). *Geochronology and thermochronology by the 40Ar/39Ar method*. New York, NY: Oxford University Press, 269.

Metcalfe, I. (1990). Allochthonous terrane processes in southeast Asia. *Phil. Trans. Roy. Soc. Lond. Math. Phys. Sci.* 331, 625–640.

Metcalfe, I. (2013). Gondwana dispersion and Asian accretion: tectonic and palaeogeographic evolution of eastern Tethys. *J. Asian Earth Sci.* 66, 1–33. doi:10.1016/j.jseaes.2012.12.020

Metcalfe, I. (1994). Gondwanaland origin, dispersion, and accretion of East and Southeast Asian continental terranes. *J. S. Am. Earth Sci.* 7, 333–347. doi:10.1016/0895-9811(94)90019-1

Metcalfe, I. (2009). Late Palaeozoic and Mesozoic tectonic and palaeogeographical evolution of SE Asia. *Geol Soc Spec Publ.* 315, 7–23. doi:10.1144/sp315.2

Metcalfe, I. (1986). Late Palaeozoic palaeogeography of Southeast Asia: some stratigraphical, palaeontological and palaeomagnetic constraints. *Geol. Soc. Malays. Bull.* 19, 153–164. doi:10.7186/bgsm19198612

Metcalfe, I. (2006). Palaeozoic and Mesozoic tectonic evolution and palaeogeography of East Asian crustal fragments: the Korean Peninsula in context. *Gondwana Res.* 9, 24–46. doi:10.1016/j.gr.2005.04.002

Metcalfe, I. (1996). Pre-Cretaceous evolution of SE Asian terranes. *Geol Soc Spec Publ.* 106, 97–122. doi:10.1144/gsl.sp.1996.106.01.09

Metcalfe, I. (2017). Tectonic evolution of Sundaland. *Bull. Geol. Soc. Malays.* 63, 27–60. doi:10.7186/bgsm63201702

Moss, S. J., Carter, A., Baker, S., and Hurford, A. J. (1998). A Late Oligocene tectono-volcanic event in East Kalimantan and the implications for tectonics and sedimentation in Borneo. *J. Geol. Soc.* 155, 177–192. doi:10.1144/gsjgs.155.1.0177

Nemchin, A. A. and Cawood, P. A. (2005). Discordance of the U-Pb system in detrital zircons: implication for provenance studies of sedimentary rocks. *Sediment. Geol.* 182, 143–162. doi:10.1016/j.sedgeo.2005.07.011

Nguyen, T. T. B., Satir, M., Siebel, W., and Chen, F. (2004). Granitoids in the Dalat zone, southern Vietnam: age constraints on magmatism and regional geological implications. *Int. J. Earth Sci.* 93, 329–340. doi:10.1007/s00531-004-0387-6

Omang, S. A. K. and Barber, A. J. (1996). Origin and tectonic significance of the metamorphic rocks associated with the Darvel Bay Ophiolite, Sabah, Malaysia. *Geol Soc Spec Publ.* 106, 263–279. doi:10.1144/gsl.sp.1996.106.01.17

Parkinson, C. D., Miyazaki, K., Wakita, K., Barber, A. J., and Carswell, D. A. (1998). An overview and tectonic synthesis of the pre-Tertiary very-high-pressure metamorphic and associated rocks of Java, Sulawesi and Kalimantan, Indonesia. *Isl. Arc.* 7, 184–200. doi:10.1046/j.1440-1738.1998.00184.x

Pearce, J. A. (2008). Geochemical fingerprinting of oceanic basalts with applications to ophiolite classification and the search for Archean oceanic crust. *Lithos* 100, 14–48. doi:10.1016/j.lithos.2007.06.016

Pearce, J. A., Harris, N. B. W., and Tindle, A. G. (1984). Trace element discrimination diagrams for the tectonic interpretation of granitic rocks. *J. Petrol.* 25, 956–983. doi:10.1093/petrology/25.4.956

Pearce, J. A. (1996). Sources and settings of granitic rocks. *IUGS Episodes* 19, 120–125. doi:10.18814/epiiugs/1996/v19i4/005

Pearce, N. J. G., Perkins, W. T., Westgate, J. A., Gorton, M. P., Jackson, S. E., Neal, C. R., et al. (1997). A compilation of new and published major and trace element data for NIST SRM 610 and NIST SRM 612 glass reference materials. *Geostand. Newsl.* 21, 115–144. doi:10.1111/j.1751-908x.1997.tb00538.x

Peccerillo, A. and Taylor, S. R. (1976). Geochemistry of Eocene calc-alkaline volcanic rocks from the Kastamonu area, northern Turkey. *Contrib. Mineral. Petrol.* 58, 63–81. doi:10.1007/bf00384745

Pieters, P. E., Abidin, H. Z., and Sudana, D. (1993a). *Geology of the long pahangai sheet area, Kalimantan. Map at 1:250,000 scale*. Bandung, Indonesia: Geological Research and Development Centre.

Pieters, P. E. and Sanyoto, P. (1993). *Geology of the pontianak/nangataman sheet area, Kalimantan. Map at 1:250,000 scale*. Bandung, Indonesia: Geological Research and Development Centre.

Pieters, P. E. and Supriatna, S. (1990). *Geological map of west, central and East Kalimantan Area scale 1:1,000,000*. Bandung, Indonesia: Geological Research and Development Centre.

Pieters, P. E., Surono, and Noya, Y. (1993b). *Geology of the nangaobat sheet area, Kalimantan. Map at 1:250,000 scale*. Bandung, Indonesia: Geological Research and Development Centre.

Pieters, P. E., Surono, and Noya, Y. (1993c). *Geology of the putussibau sheet area, Kalimantan. Map at 1:250,000 scale*. Bandung, Indonesia: Geological Research and Development Centre.

Priem, H. N. A., Boelrijk, N. A. I. M., Bon, E. H., Hebeda, E. H., Verdurman, E. A. T., and Verschure, R. H. (1975). Isotope geochronology in the Indonesian tinbelt. *Geol. Mijnbouw* 54, 61–70.

Rusmana, E., Sutrisno, Langford, R. P., Keyser, F. D., and Trail, D. S. (1993). *Geology of the sambas/siluas sheet area, Kalimantan. Map at 1:250000 scale*. Bandung, Indonesia: Geological Research and Development Centre.

Rustandi, E., Nila, E. S., Sanyoto, P., and Margono, U. (1995). *Geological map of the Kotabaru sheet, Kalimantan. 1:250,000*. Bandung, Indonesia: Geological Research and Development Centre (GRDC).

Sambridge, M. S. and Compston, W. (1994). Mixture modeling of multi-component data sets with application to ion-probe zircon ages. *Earth Planet Sci. Lett.* 128, 373–390. doi:10.1016/0012-821x(94)90157-0

Searle, M. P., Whitehouse, M. J., Robb, L. J., Ghani, A. A., Hutchison, C. S., Sone, M., et al. (2012). Tectonic evolution of the Sibumasu-Indochina terrane collision zone in Thailand and Malaysia: constraints from new U-Pb zircon chronology of SE Asian tin granitoids. *J. Geol. Soc.* 169, 489–500. doi:10.1144/0016-76492011-107

Setiawan, N. I., Osanai, Y., Nakano, N., Adachi, T., Setiadji, L. D., and Wahyudiono, J. (2013). Late Triassic metatonalite from the Schwaner Mountains in West Kalimantan and its contribution to sedimentary provenance in the Sundaland. *Berita Sedimentologi* 28 (12/2013), 4–12.

Shellnutt, J. G., Lan, C.-Y., Van Long, T., Usuki, T., Yang, H.-J., Mertzman, S. A., et al. (2013). Formation of Cretaceous Cordilleran and post-orogenic granites and their microgranular enclaves from the Dalat zone, southern Vietnam: tectonic implications for the evolution of Southeast Asia. *Lithos* 182–183, 229–241. doi:10.1016/j.lithos.2013.09.016

Sikumbang, N. (1986). Geology and tectonics of pre-tertiary rocks in the Meratus Mountains, south east Kalimantan, Indonesia. PhD thesis. London, UK: University of London.

Sircombe, K. N. (2004). AgeDisplay: an EXCEL workbook to evaluate and display univariate geochronological data using binned frequency histograms and probability density distributions. *Comput. Geosci.* 30, 21–31. doi:10.1016/j.cageo.2003.09.006

Sláma, J., Košler, J., Condon, D. J., Crowley, J. L., Gerdes, A., Hanchar, J. M., et al. (2008). Plešovice zircon - a new natural reference material for U-Pb and Hf isotopic microanalysis. *Chem. Geol.* 249, 1–35. doi:10.1016/j.chemgeo.2007.11.005

Smyth, H. R., Hall, R., and Nichols, G. J. (2008). Cenozoic volcanic arc history of East Java, Indonesia: the stratigraphic record of eruptions on an active continental margin. *Geol. Soc. Am. Spec.* 436, 199. doi:10.1130/2008.2436(10)

Spell, T. L. and McDougall, I. (2003). Characterization and calibration of 40Ar/39Ar dating standards. *Chem. Geol.* 198, 189–211. doi:10.1016/s0009-2541(03)00005-6

Steiger, R. H. and Jäger, E. (1977). Subcommission on geochronology: convention on the use of decay constants in geo- and cosmochronology. *Earth Planet Sci. Lett.* 36, 359–362. doi:10.1016/0012-821x(77)90060-7

Suggate, S. M. and Hall, R. (2014). Using detrital garnet compositions to determine provenance: a new compositional database and procedure. *Geological Society, London, Special Publications* 386, 373–393. doi:10.1144/sp386.8

Sumartadipura, A. S. and Margono, U. (1996). *Geological map of the Tewah quadrangle, Kalimantan (1:250,000)*. Bandung, Indonesia: Geological Research and Development Centre (GRDC).

Sun, S.-S. and McDonough, W. F. (1989). Chemical and isotopic systematics of oceanic basalts: implications for mantle composition and processes. *Geol. Soc. Spec. Publ.* 42, 313–345. doi:10.1144/gsl.sp.1989.042.01.19

Supriatna, S., Mragono, U., De Keyser, F., Langford, R. P., and Trail, D. S. (1993). *Geology of the sanggau sheet area, Kalimantan, 1: 250 000*. Bandung, Indonesia: Geological Research and Development Centre.

Suwarna, N., Sutrisno, de Keyser, F., Langford, R. P., and Trail, D. S. (1993). *Geology of the singkawang sheet area, Kalimantan. Scale 1:250000*. Bandung, Indonesia: Geological Research and Development Centre.

Tan, D. N. K. (1979). Lupar valley, west Sarawak. Kuala Lumpur, Malaysia: Geological Survey of Malaysia, Report 13, 159.

Tate, R. B. (1991). Cross-border correlation of geological formations in Sarawak and Kalimantan. *Bull. Geol. Soc. Malays.* 28, 63–95. doi:10.7186/bgsm28199104

Tate, R. B. (2001). *The geology of Borneo Island*. Kuala Lumpur, Malaysia: Geological Society of Malaysia.

Taylor, B. and Hayes, D. E. (1983). "Origin and history of the south China Sea basin," in *The tectonic and geologic evolution of southeast asian seas and islands, part 2 geophysical monograph series*. Editor D. E. Hayes (Washington, DC: American Geophysical Union) 27, 23–56.

Tera, F. and Wasserburg, G. J. (1972). U-Th-Pb systematics in three Apollo 14 basalts and the problem of initial Pb in lunar rocks. *Earth Planet Sci. Lett.* 14, 281–304. doi:10.1016/0012-821x(72)90128-8

van Bemmelen, R. W. (1939). De geologie van het westelijke en zuidelijke deel van de Wester-Afdelling van Borneo. *Jaarb. Mijnw. Ned-Oost-Indië*, 187–328.

van Bemmelen, R. W. (1949). "*The geology of indonesia. (3 Vols) Vol. 1a: general geology of indonesia and adjacent archipelagos. Vol.1b: Portfolio (maps, charts, indexes and references). Vol.2: economic geology*. 2nd Edn. Nijhoff, The Hague: Govt. Printing Office, 732.

van Emmichoven, C. P. A. Z. (1939). De geologie van het centrale en oostelijke deel van de Westerafdeeling van Borneo. *Jaarboek Mijnwezen Nederlandsch Oost Indië, Verhandelingen* 68, 7–186.

van Hattum, M. W. A., Hall, R., Pickard, A. L., and Nichols, G. J. (2013). Provenance and geochronology of Cenozoic sandstones of northern Borneo. *J. Asian Earth Sci.* 76, 266–282. doi:10.1016/j.jseaes.2013.02.033

van Leeuwen, T., Allen, C. M., Elburg, M., Massonne, H.-J., Palin, J. M., and Hennig, J. (2016). The palu metamorphic complex, NW Sulawesi, Indonesia: origin and evolution of a young metamorphic terrane with links to Gondwana and Sundaland. *J. Asian Earth Sci.* 115, 133–152. doi:10.1016/j.jseaes.2015.09.025

Viete, D. R., Forster, M. A., and Lister, G. S. (2011). The nature and origin of the Barrovian metamorphism, Scotland: 40Ar/39Ar apparent age patterns and the duration of metamorphism in the biotite zone. *J. Geol. Soc.* 168, 133–146. doi:10.1144/0016-76492009-164

Viete, D. R., Richards, S. W., Lister, G. S., Oliver, G. J. H., and Banks, G. J. (2010). Lithospheric-scale extension during Grampian orogenesis in Scotland. *Geol. Soc. Spec. Publ.* 335, 121–160. doi:10.1144/sp335.7

Wakita, K., Miyazaki, K., Zulkarnain, I., Sopaheluwakan, J., and Sanyoto, P. (1998). Tectonic implications of new age data for the Meratus complex of South Kalimantan, Indonesia. *Isl. Arc* 7, 202–222. doi:10.1046/j.1440-1738.1998.00163.x

Wetherill, G. W. (1956). Discordant uranium-lead ages, I. *Trans. AGU* 37, 320–326. doi:10.1029/tr037i003p00320

Whalen, J. B., Currie, K. L., and Chappell, B. W. (1987). A-type granites: geochemical characteristics, discrimination and petrogenesis. *Contrib. Mineral. Petrol.* 95, 407–419. doi:10.1007/bf00402202

White, L. T., Graham, I., Tanner, D., Hall, R., Armstrong, R. A., Yaxley, G., et al. (2016). The provenance of Borneo's enigmatic alluvial diamonds: a case study from Cempaka, SE Kalimantan. *Gondwana Res.* 38, 251–272. doi:10.1016/j.gr.2015.12.007

Wilford, G. E. and Kho, C. H. (1965). Report No.: 2. Penrissen area, west Sarawak, Malaysia: Malaysian geol. Survey, Borneo region, 195.

Williams, I. S. (1997). "U-Th-Pb geochronology by ion microprobe," in *Applications of microanalytical techniques to understanding mineralizing processes*. Editors M. A. McKibben, W. C. Shanks III, and W. L. Ridley (Littleton, CO: Society of Economic Geologists). doi:10.5382/rev.07.01

Williams, P. R., Johnston, C. R., Almond, R. A., and Simamora, W. H. (1988). Late Cretaceous to early Tertiary structural elements of West Kalimantan. *Tectonophysics* 148, 279–297. doi:10.1016/0040-1951(88)90135-7

Witts, D., Hall, R., Nichols, G., and Morley, R. (2012). A new depositional and provenance model for the Tanjung Formation, Barito Basin, SE Kalimantan, Indonesia. *J. Asian Earth Sci.* 56, 77–104. doi:10.1016/j.jseaes.2012.04.022

Wu, J. M. and Yang, M. Z. (1994). Age analysis of seismic sequences in the southwestern South China Sea. *Geol. Res. South China Sea* 6, 16–29. [in Chinese].

Xu, C., Shi, H., Barnes, C. G., and Zhou, Z. (2016). Tracing a late Mesozoic magmatic arc along the Southeast Asian margin from the granitoids drilled from the northern South China Sea. *Int. Geol. Rev.* 58, 71–94. doi:10.1080/00206814.2015.1056256

Yan, Q., Shi, X., and Castillo, P. R. (2014). The late Mesozoic-Cenozoic tectonic evolution of the South China Sea: a petrologic perspective. *J. Asian Earth Sci.* 85, 178–201. doi:10.1016/j.jseaes.2014.02.005

Zhou, D., Sun, Z., Chen, H.-Z., Xu, H.-H., Wang, W.-Y., Pang, X., et al. (2008). Mesozoic paleogeography and tectonic evolution of South China Sea and adjacent areas in the context of Tethyan and Paleo-Pacific interconnections. *Isl. Arc* 17, 186–207. doi:10.1111/j.1440-1738.2008.00611.x

Zimmermann, S. and Hall, R. (2019). Provenance of Cretaceous sandstones in the Banda Arc and their tectonic significance. *Gondwana Res.* 67, 1–20. doi:10.1016/j.gr.2018.09.008

Zimmermann, S. and Hall, R. (2016). Provenance of triassic and jurassic sandstones in the Banda arc: petrography, heavy minerals and zircon geochronology. *Gondwana Res.* 37, 1–19. doi:10.1016/j.gr.2016.06.001

Conflict of Interest: Author HTB and co-author JH-B are currently employed at Chemostrat Ltd. Co-author LD is currently managing dircetor of Petryx. This research took place prior to the commencement of any commercial affiliations associated with the authors, and was conducted as part of a PhD and post-doctoral research positions at the Royal Holloway University of London.

The remaining authors declare that the research was conducted in the absence of any commercial or financial relationships that could be construed as a potential conflict of interest.